UNIVERSITY OF SOUTHERN QUEENSLAND

DETERMINING BROADACRE CROP AREA ESTIMATES THROUGH THE USE OF MULTI-TEMPORAL MODIS SATELLITE IMAGERY FOR MAJOR AUSTRALIAN WINTER CROPS

A Dissertation submitted by:

Andries B Potgieter, MSc. Mathematical Statistics

For award of

Doctor of Philosophy

2009

To my parents

Abstract

Since early settlement, agriculture has been one of the main industries contributing to the livelihoods of most rural communities in Australia. The wheat grain industry is Australia's second largest agricultural export commodity, with an average value of $3.5 billion per annum. Climate variability and change, higher input costs, and world commodity markets have put increased pressure on the sustainability of the grain industry. This has lead to an increasing demand for accurate, objective and near real-time crop production information by industry. To generate such production estimates, it is essential to determine *crop area planted* at the desired spatial and temporal scales. However, such information at regional scale is currently not available in Australia.

The aim of this study was to determine broadacre crop area estimates through the use of multi-temporal satellite imagery for major Australian winter crops. Specifically, the objectives were to: (i) assess the ability of a range of approaches to using multi-temporal Moderate Resolution Imaging Spectroradiometer (MODIS) imagery to estimate total end-of-season winter crop area; (ii) determine the discriminative ability of such remote sensing approaches in estimating planted area for wheat, barley and chickpea within a specific cropping season; (iii) develop and evaluate the methodology for determining the predictability of crop area estimates well before harvest; and (iv) validate the ability of multi-temporal MODIS approaches to determine the pre-harvest and end-of-season winter crop area estimates for different seasons and regions.

MODIS enhanced vegetation index (EVI) was used as a surrogate measure for crop canopy health and architecture, for two contiguous shires in the Darling Downs region of Queensland, Australia. Multi-temporal approaches comprising principal component analysis (PCA), harmonic analysis of time series (HANTS), multi-date MODIS EVI during the crop growth period (MEVI), and two curve fitting procedures (CF1, CF2) were derived and applied. These approaches were validated against the traditional single-date approach. Early-season crop area estimates were derived through the development and application of a metric, i.e. accumulation of consecutive

16-day EVI values ≥ than 500 ($\sum \Delta EVI_{T500}$), at different periods before flowering. Using ground truth data, image classification was conducted by applying supervised (*maximum likelihood*) and unsupervised (*K-means*) classification algorithms. The *percent correctly classified* and *kappa coefficient* statistics from the *error matrix* were used to assess pixel-scale accuracy, while shire-scale accuracy was determined using the *percent error* (PE) statistic. A simple linear regression of actual shire-scale data against predicted data was used to assess accuracy across regions and seasons. Actual shire-scale data was acquired from government statistical reports for the period 2000, 2001, 2003 and 2004 for the Darling Downs, and 2005 and 2006 for the entire Queensland cropping region.

Results for 2003 and 2004 showed that multi-temporal HANTS, MEVI, CF1, CF2 and PCA methods achieved high overall accuracies ranging from 85% to 97% to discriminate between crops and non-crops. The accuracies for discriminating between specific crops at pixel scale were less, but still moderate, especially for wheat and barley (lowest at 57%). The HANTS approach had the smallest mean absolute percent error of 27% at shire-scale compared to other multi-temporal approaches. For early-season prediction, the $\sum \Delta EVI_{T500}$ metric showed high accuracy (94% to 98%) at a pixel scale and high R^2 (0.96) for predicting total winter crop area planted.

The rigour of the HANTS and the $\sum \Delta EVI_{T500}$ approaches was assessed when extrapolating over the entire Queensland cropping region for the 2005 and 2006 season. The combined early-season estimate of July and August produced high accuracy at pixel and regional scales with percent error of 8.6% and 26% below the industry estimates for 2005 and 2006 season, respectively. These satellite-derived crop area estimates were available at least four months before harvest, and deemed that such information will be highly sought after by industry in managing their risk. In discriminating among crops at pixel and regional scale, the HANTS approach showed high accuracy. Specific area estimates for wheat, barley and chickpea were, respectively, 9.9%, -5.2% and 10.9% (for 2005) and -2.8%, -78% and 64% (for 2006). Closer investigation suggested that the higher error in 2006 area estimates for barley and chickpea has emanated from the industry figures collected by the government.

Area estimates of total winter crop, wheat, barley and chickpea resulted in R^2 values of 0.92, 0.89, 0.82 and 0.52, when contrasted against the actual shire-scale data. A significantly high R^2 (0.87) was achieved for total winter crop area estimates in Augusts across all shires for the 2006 season. Furthermore, the HANTS approach showed high accuracy in discriminating cropping area from non-cropping area and highlighted the need for accurate and up-to-date land use maps.

This thesis concluded that time-series MODIS EVI imagery can be applied successfully to firstly, determine end-of-season crop area estimates at shire scale. Secondly, capturing canopy green-up through a novel metric (i.e. $\sum \Delta EVI_{T500}$) can be utilised effectively to determine early-season crop area estimates well before harvest. Finally, the extrapolability of these approaches to determine total and specific winter crop area estimates showed good utility across larger areas and seasons. Hence, it is envisaged that this technology is transferable to different regions across Australia. The utility of the remote sensing techniques developed in this study will depend on the risk agri-industry operates at within their decision and operating regimes. Trade-off between risk and value will depend on the accuracy and timing of the disseminated crop production forecast.

Certification of Dissertation

I certify that the ideas, experimental work, results, analyses, software and conclusions reported in this dissertation are entirely my own effort, except where otherwise acknowledged. I also certify that the work is original and has not been previously submitted for any other award, except where otherwise acknowledged.

_____ _____

Signature of Candidate Date

ENDORSEMENT

_____ _____

Signature of Supervisor Date

Associate Professor Armando Apan

Preface

"My son, farming (the farm) and I can not provide you with what an education can equip you with, and most of all, it (education) can't be taken away from you."

Dad, 1986; South Africa

Growing up on a mixed cropping farm in the Free State, South Africa, I have seen, experienced and lived through the emotions of the negative and positive impacts of climate variability on our farm, during the 80s and 90s. The effect, physically and emotionally, affected my parents more severely, in particular my father who never gave up, but instead persevered year-after-year working the land, until the end of his life in 1990. The interplay of colours, patterns and depth created by the hue reflectance of pastures, crops and landscapes, approaching the farm from the hill, is still vivid in my mind. These images are akin to a painter's palette. Thus, I want to dedicate my thesis specifically, to my late father, but also to farmers in general, who sturdily facing enormous physical, economical and ecological challenges each day, and unintentionally contributing to the ever changing mosaic of vivid images when viewed from space, i.e. "*a farmer's palette"*.

During these years and particularly during the end of my *master degree*, the idea of doing a PhD study program was seeded. It was not until 1995, when I met Dr Graeme Hammer from Australia, and specifically, in 1997 during a conversation with him in South Africa, that the idea of a PhD became more than just an idea. However, at that stage it was still only a dream.

In 1999, I was appointed as a research scientist to the Queensland Department of Primary Industries (QDPI), Australia. My job was made easier by the kind and friendly acceptance I received from the DPI, and specifically the Agricultural Production Systems Research Unit (APSRU) group, though sometimes I must have caused laughs with my pronunciation and word choice, which very quickly could get me into awkward situations. Nonetheless, it was and is still great working with colleagues from APSRU. Under the supervision of Dr Graeme Hammer, my job was

to develop and operationalise a regional scale commodity forecasting system. The uptake by industry confirmed the success of the system, which soon lead to the need for accurate production estimates.

The *missing link* however, is the availability of objective accurate and in-time crop area estimate, across large areas, well before harvest. In early 2003, the impetus and objective of the current thesis took shape and became a reality in a conversation with Graeme Hammer. I became a part-time PhD candidate not long after.

Acknowledgements

Many people and institutions, have contributed, assisted and encouraged me during the course of my research and deserve a special word of thanks. Queensland Department of Primary Industries & Fisheries (QDPI&F) and Dr Roger Stone approved and endorsed my post graduate research through its early stages. Dr Holger Meinke, who was the program leader during the main part of my study period and Dr Daniel Rodriguez, who is currently my program manager, provided me their full support.

My research involved frequent field trips to collate ground truth crop type samples during 2003 to 2006 across the entire Queensland cropping region. I want to thank Kym McIntyre and Brendan Lynch from QDPI&F who accompanied me on various field trips and their willingness and support in collating this information. Particularly, agronomist Stuart Thorn (MCA Goondiwindi PTY Ltd.) keenly helped me in providing sound data points for the Waggamba shire during the 2005 and 2006 seasons. Leanne Lawrence of the Australian Bureau of Agricultural and Resource Economics (ABARE) provided actual state level crop data, which was essential in validation of the remote sensing methodologies. Greg McLean and Al Doherty helped in downloading MODIS imagery at critical periods. Brendon Power assisted me in programming the curve fitting code in the R-statistical package environment, while Sarah Lennox gave excellent advice and helped with making sure my mathematical algorithms were robust.

This thesis was made possible by the critical assessment and guidance of my supervisors. Therefore, I want to thank my supervisor, Associate Professor Armando Apan, for his support, energetic guidance and subtle way of pushing me to keep me on track with my research and thesis milestones. Dr Peter Dunn, co-supervisor, gave countless comments on the application of statistics. My profound appreciation to Professor Graeme Hammer, co-supervisor, for his remarkable insight and prudent vision in addressing the research questions at hand.

My parents (Philip and Marietjie), for mentoring me, always believing in me and most of all, providing me with the opportunity and financial support to follow a university degree; "*This work is dedicated to you mum (and dad who passed away in the early 90s)*."

Last but not least, my effervescent wife, Marlene, for your continuing support and perseverance during this period. Thank you for your encouragement and believing in me, which helped me to keep pushing on with my studies towards the end. Sorry (again), for the times I came home from work irritated. I will make up for it in the future. To my two beautiful children, Philip and Imann-jana, thanks for your love and care. And finally, thanks to my Creator – to whom I stand in awesome wonder.

Publications Resulted from this Thesis

Refereed Journal

Potgieter, A, Apan, A, Dunn, P & Hammer, G 2007, 'Estimating Crop Area Using Seasonal Time Series of Enhanced Vegetation Index from MODIS Satellite Imagery', *Australian Journal of Agricultural Research*, vol. 58, pp. 316-25.

Conference Papers

Potgieter, AB, Apan, A, Dunn, P & Hammer, GL 2008, 'Estimating Winter Crop Area across Seasons and Regions in Queensland Using Multi-Temporal MODIS Satellite Imagery', paper presented to the 14th Australasian Remote Sensing & Photogrammetry Conference, Darwin, 29th September - 3rd October 2008.

Potgieter, AB, Hammer, GL & Doherty, A 2007, 'Integrating Crop Models, Satellite Data and Seasonal Climate Prediction to Forecast Regional Crop Production in Australia', paper presented to The 6th Asian Crop Science Association Conference and the 2nd International Conference on Rice for the Future, Bangkok, Thailand. (ISBN 978-974-229-500-4), 5-9 November 2007.

Potgieter, AB, Apan, A & Kelly, R 2003, 'The Potential of Multi-Temporal MODIS Imagery for Mapping Agricultural Areas in Support of Regional Commodity Forecasting', paper presented to Spatial Sciences Coalition Conference, Canberra, 22-26 September 2003.

Abbreviations

ABARE	Australian Bureau of Agricultural Resource Economics
ABS	Australian Bureau of Statistics
ACRES	Australian Centre for Remote Sensing
APSIM	Agricultural Production Systems sIMulator
APSRU	Agricultural Production Systems Research Unit
AVHRR	Advance Very High Resolution Radiometer
CF1, CF2	Curve Fitting Procedures
EVI	Enhanced Vegetation Index
HANTS	Harmonic Analysis of the Time-series
JM	Jeffries-Matusita
KC	Kappa Coefficient
LAI	Leaf Area Index
MAPE	Mean Absolute Percent Error
MEVI	Multi-date Enhanced Vegetation Index approach
MLC	Maximum Likelihood Classification
MDC	Minimum Distance Classifier
MODIS	Moderate Resolution Imaging Spectroradiometer
NDVI	Normalized Difference Vegetation Index
NOAA	National Oceanographic and Atmospheric Administration
PE	Percent Error
PEVI	Peak Enhanced Vegetation Index approach; single date EVI MODIS image acquired around the peak of the average EVI profile
PC	Principal Component
PCA	Principal Component Analysis
PCC	Percent Correctly Classified
RMSE	Root Mean Square Error
ROI	Region of Interest
TM	Thematic Mapper
TD	Transformed Divergence
USDA	United States Department of Agriculture
WAOB	World Agricultural Outlook Board

Table of Contents

List of Figures

List of Tables

Chapter 1

Introduction

*"It is our will and pleasure that you do immediately upon your landing after taking measures for securing yourself and the people who accompany you from any attacks or interruptions of the natives…**proceed to the cultivation of the land** [emphasis provided] …and with all convenient speed transmit a report of the actual state of the soil…and the most effectual means of improving and cultivating the same."*

King George III (1787)

1.1 Crop Production *Then and Now*

Agriculture and crop production is an intrinsic commission in securing the survival of the human species. This was very much evident when the first settlers landed on the east coast of Australia and is illustrated through the above quotation from one of the earliest documents related to settlement in the continent (Commonwealth of Australia 1914). This was the order approximately 200 years ago by King George III (England) to Governor Philip before he set out to establish the new penal settlement at Botany Bay in New South Wales, Australia (Shaw 1993). Crop production was at the heart of these pioneers as they started a new life, on a new continent, with its many unknown vagaries.

Today, through the evolution of agricultural technology in crop varieties, management practices and farming equipment, along with other factors, wheat production in Australia (Figure 1.1) has significantly increased from 500 thousand tonnes in the mid 19th century to nearly 20 million tonnes in the last decade (ABS 2004). For barley, the degree of increase in production over the last century was much higher. The production started ~10,000 tonnes in the late 19th century, and has increased to ~4 million tonnes on average today. A major advance for wheat production occurred during the last part of the 20th century when an increase of up to

30 percent in decadal yield occurred (Knopke et al. 2000). This makes cereal crop production, specifically wheat, one of the most important agricultural commodities (after beef) for the continent.

In spite of this significant increase in crop production, the economic survival of the producer is still highly dependent on the environment in which they operate. Currently, however, the operating environment has become increasingly challenging due to factors like domestic and world markets that are affecting commodity price regimes, climate variability and climate change that influence production risk, and increasing costs of inputs, which impinge on business profitability. Furthermore, these factors operate at different temporal and spatial scales (Meinke et al. 2006a) and cause current producers to be risk orientated and, thus, more vigilant in their decision making processes in order to ensure social, economical and environmental sustainability. This is very different from the physical and cognitive *well-being* regimes (i.e. decisions were more likely focussed on how to survive from day to day or week to week) associated with their ancestors during early and late 19th century settlement on the Australian continent.

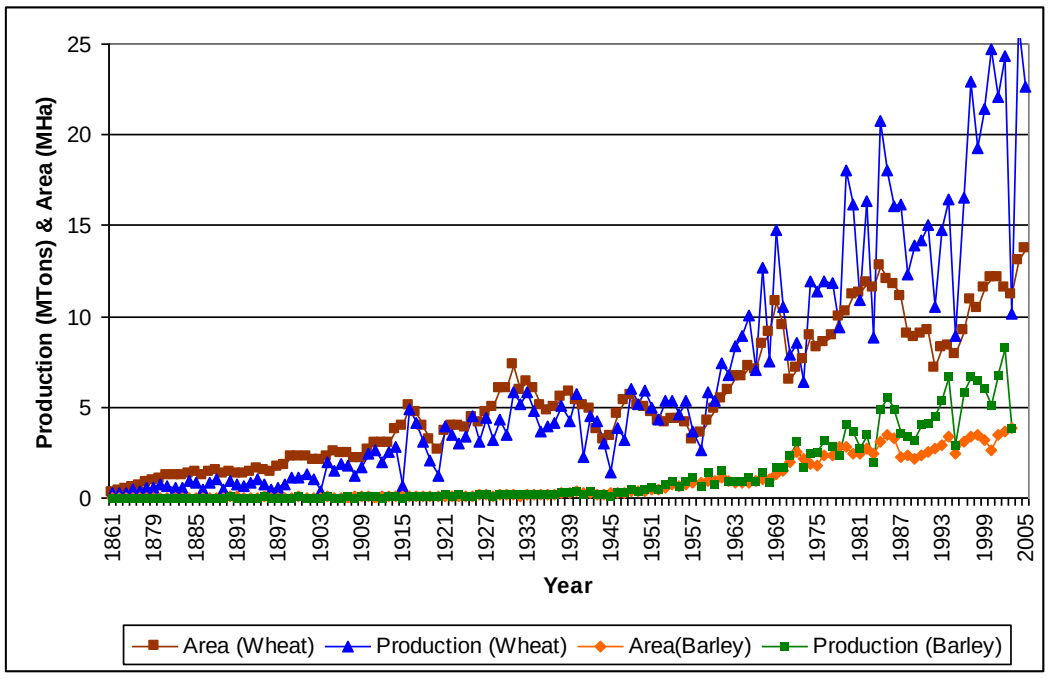

Figure 1.1: Time series of total area planted for wheat (orange line) and barley (brown line) and total production for wheat (blue line) and barley (green line) for Australian from 1862 to 2004 (ABS 2004).

1.2 Statement of the Problem

In Australia, like in many other semi-arid continents, wheat production is mainly affected by climate variability (Nix 1975). Thus, to remain economically viable in an internationally competitive market, the producer needs to have a sound understanding of the sources of climate variability, their predictability and access to objective tools and information, which can be used to assess specific management options in agronomic, economic, and environmental terms (Meinke et al. 2003). Having access to such decision support tools has become increasingly necessary to the producer to better deal with production risk. Numerous objective decision-making tools have been designed to assist agri-industry in managing production risk at paddock/farm level (Hammer et al. 2001; Nelson et al. 2002). During the past decade, this development has extended to the regional level (Potgieter et al. 2002; Stephens et al. 2000) with objective systems for estimating regional crop production that provide information to support policy (e.g. drought declarations) and industry (e.g. commodity storage and trading).

During the late 20th century, most regional crop estimate frameworks were based on local knowledge from local experts (e.g. extension officers, farmers, grain traders etc.). Hence, they depended heavily on how well the experts knew their regions. These estimates were often based on historical regional, state and national level statistics, which were, and still are, collated by the Australian Bureau of Statistics (ABS) via an agricultural census/survey at the shire (statistical local area) scale. This approach forms the basis on which various government bodies (e.g. Australian Bureau of Agricultural Resource Economics (ABARE), Bureau of Resource Science (BRS), Queensland Government (QG)) make decisions, such as, which shires should be classified as drought stricken during drought years. Such decisions have a major impact on the coping ability of communities.

In the late 1990s, the ABS census was changed to a yearly survey and a 5-yearly census, which further confounded the availability of accurate crop information. In addition, the statistics collated during survey years by ABS, such as the 2002 season,

are disseminated at a statistical division level (group of shires) (Lester 2008). Lack of detailed shire scale information during 4 out of 5 years further emphasises the need for alternative of near real-time accurate and objective crop production estimates to assist agri-industry decision-making at regional scale. This has been especially the case during the last five years when, for example, the severe drought of 2002 reduced the economic growth of the Australian economy by approximately 0.75 percentage points (Penm 2002).

The Regional Commodity Forecasting System (RCFS), which is being used operationally by the Queensland Department of Primary Industries & Fisheries (QDPI&F) to predict shire-scale wheat and sorghum yield on a monthly basis (www.dpi.qld.gov.au/fieldcrops) is an example of the type of system required to deliver objective information to industry in a timely manner. This system, which commenced in 1999, generates a yield forecast distribution of wheat and sorghum on a monthly basis through the integration of a simple stress index model (Potgieter et al. 2005a; Potgieter et al. 2006; Stephens et al. 1998) and the El Niño Southern Oscillation (ENSO) based climate forecast system generally known as the SOI phase system (Stone et al. 1996b). This is run for each month throughout the crop-growing season (winter and summer) for all main crop-producing shires in Australia to generate updated forecasts as the season unfolds. A shortcoming of this system, however, is that it generates an estimate of yield per unit area—not total production. This estimate is being used by decision-makers in conjunction with their subjective knowledge of total area planted at a shire or broader scale to calculate total production. Thus, in order to generate total production predictions, a real-time estimate of the crop area planted is needed. This is necessary in determining near real-time production figures for updating supply chain information at the regional, state and national levels.

While there are alternative methods (e.g. survey or census) to derive information on crop area planted, the use of satellite information offers more objectivity, timeliness, repeatability as well as likely increased accuracy. Over the years, satellite-based derived information in agriculture, using high spatial resolution imagery to low spatial resolution imagery, has been invaluable in decision-making processes of

governments (e.g. disaster relief), business and natural resource managers (e.g. extent and impact of floods or hail) and producers (e.g. precision agriculture) across different scales (Figure 1.2). Until now, the potential for remotely sensed based regional crop-forecasting systems has not been fully realised because of the high resource costs (i.e. imagery, computer disk space and speed) and the difficulty in applying high spatial resolution imagery to large areas. However, the advent of *Moderate Resolution Imaging Spectroradiometer* (MODIS) imagery, launched in April 2000, provides significant opportunity to address the issues of cost and useable pixel size for regional applications. In this study, it was proposed to use MODIS imagery to determine crop area planted as a means to aid targeted agricultural forecasting systems in estimating crop production at a regional scale (Figure 1.2).

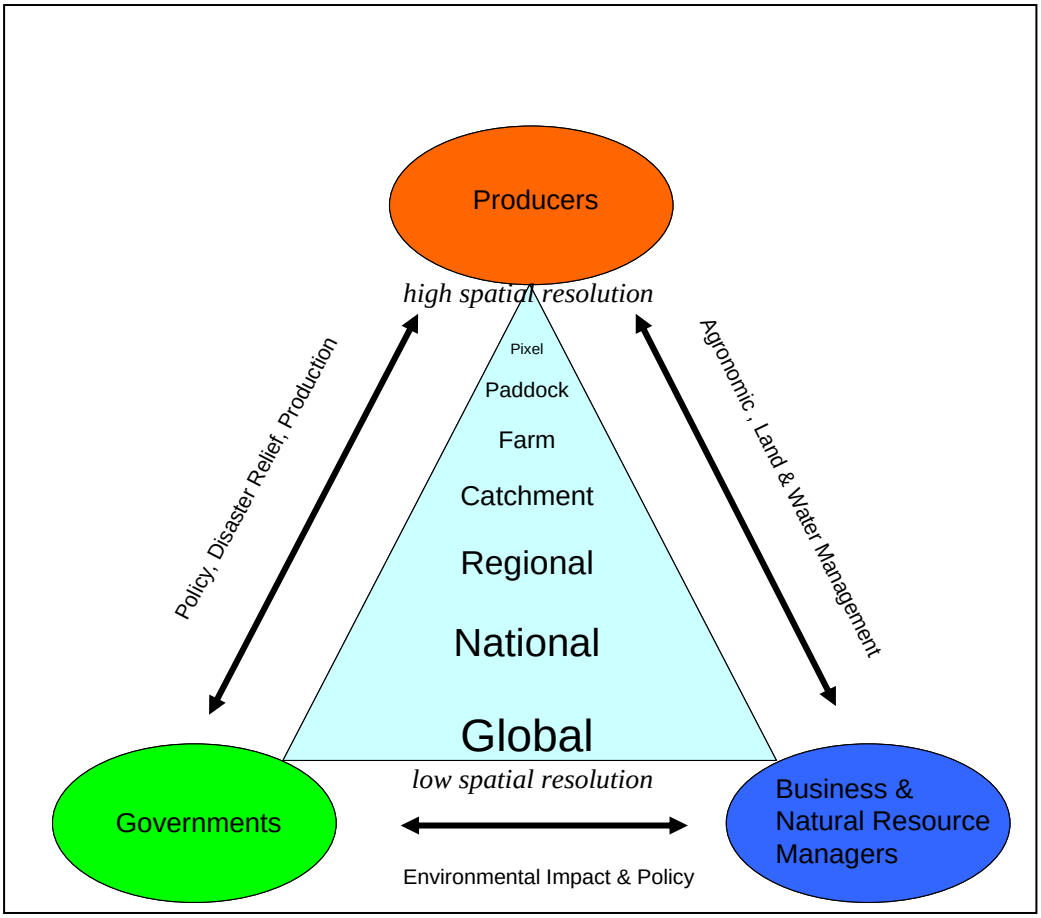

Figure 1.2: Information flow between decision-makers at the different scales and application levels of remotely sensed data. This thesis targets data outputs at the regional scale.

Although various international studies have utilised MODIS in determining land use patterns (Muchoney et al. 2000; Price 2003; Zhan et al. 2002), vegetation phenology (Zhang et al. 2003) or rice production in the northern Hemisphere (Xiao et al. 2005), no specific studies on its utility for determining total and crop specific winter crop area estimates well before harvest have been reported.

Therefore, given the potential integration of MODIS with a rigorous regional agro-climatic crop forecasting system, such approach is expected to lead to rapid, objective and sound production estimates that have the potential to underpin better-informed production risk decisions at a regional level.

1.3 Significance of the Study

Accurate, objective and near real-time estimates of crop area planted are intrinsic to determining regional production estimates for any crop. Currently, no accurate near real-time estimates of wheat area planted at shire scale exist in the public domain in Australia. Information is available currently via the ABS survey and census data with a lag of 2 to 3- years after the event; an example was the 2005/2006 census year, when the agricultural statistics at shire scale was released only in early 2008 (ABS 2008).

Many within the grains industry (from bulk handlers to government policy makers), particularly in the recently deregulated marketing environment, seek advance information on likely production and its geographical distribution to assist them in sound production risk management processes. Such information is also sought by government agencies (e.g. ABARE) in relation to policy interventions triggered by the degree of exceptional circumstances (e.g. drought, bumper crops, etc.). The current regional commodity forecasting system (RCFS) of QDPI&F partially addresses this need through its monthly crop outlook report. However, this report only disseminates wheat yield per unit area (t/ha) at a shire scale and does not address the issue of area planted and, hence, total crop production. This information on *yield only* (as derived from the simple agro-climatic model) can be sometimes misleading; an example was the case in the 2004 winter crop season for south-east Queensland (QLD). During this season, an average wheat yield crop was forecast for

most of the Darling Downs shires. However, the total production for wheat was below to very much below average crop for the 2004 season. This anomaly was caused by the lack of widespread sowing rainfall throughout the region, which resulted in the area sown to winter crop to be well below the potential area that could be planted. Thus, having the additional knowledge about crop area planted is critical to providing reliable forecasts of crop production.

This clearly illustrates the need for developing a system that can address the *missing link*: i.e. an accurate and objective way of determining winter crop area planted at a shire scale. The accessibility of up-to-date, objective and accurate agricultural statistics is of utmost importance to assist government and industry in decision-making processes well before harvest. Moreover, the change of the agricultural statistics census from an annual to a 5-yearly time frame by ABS, has elevated the need for an objective regional commodity/crop production forecast to an even higher priority.

1.4 Research Objectives

The aim of this study was to develop remote sensing techniques to determine winter crop area estimates at different spatial scales through the use of multi-temporal MODIS satellite imagery. More specifically, the objectives were to:

- Assess the ability of a range of approaches in using multi-temporal MODIS imagery to estimate total end-of-season winter crop area;
- Determine the discriminative ability of such remote sensing approaches in estimating area totals for wheat, barley and chickpea within a specific cropping season;
- Develop and evaluate the methodology for determining the predictability of crop area estimates well before harvest (early-season) for wheat, barley and chickpea; and
- Validate the ability of multi-temporal MODIS approaches, as derived in the study region, to determine the pre-harvest and end-of-season winter crop area estimates for different seasons and regions.

1.5 Organisation of the Thesis

Chapter 1 presents a brief history of winter crop production trends in Australia and provides background and justification for the thesis. The research gap (i.e. the need for winter crop area estimates) was identified, and the aim and specific objectives of the research study were presented. Chapter 2 reviews the literature on the current state of knowledge on regional scale crop area estimate approaches. This includes crop area estimates using remotely sensed data, the importance of temporal and spatial resolution, the advent of MODIS, and the ability of satellite imagery to discriminate among crops. In Chapter 3, the common research design and protocols to achieve the specific objectives are discussed. This includes the delineation of the study region, common data resources, classification approaches and the validation approach used.

Comparing the efficacy of different approaches to using multi-temporal MODIS data to determine end-of-season crop area estimates and their ability to discriminate between specific winter crops is addressed in Chapter 4. This addresses the first two specific objectives as discussed in the previous section. Chapter 5 addresses the third objective on exploring early season crop area estimates through the use of multi-temporal MODIS imagery. Chapter 6 examines the ability of the derived approaches (Chapters 4 and 5) to determine crop area estimates across seasons and regions, which addresses the fourth objective of this research. The overall summary, general conclusions and recommendations of the research study are given in Chapter 7.

Chapter 2

Literature Review

"Knowledge is of two kinds. We know a subject ourselves, or we know where we can find information on it."

Samuel Johnson (1709 - 1784), *quoted in Boswell's Life of Johnson*

2.1 Introduction

During the last century, seasonal climate and ensuing crop production have become more variable. This has prompted those in the industry to become better risk managers in order to achieve economic, social and environmental sustainability (Chapter 1). Furthermore, the sustainability of agricultural industries is not only impacted by world economies, price volatility or government drought policy but also by the fluctuation and change in climate (Meinke et al. 2006b). Recent research has suggested that El Niño-like events, i.e. usually associated with a reduction in rainfall over most parts of north-eastern Australia, may increase in magnitude and frequency due to existing climate change trends (IPCC 2001, 2007). Therefore, accurate and timely agricultural information (i.e. production statistics) has become highly sought after by the industry and government decision-making agencies (Hammer et al. 2001). However, there is no efficient, operational, near-real time production information system for Australia, similar to that used by the United States Department of Agriculture to assess yearly and half-yearly crop status through area-frame surveys (http://www.usda.gov). There is a clear need to develop and operationalise a system for regional scale crop area estimates in Australia. Currently, Australia has no operational remotely sensing based framework exists to determine regional scale winter crop area estimates.

In this chapter, the scientific literature relating to crop area estimate approaches is examined. Issues relating to accuracy, scale and costs are reviewed in section 2.2, while the evolution of remote sensing in agriculture is briefly described in section 2.3. Sections 2.4 and 2.5 deal with issues relating to the temporal and spatial resolution of

remotely sensed data. The advent of the MODIS platform is reviewed in section 2.6, while section 2.7 addresses the evolution of vegetation indices. The ability to discriminate between specific crops through the application of remotely sensed data is discussed in section 2.8. Traditional classification approaches in remote sensing is elaborated in section 2.9. Further literature reviews, specific to chapter objectives, will be presented in Chapters 3, 4, 5 and 6.

2.2 Accuracy, Scale and Cost of Remote Sensing Systems

In Australia, various crop yield forecasting methods exist. They predict crop yield at point/paddock/farm scale (Keating et al. 2003; Nelson et al. 2002) and regional/state/national scale (Potgieter et al. 2002; Potgieter et al. 2005a; Potgieter et al. 2006; Stephens et al. 1989), through the use of detailed to parsimonious crop simulation models. Attempts to using remotely sensed data to estimate crop yield at a shire scale have also been reported for Western Australia (WA). Those studies related crop yield to traditional monthly aggregated Normalised Difference Vegetation Index (NDVI) values (Smith et al. 1995; Stephens 1995). They have shown that a significant moderate relationship existed (R^2 ranged from 46% to 56%) between the NDVI Advance Very High Resolution Radiometer (AVHRR) green vegetation cover index and shire scale wheat yield across most of the WA broad cropping region. However, outcomes from these studies have not been integrated in an operational remote sensing based framework to determine total winter crop area/yield estimates as well as areas planted to specific crops at a regional scale. The lack of successful integration of such remotely sensed system is likely attributed to the higher accuracies of agro-climatic and empirical rainfall index models to predict shire scale wheat yields in WA.

Previous research efforts addressed the issue of determining crop area estimates and incorporating such outcomes into an operational system. For example, the ability of a range of approaches to predict broad-scale crop yield and planted area were contrasted in a detailed study in 1996 (Hammer et al. 1996). In this study, numerous crop yield prediction models ranging from empirical regression models, simple agro-climatic models and detailed dynamic crop models were contrasted. They also examined the application of remote sensing (Landsat Thematic Mapper (Landsat TM)

and AVHRR satellite imagery) to predicting shire-scale crop area. This study found that the medium resolution (30 m) imagery of Landsat TM showed significantly higher accuracy (R^2 = 0.91) in predicting actual total winter crop area planted at a state level (i.e. Queensland), than the coarse resolution (1.1 km) AVHRR system (R^2 = 0.76). However, the Landsat TM system could not be applied operationally because of the high cost of imagery (at least in previous years) and low repeat cycle, which is a major impediment in near-real time operational crop forecasting. Although the AVHRR system is less likely to be constrained by cloud cover because of its high temporal frequency (i.e. daily), its pixel size of 1.1 km resulted in much lower predictive accuracy. In addition, although the AVHRR system showed appreciable potential in mapping of broad cropping areas, it has no discriminatory power in the classification of crop species (e.g. wheat, barley) at any given location (Hammer et al. 1996).

The uptake and implementation of finer resolution satellite platforms like Landsat TM has been hampered by cost when an operational mode is considered. For example, to acquire Landsat 5/7 ortho-corrected images costs $1200 per scene. To cover the whole cropping region of Queensland, the data would thus cost ~ $15600 (13 full images x $1200) (www.ga.gov.au/acres/prod_ser/). This is further confounded by the infrequent satellite passes over an area (~16 day intervals) and the degree of cloud cover during such overpass.

The latter approach is more accurate, but it is costly and time-consuming when applied to large areas. Applications from the AVHRR and recently launched Moderate Resolution Imaging Spectroradiometer (MODIS) platforms have attributes of low-cost and rapidness, but has a restricted spatial resolution, specifically the AVHRR platform (Chen et al. 2008). This emphasises the need for a remote sensing system, which is inexpensive, has a high temporal resolution (e.g. 1-2 days) and more importantly, has a relatively good spatial resolution (e.g. 250 m pixel size).

2.3 Remote Sensing in Agriculture

The practice of remote sensing, which focuses on the examination of images of the earth's surface, has rapidly evolved since the discovery of the infrared spectrum and photography in the early 1800s (Campbell 2002). Various milestones in history (specifically war time research) have shaped the discipline we today know as remote sensing. One such clear milestone in the development of this field was the work done by Robert Colwell in 1965 on small-grain cereal crops and their diseases through the use of colour infrared film (also known as *camouflage detection film*). His work delineated the boundaries of modern remote sensing and anticipated many of the opportunities and difficulties of this field of reconnaissance. After 1960, when the first meteorological satellite was launched, a rapid sequence of events followed. During the 1970s and 1980s digital image processing came of age. During the early 1990s university degrees in remote sensing became available at most universities, which also lead to the integration of this science with other geographic sciences (including cartography, surveying and geographic information systems, to name a few) (Jensen 2007). In 1999, the National Aeronautics and Space Administration (NASA) launched Terra-1, which was the first satellite system specifically designed to acquire global coverage to monitor changes in nature and the extent of the earth's ecosystems. This marked the advent of an era of broad-scale remote sensing of the earth (Campbell 2002).

Globally, during the last decade, satellite imagery has been extensively used in various studies to determine the spatial and temporal dimensions of agricultural characteristics like net primary production (Markon et al. 2002; Prince 1991; Prince et al. 1995), vegetation cover (Fensholt 2004; Gitelson et al. 2002; Rondeaux 1995; Zhang et al. 2003), land use patterns (Muchoney et al. 2000; Price 2003; Xiao et al. 2005; Zhan et al. 2002) and the impact of climate variability on vegetation dynamics at the earth's surface (Roerink et al. 2003). Furthermore, the estimation of crop yield through the correlation of composite normalised difference vegetation index (NDVI) values and observed average district/state yield (Boken et al. 2002; Doraiswamy et al. 1995; Fuller 1998; Granados-Ramirez et al. 2004; Groten 1993; Labus et al. 2002; Stephens 1995), and the integration of the Food and Agriculture Organisation's (FAO) crop specific water balance with NDVI at the state level (Reynolds et al. 2000) have shown appreciable promise. However, none of these studies have focussed on

determining crop area of more than one crop (e.g. wheat and barley) within the same growing period when calculating the NDVI value for a specific region. Instead, they used the total aggregated NDVI value within the cropping land use mask for a specific shire to monitor crop condition or biomass. The use of multi-temporal "peak' NDVI to determine three different land use cover percentages (Defries et al. 2000) and to discriminate between irrigated rice and non-irrigated rice in an invariant climate environment (Kamthonkiat et al. 2005) showed reasonable accuracy (i.e. 69% to 89%). However, by using the point of maximum canopy growth, such an approach ignores likely additional information about crop canopy vigour intrinsic to the entire crop growth profile.

The Large Area Crop Inventory Experiment (LACIE), which is a joint project between NASA, the United States Department of Agriculture and National Oceanographic and Atmospheric Administration (NOAA) commenced in 1974 and is probably one of the first frameworks to integrate low-resolution Landsat imagery, a weather monitoring system and crop yield models to monitor global wheat production (MacDonald et al. 1980). Although LACIE had appreciable accuracy in determining global wheat production, it was very labour intensive and expensive to implement.

Another example of near real-time crop area and yield estimates is the Monitoring Agriculture through Remote Sensing techniques (MARS) project, which is a crop forecasting project operated and developed by the Directorate General Joint Research Centre (JRC) of the European Commission in Ispra (Italy) (http://www.marsop.info/). This project generates advance and timely production statistics for all the main European crops published in monthly MARS bulletin. Although very expensive (~ 1000,000 Euro), it is an excellent example of collaboration between governments (i.e. policy makers) and independent R&D institutions.

Other studies have shown that satellite-based vegetation indices could successfully be used in the monitoring of crop yield, production and crop condition over large areas (Dabrowska-Zielinska et al. 2002; Doraiswamy et al. 2004; Granados-Ramirez et al. 2004; Wannebo et al. 2000; Weisssteiner et al. 2005; Zang et al. 2005). Particularly, the development of indices measuring leaf canopy structure,

i.e. leaf area index (LAI), which was incorporated into a climate-variability impact index (Zang et al. 2005; Zhang et al. 2006) to monitor corn production across wide areas in the USA corn-belt showed satisfactory predictions (R^2 = 60%).

Other sensors like SPOT (Satellite Pour I'Observation de la Terre), ASTER (Advanced Spaceborn Thermal Emmision and Reflection Radiometer), high-resolution commercial satellites (e.g. IKONOS and Quickbird), microwave imaging sensors like RADARSAT, to name a few, and recently the hyper spectral image spectrometer, Hyperion, on NASA's observing-1 platform have all contributed to the advance in application of remotely sensed technology within the agricultural, ecological and oceanographic research community (Mather 1999). Relaxation in the remote sensing copy right specifically, with Landsat TM (and maybe others to follow later on) will further enhance the uptake of such technology (USGS 2009).

Since the launch of MODIS, data outputs from it were extensively used in the monitoring of biophysical aspects of vegetation and crop canopy conditions (e.g. biomass, leaf area index). Although it has a relatively low spatial resolution (i.e. 250 m x 250 m pixel size), it has the advantage of a high temporal resolution. The success of agricultural applications using MODIS approaches can be partly attributed to the high temporal and moderately low spatial resolution, as well as availability of the needed MODIS products (Chen et al. 2008).

2.4 Spatial Resolution of Satellite Imagery

Up to now, the most common satellite system used in broad-scale agricultural applications is the Advanced Very High Resolution Radiometer (AVHRR) carried by NOAA's Polar Orbiting Environmental Satellites. This satellite platform has been used in global impact studies (Prince 1991; Prince et al. 1995) because of its coarse spatial resolution of 1.1 km (~121 ha pixel size) and near-daily repeat cycle, which counteracts the likeliness of cloud cover at a global scale. Remarkably the difference in spatial resolution had little effect on the final area estimates for large areas as elucidated by an earlier study (Price 2003). Another study showed overall accuracies of 74% and 83% using the Landsat TM (30 m) and the Landsat MSS (80 m) products,

respectively, to classify vegetation cover (Toll 1985). Although both studies found no significant decrease in accuracy in using lower resolution satellite-based systems, results might differ from region to region and further research is necessary to determine the value of coarse resolution satellite imagery in discriminating among different crops (e.g. wheat and barley) within a growing season.

The interplay between scale and pixel size is an important issue, particularly in heterogeneous cropping areas. For example, large pixel size gives an increased chance of recording *mixed* brightness values. This *mixed* spectral response is further confounded by established local crop management practices, such as found in some areas of southern Queensland, where crops are planted in 50 m to 250 m strips (Figure 2.1) and alternated with an uncropped band (e.g. bare soil or stubble) of similar size to the cropped strip. Thus, pixels that are not completely within a single homogeneous feature (e.g. forest, vegetation, wheat crop etc.) have average brightness values as a consequence of more than one feature within the pixel area. Such pixels are know as *mixels* and are ubiquitous in cropland mapping (Chen et al. 2008).

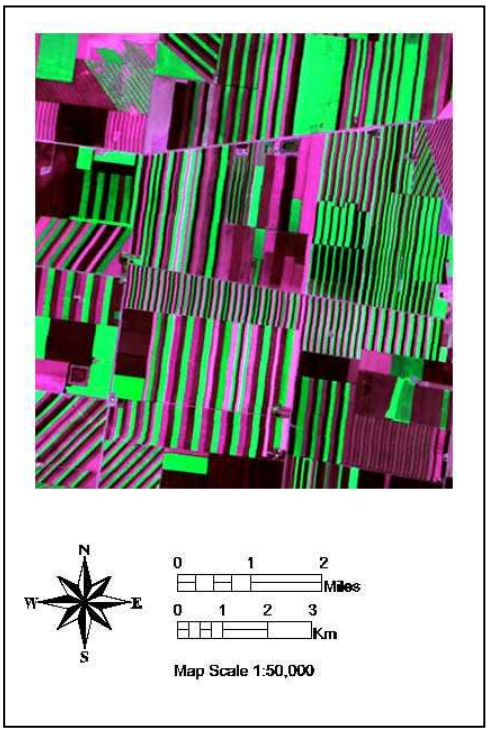

Figure 2.1: Zoomed view within the study area of a Landsat image acquired on 16th September 2003. The range in strip sizes (width and length) is noticeable.

Mixels have a composite spectral response or signature, which does not match the pure signature ideal for determining the total cultivated area of a specific crop (e.g. wheat). Mixed pixel responses add an additional source of error or confusion to the classification process and reduce the discriminating power (i.e. between crops) of such an analysis.

The selection of pixels, which consist completely of homogeneous crop canopies, will have average brightness values very similar to the object of interest and consequently a high signal to noise ratio (i.e. higher classification accuracy). Furthermore, contrasting mixel reflectance from the AVHRR satellite system to actual observed values of biomass, LAI or yield at that specific pixel location, is a major impediment to the usefulness of such an operational system (Prince 1991). There is a direct positive relationship between pixel purity and accuracy (Badhwar et al. 1982b).

2.5 Temporal Resolution of Satellite Imagery

Agricultural production has specific crop characteristics and capturing of all possible reflectance data throughout the growth of the crop is vital in determining accurate crop biomass, acreage or LAI. Any satellite-based platform needs to be able to cover most of the key phenological stages of cropping systems in order to be efficient (Thenkabail et al. 2000).

Although Landsat TM can be regarded as a suitable satellite imaging system for regional crop forecasting (mainly due to its swath width and spatial resolution), its major drawback is the relatively low temporal resolution (repeat cycle) of 16 days. Clouds and other atmospheric factors (e.g. pollution through large fires and volcanic eruptions) confound the use of such a system even further. Furthermore, the accuracy of a single date Landsat image to map crop area planted was found to be lower than that of multi-date approaches (Lobell et al. 2003; Van Niel et al. 2004). Although multi-date imagery can improve the mapping accuracy, such an approach will result

in a rapid increase in costs when extrapolated over time and across very large areas when using Landsat TM imagery.

AVHRR data has often been used to assess the impact of climate variability on vegetation vigour at seasonal and intra-seasonal time scales. However, because AVHRR was never designed for land applications, its data are not well suited for vegetation monitoring studies (Zhang et al. 2003). Specifically, the lack of precise calibration, poor geometric registration, and difficulties involved in cloud screening resulted in AVHRR having high levels of *noise*. The recently launched MODIS system, onboard NASA's Terra spacecraft, has improved atmospheric and cloud screening algorithms and provides a substantially improved basis for biophysical studies at the earth's surface (Zhang et al. 2003).

2.6 MODIS – The New Kid on the Block

The advent of MODIS is expected to enhance the application of remote sensing in targeted agricultural systems, such as crop forecasting. This relatively new satellite system, with its 36-spectral bands between 405 and 14385 nanometres (nm) (Table 2.1), provides global datasets that were previously unavailable (Justice et al. 2002). It has combined characteristics from both the AVHRR and Landsat TM platforms and provides new and improved capability for terrestrial satellite remote sensing research in agricultural systems. With a repeat cycle of 1-2 days, a pixel resolution of 250-m (~6.25 ha), 500-m (~25 ha) and 1-km (~100 ha), and a swath width of 2330 km, it also has readily available products such as NDVI, Enhance Vegetation Index (EVI) and LAI (Justice et al. 2002; Justice et al. 1998). MODIS satellite products are available through the ordering or downloading from the NASA's Earth Observing System (EOS) (http://edcimswww.cr.usgs.gov) website. MODIS data are captured through instruments onboard two spacecrafts (Terra and Aqua), which then send data through to the ground stations in the USA and other countries. Many data products are derived from MODIS observations which describe features of the land, oceans and the atmosphere that can be used for studies of processes and trends on local to global scales (TBRS 2007).

The range of spectral bands available, as well as the spatial and temporal resolution, makes MODIS imagery ideal for integration in a multi-temporal classification approach for determining not only crop area planted and yield per unit area. With a swath width of 2330 km, it is ideal for identifying crop types over large areas. Furthermore, given the potential integration of such a system with a rigorous regional agro-climatic crop forecasting system, the use of MODIS imagery is expected to lead to rapid, objective and sound production estimates that have the potential to underpin better-informed production risk decisions at a regional level.

Table 2.1: Spectral bands of the MODIS satellite platform (TBRS 2007).

BAND	Range (nm) reflected	Range (nm) emitted	Key Application
1	620-670		Absolute Land Cover Transformation, Vegetation, Chlorophyll
2	841-876		Cloud Amount, Transformation, Vegetation, Transformation
3	459-479		Soil/Vegetation Differences
4	545-565		Green Vegetation
5	1230-1250		Leaf/Canopy Differences
6	1628-1652		Snow/Cloud Differences
7	2105-2155		Cloud Properties, Land Properties
8	405-420		Chlorophyll
9	438-448		Chlorophyll
10	483-493		Chlorophyll
11	526-536		Chlorophyll
12	546-556		Sediments
13h	662-672		Atmosphere, Sediments
13l	662-672		Atmosphere, Sediments
14h	673-683		Chlorophyll Fluorescence
14l	673-683		Chlorophyll Fluorescence
15	743-753		Aerosol Properties
16	862-877		Aerosol Properties, Atmospheric Properties
17	890-920		Atmospheric Properties, Cloud Properties
18	931-941		Atmospheric Properties, Cloud Properties
19	915-965		Atmospheric Properties, Cloud Properties
20		3.660-3.840	Sea Surface Temperature
21		3.929-3.989	Forest Fires & Volcanoes
22		3.929-3.989	Temperature, Surface Temperature
23		4.020-4.080	Temperature, Surface Temperature
24		4.433-4.498	Cloud Troposphere Temperature
25		4.482-4.549	Cloud Troposphere Temperature
26	1360-1390		Cloud Fraction (Thin Cirrus), Troposphere Temperature
27		6.535-6.895	Mid Troposphere Humidity
28		7.175-7.475	Upper Troposphere Humidity
29		8.400-8.700	Surface Temperature
30		9.580-9.880	Total Ozone
31		10.780-11.280	Cloud Temperature, Forest, Fires & Volcanoes, Surface Temperature
32		11.770-12.270	Cloud Height, Forest, Fires & Volcanoes, Surface Temperature
33		13.185-13.485	Cloud Fraction, Cloud Height
34		13.485-13.785	Cloud Fraction, Cloud Height
35		13.785-14.085	Cloud Fraction, Cloud Height
36		14.085-14.385	Cloud Fraction, Cloud Height

2.7 Remotely Sensed Vegetation Indices

In biophysical land cover studies, plant growth responses are traditionally measured through a variety of vegetation indices (VI) that attempt to measure biomass or vegetative vigour. Spectral response of crop and vegetation canopies are mainly determined by five physical attributes (i) leaf optical properties, (ii) canopy geometry (e.g. LAI and leaf angle distribution), (iii) soil reflectance, (iv) solar illumination and view angles, and (v) atmospheric transmittance. The effects of the last three factors are traditionally corrected by remotely sensed algorithms, and thus leaving the first two attributes to directly describe reflectance of final crop parameters or crop status (Bauer 1985; Dadhwal et al. 2000).

Different canopy types have different reflectance responses across the wavelength spectrum. Variability in leaf optical properties is wavelength dependent with green leaves having the smallest variation in the visible wavelength region (VIS), while the largest variation is in the near-infrared region (NIR). Woody stem material showed opposite trends to that of green leaves. Canopy reflectance data is predominantly controlled by LAI and leaf angle within and across different landscapes. Leaf visual properties are mainly expressed at the canopy level within the NIR wavelength region (Asner 1998). The ability to capture canopy reflectance properties have been tried through a range of vegetation indices.

The typical pattern for a healthy vegetation cover shows high absorption due to chlorophyll at 650 nm (Red (R) region), and high reflection due to leaf internal structure at the 750 nm (NIR region). The simplest form of a VI is a ratio between two digital values from separate spectral bands, i.e. near-infrared and red bands. VI indices give an indication of broadband greenness derived from the amount and quality of photosynthetic material in vegetation canopy (Campbell 2002; Dadhwal et al. 1991; Lillesand et al. 2004). Another index is the AVHHR NDVI, which is one of the oldest and most commonly used VI in remote sensing studies. Green vegetation areas will generally yield high because of the high reflectance in NIR band and low reflectance in the R or visible region. NDVI is computed from the following equation:

$$NDVI = \frac{(NIR - R)}{(NIR + R)} \qquad [2.1]$$

This index is mainly used to determine biomass or vegetative canopy vigour over large areas (Campbell 2002). Conventional remote sensing approaches use multi-temporal composite NDVI images through the crop growth period and are typically derived from AVHRR imagery (Boken et al. 2002; Doraiswamy et al. 1995; Granados-Ramirez et al. 2004; Kalubarme et al. 2003; Labus et al. 2002).

Other forms of VIs exist such as greenness (GVI), perpendicular (PVI), transformed soil adjusted (TSAVI), soil adjusted (SAVI), atmospheric resistant (ARVI), soil and atmospheric adjusted (SARVI) and modified normalised difference (MNDVI) vegetation indices (Huete et al. 1997; Wiegand et al. 1991). Other simpler spectral band ratios were investigated for their ability to discriminate between vegetative growth profiles as a result of water stress with limited success (Jackson 1983).

The main constraint for VI metrics is the effect of the atmosphere and soil background on reflectance values in the red, near infrared, blue and green wavelength regions. The reduction in ambient contamination of measured reflectance has induced the variety of VIs noted above (Huete et al. 1997). A further effort to reduce the background "noise" (i.e. soil, atmosphere) has lead to the development of the Enhanced Vegetation Index (EVI) (Liu et al. 1995). This was done by including the blue reflectance band to correct for soil background and atmospheric perturbations. Not only does it minimise canopy background and atmospheric influences, it also optimises the vegetation signal with improved sensitivity in the high biomass regions, which is a major improvement on the traditional NDVI measure (Huete et al. 2002; Huete et al. 1997).

Another valuable metric that are produced on the MODIS platform is the satellite-based leaf area index (LAI). This measure responds rapidly to abiotic and biotic influences and can therefore integrate a range of conditions affecting plant growth through the various phenological stages (Holben et al. 1980). LAI is also highly correlated to crop yield since it captures both magnitude and duration of photosynthetic activity (Tucker et al. 1980). In recent studies, MODIS LAI product

showed reasonable success in measuring the impact of climate variability on crop production across large regions (Zhang et al. 2005; Zhang et al. 2006). However, the MODIS LAI product has a much lower spatial resolution (~ 1 km) than the MODIS EVI and NDVI products. In addition, some calibration is needed, either through ground experiments or broad scale land cover maps, in order to relate different magnitudes of satellite-based LAI measures to specific vegetation canopy types on the ground.

2.8 Crop Discrimination from Satellite-based Images

The simplest form of crop discrimination is the classification of imagery into broad-scale classification categories into which all agricultural land is grouped together. This is also known as level-1 land use cover classification (Campbell 2002). From this level of classification, classes can be grouped into cropping and non-cropping regions. Creation of level-1 classification maps is usually done by creating land use maps of specific regions through the concurrent use of Landsat TM and NOAA AVHRR imagery assisted by detail land use identification strategies (e.g. expansive field trips). This makes it a highly expensive exercise when large regions are covered. These classification types are very informative regarding longer-term cropping/vegetation patterns within a region.

The aim of this study, however, was to discriminate among small grain crops (wheat – *Triticum aestivum*, and barley – *Hordeum vulgrae*) and a winter grain legume (chickpea – *Cicer arietinum*) within a single cropping season. Discrimination between different crop canopies is a challenge, especially, separating wheat from barley since they have similar canopy architecture and phenology. The life cycle in crop plants consists mainly of three main phases i.e. (i) a vegetative stage, (ii) reproductive phase and (iii) a grain-filling stage. The overall length of the life cycle and the relative length of each phenological stage in it depend mainly on the daylength or temperature during the crop growth period (Evans et al. 1976). Wheat, barley and chickpea are known as temperate species and are largely dependent on sufficient moisture availability throughout the growing period but especially around specific phenological phases such as flowering and grain filling. Barley and wheat

were first domesticated in the Fertile Crescent (Figure 2.2) around 10,000 BC. Barley is closely related to wheat, but despite the similarities barley is generally regarded as the inferior staple to wheat, and thus the *poor man's bread*. However, barley is the hardier of the two species, which ensured its continued cultivation throughout history and specifically, in drier highly variable climate environments like north-eastern Australia (Langridge et al. 2003).

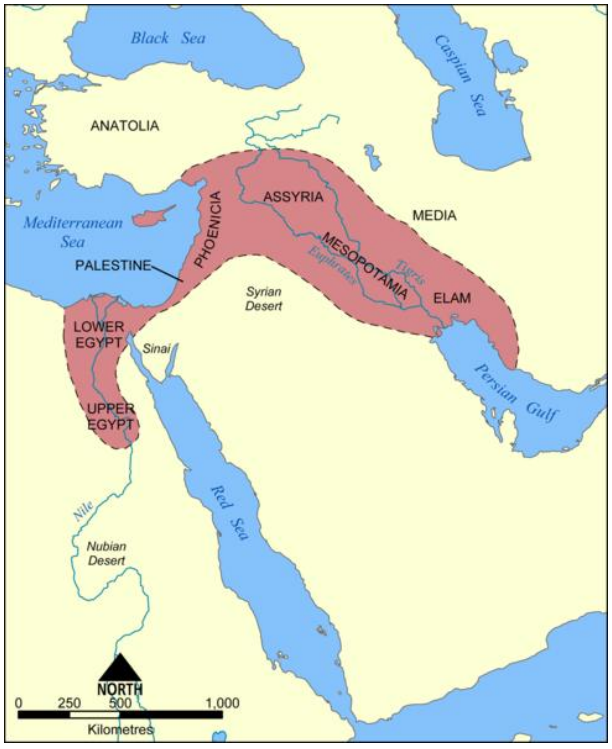

Figure 2.2: The Fertile Crescent is a region in the Middle East incorporating Ancient Egypt, the Levant, and Mesopotamia (Wikipedia 2008).

Figure 2.2 shows a map of the broad winter cropping region, the broad crop calendar for winter crops, and the breakdown of the percentage contribution of each state to the total national wheat production for Australia. Planting of temperate crops in Australia occurs during April to June (and can be extended into July and August for chickpea) followed by tillering and vegetative stages through June to August up to early September after which flowering, grain filling and maturity is reached during the late September to October period. Crops are generally harvested during late November to end of December depending on sowing times (Kelleher 2003).

The ability to discriminate between crops is directly related to the amount of reflectance, specifically in the NIR bandwidth, by the leaf and canopy structures (Campbell 2002). The main factor contributing to differences in canopy growth and, thus, canopy reflectance, between wheat and barley relates to canopy architecture and density (usually referred to as leaf area index), which is a function of the number of tillers and rate of growth (Kelleher 2003).

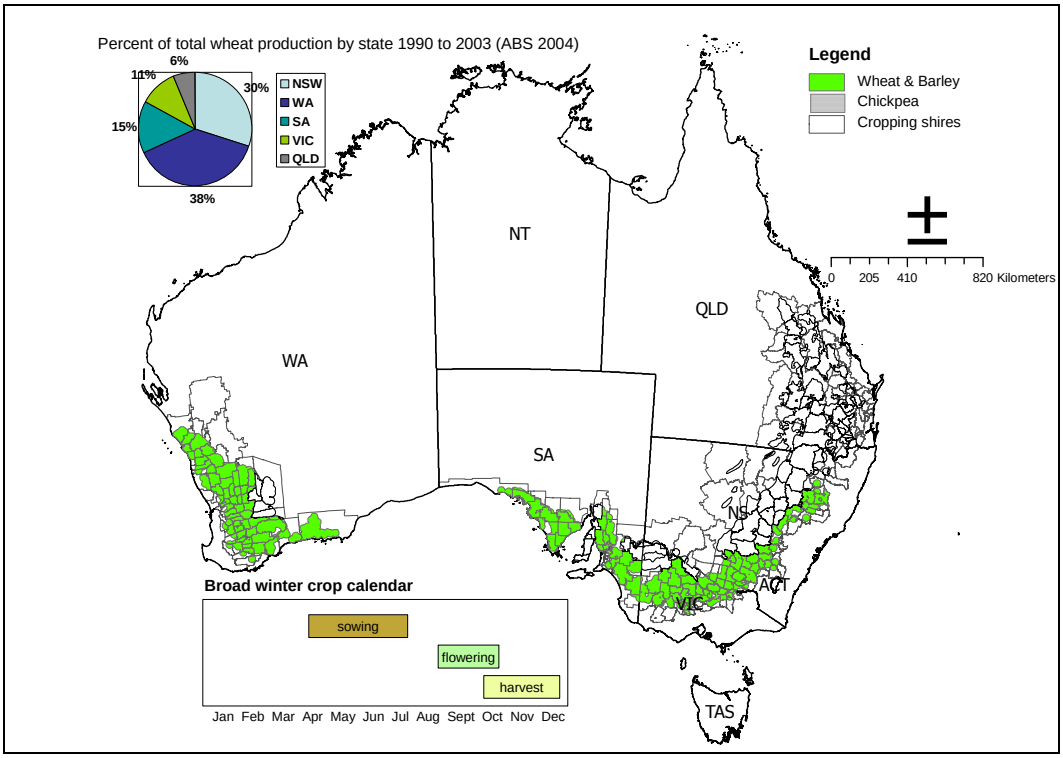

Figure 2.3: The broad winter cropping region, crop calendar for winter crops and the breakdown of the percentage contribution of each state to the total national wheat production for Australia. Wheat and barley is traditionally produced in the green coloured area while the cross hatched area indicates the location of chickpea production (Kelleher 2003).

For barley, early tillering and growth rate are nearly double that of wheat, causing crop canopy closure much quicker than in the case of wheat (Meinke 1996; Yunasa et al. 1993). This is a significant feature and it is likely that any discriminating ability would be derived from differences in reflectance values relating to rate of canopy closure mainly before the grain filling stage of crop development.

The different crop physiology and phenology of chickpea causes its leaf and canopy structure development to be quite different from wheat and barley (Figure 2.4) (Thomas et al. 1995). Discrimination of chickpea from wheat and barley is thus likely. The use of a vegetation index (which is highly sensitive to leaf and canopy architecture) and density, is thus imperative to the ability to discriminate between wheat and barley crops.

Figure 2.4: Showing the difference in canopy structure between (a) chickpea, and (b) barley (bottom left) and wheat (bottom right). Note the

difference in canopy structure with barley having large-awned ears and ears horizontal and a little more advance than wheat. The canopy differences between chickpea and wheat and barley are more prominent.

2.9 Traditional Classification Procedures in Remote Sensing

The main aim of classification procedures is to group pixels into a similar region of land use/cover classes or themes. This can be done by either *supervised* or *unsupervised* classification approaches (Lillesand et al. 2004). These approaches use algorithms that examine the unknown pixels in an image and aggregate them into a number of themes based on natural groupings or clusters present in the image. These classes are then related to a training or reference set after classification and categories are labelled with the name of the category it resembles. On the other hand, the pixel categorisation is supervised by specifying to the algorithm the spectral characteristics of specific themes based on reference data or ground truth data. Each image pixel is then compared numerically (through an algorithm) to the reference theme attributes and classified accordingly.

Unsupervised classification procedures are based on non-parametric statistical approaches such as *ISODATA* (Tou et al. 1974) and *K-means* (Johnson et al. 1988) algorithms and are the two most commonly used. Supervised classification is derived from parametric statistical approaches and the most commonly used are the parallelepiped classifier, the *maximum likelihood classifier* (MLC) and the *Malhalanobis classifier* (Johnson et al. 1988). The MLC approach forms the backbone of most multi-spectral remote sensing analyses today (Wessel et al. 2004).

A combination between unsupervised and supervised classification procedures is known as hybrid classification and is generally applied where complex variability in the spectral response of specific cover types exists. Furthermore, the classification of mixels (i.e. pixels with mixed spectral response) are made possible by more complex approaches such as spectral mixture analysis (SMA), which is based on the unmixing of spectral values within a pixel. This approach showed moderate to high accuracy in classifying heterogeneous cropland systems into land classes (Lobell et al. 2004).

Another approach is the *neural network* or *artificial neural network* (ANN), which are algorithms designed to simulate human learning processes through establishment and reinforcement of pathways between input data and output data. ANN has been found to be accurate in classification of remotely sensed data, although accuracy gain has been minimal or slightly worse than the traditional MLC. This was exemplified when determining soil moisture and agricultural variables by microwave radiometry using neural networks (Del Frate et al. 2003).

In recent years, *object-orientated* methods have become more popular in classification of satellite-based imagery mainly because of the availability of the software called *E-Cognition*. This approach refers to analysing the image in object space (i.e. groupings of pixels with similar spectral and spatial properties) rather than pixel space. Objects are used as primitives for image classification rather than pixels (Navulur 2007). This software uses a region-growing approach at different scale levels from coarse to fine, using both spectral properties and geometric attributes of the regions, such as shape (Campbell 2002). Although this approach showed slightly higher accuracy (~ 8%) than the MLC, the MLC approach still had a surprisingly high accuracy of 85% (Mather 1999).

Various other approaches to image classification exist, too many to discuss here, which are often adapted from existing approaches. The different classification methods should be seen as complementary rather than an alternative. Therefore, no single classification method should be seen as the ultimate classification approach, or panacea, when it comes to analysing remotely sensed imagery.

2.10 Concluding Remarks

Applications of remotely sensed data in agriculture have rapidly evolved since the end of the 20th century. Most recently (start of the 21st century), the advent of the MODIS satellite platform has enhanced the potential application of remotely sensed data to determine and monitor vegetation vigour at a regional level with appreciable success. Although MODIS has a relatively coarse spatial resolution, the imagery has been shown to be as accurate (at regional scale) as the finer resolution and the more

expensive Landsat TM. Furthermore, the near diurnal repeat cycle (~1 to 2 days) and its swath width of 2330 km makes the MODIS imagery ideal for application in determining regional crop area estimates. The evolution of vegetation indices has been reviewed, and it is evident that the recently developed enhanced vegetation index (EVI) has a significantly better ability to deal with ambient contamination such as soil background and atmospheric noise. In addition, EVI has an improved capability in discriminating reflectance values at higher biomass level. This makes EVI an ideal vegetation index metric in determining total, as well as specific winter crop, area estimates at a shire scale. The ability of multi-temporal MODIS imagery to determine total winter crop area estimates and discriminate between specific crops at the end of the cropping season is investigated in Chapter 4.

Chapter 3

Overview of Study Design and Protocols

"No good workman without good tools."

Thomas Fuller (1608 AD - 1661 AD)

3.1 Introduction

This chapter outlines the general research design, including description of the shire study area, data acquisition and pre-processing, the enhanced vegetation index, feature classification approaches and validation statistics. Specific methods are detailed in ensuing chapters. The frameworks and methods developed for crop area estimation in this thesis were targeted at shire, state and national levels. However, the methodology was firstly derived, applied and tested for two contiguous shires in the Darling Downs region in southeast Queensland (Chapters 4 and 5). Those methodologies were then applied and evaluated for different regions and seasons (Chapter 6).

3.2 Overview of Study Design

One of the main challenges in determining crop growth vigour or biomass from remotely-sensed images is the alignment of the acquisition date of the image with the optimal crop growth period. As discussed in section 2.5, this makes the single date approach, which is still often used, analogous to a *hit and miss* approach. Increasing the temporal frequency of image acquisition addresses this problem but can be costly, especially, in the case of fine resolution (i.e. high spatial resolution) platforms. However, with MODIS being available at a relatively small cost (usually free), composite 16-day EVI MODIS data (~250 m x 250 m pixel size) throughout the entire crop growth period was used for this research. This ensured a continuous vegetation index profile, which captured land use patterns (e.g. fallow, cropping) before and during the growing period of winter crops.

The measured 16-day aggregated MODIS EVI was used as temporal input for quantifying and understanding the crop growth *trajectory* at each pixel. Standard and advanced image processing techniques were applied to the multi-date EVI imagery. These methods included geometric corrections, image enhancement and transformation, re-projection, supervised and unsupervised classification, and classification accuracy assessment (Figure 3.1). Temporal classification methodology and multi-temporal algorithms were adapted, developed and tested at the shire level in order to determine crop area planted for different crop types (e.g. wheat, barley and chickpea) at the end of the crop growing season (Chapter 4) as well as for early-season estimates (Chapter 6).

The accuracy of four analytical approaches used to analyse the multi-temporal datasets was examined in Chapter 4. These approaches were: (i) clustering of *multi-date* MODIS EVI (MEVI) image values between day of year (DOY) 97 (i.e. early April) and DOY 305 (i.e. end of October); (ii) *Harmonic Analysis of the Time-series* (HANTS) (Jakubauskas et al. 2001, 2002) of EVI data; (iii) *principal component analysis* (PCA) (Richards et al. 1999) of the time series of EVI data; and (iv) *fitting of curves* to the multi-date MODIS imagery (CF) (Badhwar 1980; Crist et al. 1980). Images were trained and classified into specific land cover types/features (i.e. wheat, barley, chickpea, fallow, etc.) using the ground truth pixel data (also known as region of interest). The methods were assessed based on their ability to correctly classify independently selected pixels (training pixels) for each crop feature. Figure 3.1 depicts the steps involved in determining which approach had the highest accuracy in determining total area planted, as well as the best discriminative ability among crop species within a specific season.

These training pixels were collated during various field trips over a period of two years (2003 and 2004). Data collection started in the 2003 winter cropping season, which coincided with the start of the research study. Validation of aggregated crop area estimates was determined based on the degree of association with surveyed shire-scale crop area data (ABARE 2005b; ABS 2008). In addition, these approaches

were contrasted with the results obtained for the single-date EVI MODIS classifications (i.e. benchmark) to determine the best multi-temporal approach (Chapter 4). Further development and analysis were undertaken to derive predictive capability within a specific season (Chapter 5).

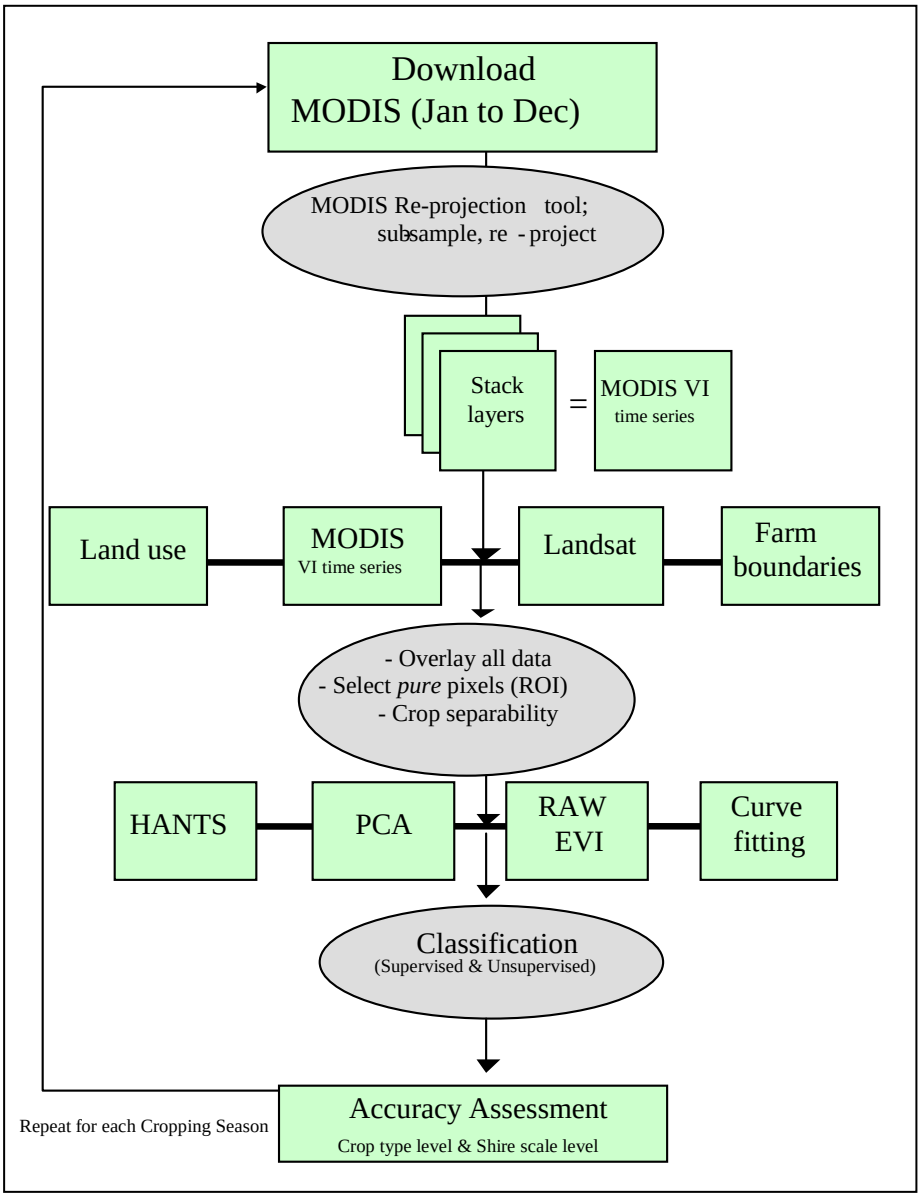

Figure 3.1: Diagram depicting the processes involved in determining the best approach for predicting shire scale winter crop area estimates.

The EVI spectral vegetation index was used to perform supervised classifications. The final classified image was subjected to rigorous accuracy assessment using the error matrix through the use of the independent selected reference pixels collated

during field trips. Aggregated shire level area estimates, derived from each approach, were contrasted with observed shire data obtained from ABARE. The process was repeated for a second crop-growing season to validate the analytical methodology determined during the first winter crop season. Determining early-season predictive capability of the multi-date approaches were undertaken for both seasons.

3.3 Study Area

The study area is located in the central Darling Downs region, ~150 km west of Brisbane, Queensland, Australia (Figure 3.2 and 3.3). The Jondaryan and Pittsworth shires (ca. 200 000 ha) were selected for this study. The typical crop area planted in a single season in both shires equates to nearly half of the total potential cropping area for winter and summer cropping seasons combined. Crop management practices are variable, and paddock sizes can range from small (~20 ha) to very large (>400 ha). Some larger paddocks might be divided into cropping strips. These strips can vary in width from 50 m to 180 m in some areas and are usually used in crop rotation practices (Figure 3.3). The practice of strip cropping was introduced as a preventative measure to counteract the potential loss of topsoil via water runoff and erosion during wet seasons.

Soils in this region are generally deep and high in clay content and therefore have very high potential soil water-holding capacities. In addition, the high variability in in-crop (i.e. May–October period) rainfall[1], combined with the advantage of deep soils and high soil moisture-storing capacity, has shaped crop-management practices in the northern region to be more dependent on starting soil moisture at sowing, than regions further south in the more winter-dominant rainfall areas (Nix 1975). The summer-dominant rainfall makes the region highly suited to summer cropping and the soil storage capacity makes it favourable for winter cropping (e.g. wheat, barley and chickpea).

The sowing of winter crops occurs between middle of April and the end of June. Rotations traditionally incorporate both winter and summer crops.

[1] Coefficients of variation for in-crop (i.e. May to October period) shire rainfall was > 46% for the period 1977 – 2004, with rainfall station data weighted within a shire based on area represented.

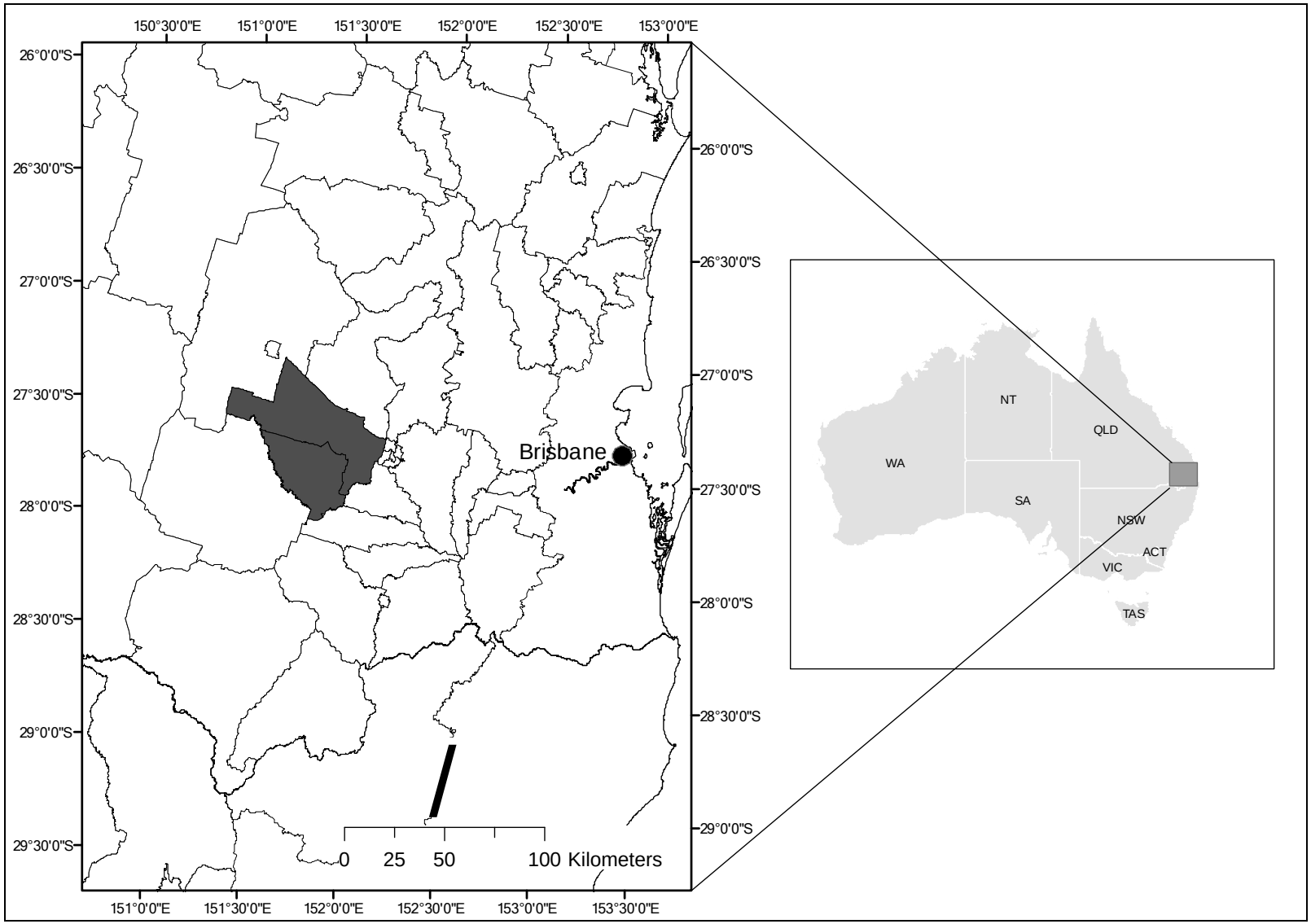

Figure 3.2: The geographical location of the Jondaryan and Pittsworth shires within the north-eastern region of Australia.

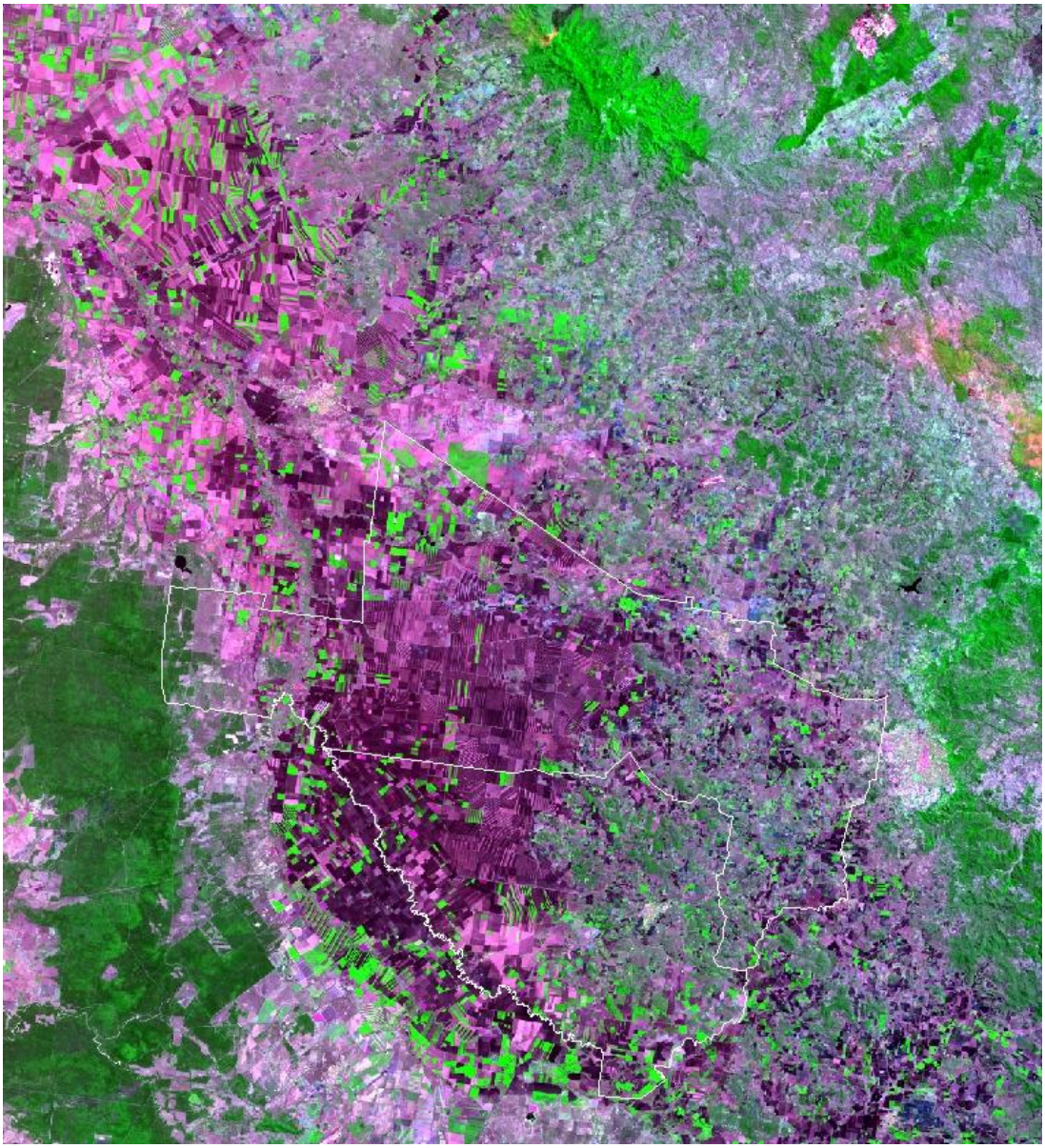

Figure 3.3: Image acquired by the Landsat 5 satellite sensor on the 14th September 2004. The image shows the land use patterns for the 2004 winter crop season for the Jondaryan and Pittsworth shires (centre of the map). Boundaries are delineated in solid white lines while healthy vegetation and forest are depicted in shades of green. Fallow and bare soils are depicted in shades of magenta (ACRES 2004).

In these shires, the land-use patterns over the last decade have been dominated by cropping (78% of total shire area in both shires), with total winter crop area planted (including wheat and barley) very similar to summer crop area planted (including sorghum and cotton) as noted in Table 2.1 (Gutteridge et al. 2002).

The spatial variability of crop yield within a specific season can be caused by either variability in rainfall amount, soil type, crop management practices, timing of rainfall, or any combination of these factors. Although variability in rainfall amount might be small across the study area in some years (e.g. 2004), there is significant variability in other factors, generating a spatially heterogeneous cropped landscape.

Table 3.1: The 10-year (1990 to 2000) average area planted for principal crops for the Pittsworth and Jondaryan shires (Gutteridge et al. 2002).

	Jondaryan		Pittsworth	
Crop group	**Hectares**	**% All crops**	**Hectares**	**% All crops**
Wheat grain	11,943	14.05	8,724	15.51
Barley grain	15,244	17.94	8,948	15.91
Fed-off, silage, hay, lucerne	8,565	10.08	4,240	7.54
Cotton irrigated & dry land	8,888	10.45	8,557	15.22
Sorghum grain	23,777	27.98	14,755	26.24
Legume grain	3,295	3.88	3,057	5.44
Oilseed	4,263	5.02	2,197	3.91
Other	187	0.23	115	0.21

This was evident in the differences in aggregated shire wheat and barley yields of 2.96 t/ha and 2.69 t/ha for the 2003 season for the Jondaryan and Pittsworth shires, respectively. Differences in aggregated shire wheat and barley yields were less during drier seasons such as 2004, with 2.52 and 2.50 t/ha for the Jondaryan and Pittsworth shires, respectively (Table 3.1) (ABARE 2005b).

3.4 Data Acquisition and Pre-processing

3.4.1 Imagery Used and Re-projection

The "MOD13Q1" MODIS satellite product, which includes the 16-day 250 m VI data, was downloaded from NASA's Earth Observing System (EOS) (http://edcims.cr.usgs.gov) website for the period 2003 to 2004. This resulted in 46 images (i.e. 23 images x 2-years) each of which had a file size of 500 megabytes. The 23 images within each season covered the period from January to December (in 16-day intervals). The NDVI and EVI MODIS products were geometrically, atmospherically and bidirectional reflectance distribution fraction (BRDF) corrected, validated and quality assured through the EOS program (Huete et al. 2002; Justice et

al. 2002). The MODIS re-projection tool (http://edcdaac.usgs.gov /datatools.asp) was used to sub-sample the *granule* to an area covering the study area. An image was created by stacking the 23 images for each season, with a GDA94 projection in ENVI software (RSI, 2005), thus creating a single image file with 23 layers. This resulted in a continuous sequence of EVI temporal values for each pixel for each cropping season.

Landsat TM 5 images (14 Sept 2004 and 16 Sept 2004), in combination with farm boundaries and the 1999 land use map (Department of Natural Resources and Water 2006) of the study area, were used to assure that selected ground truth points were *pure*, i.e. each selected pixel was near the centre of a paddock and that the pixels were mainly from large paddocks. This avoided erroneous EVI values being selected due to mixed crop canopy reflectance within a 6.25 ha pixel.

3.4.2 Vegetation Indices

The MODIS vegetation indices (VI), including NDVI and EVI, are robust spectral measures of the amount of vegetation present at the earth's surface. These indices involve transformations of the red band (R, 620-670 nanometres), near infra-red band (NIR, 841-876 nanometres) and the blue band (B, 459-479 nanometres), which were designed to enhance the vegetation signal and thus allow for more accurate contrasts of spatial and temporal variations in terrestrial photosynthetic activity (Huete et al. 2002). This index was specifically developed to optimise the vegetation signal with improved sensitivity in high biomass regions and improved vegetation monitoring through the decoupling of the canopy background signal and reduction in atmosphere influences (Figure 3.4). Given the spatial variability in land use patterns across the study area and future extrapolation of this methodology to other regions within Australia, the EVI index was utilised.

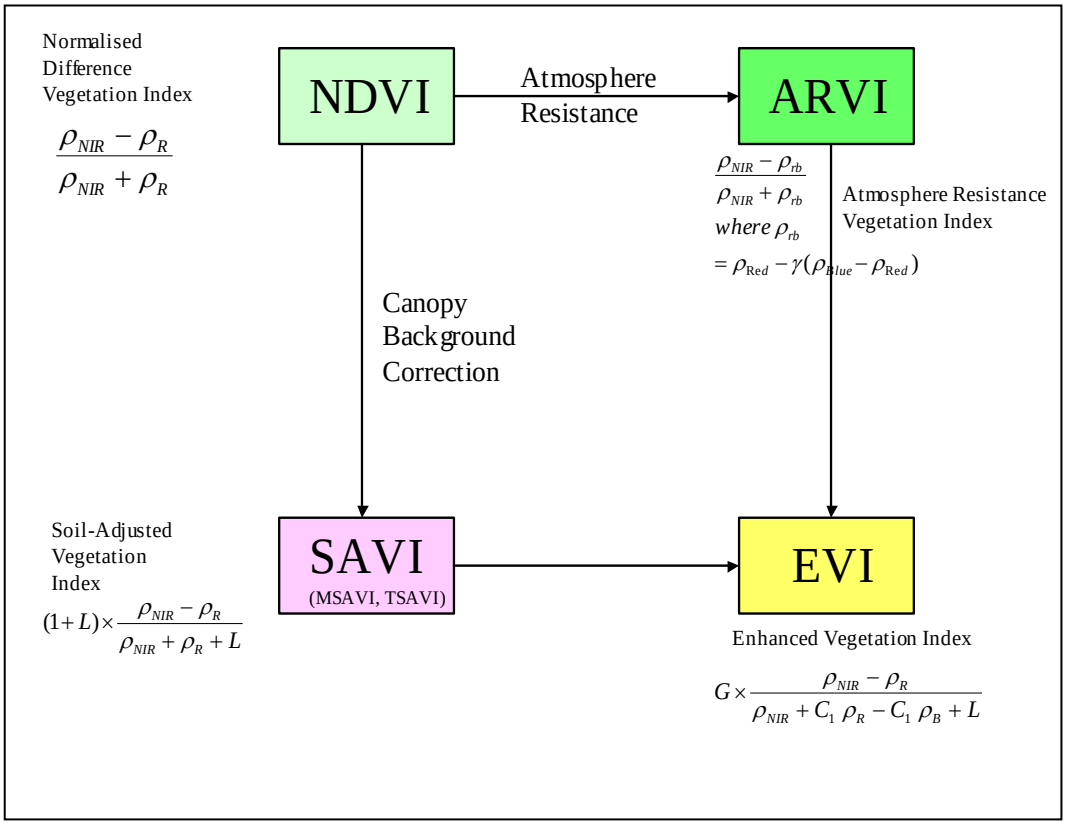

Figure 3.4: The evolution of EVI. The NDVI was adapted to address the issue of canopy background and atmospheric *noise*.

The EVI equation is computed as,

$$EVI = G \frac{\rho_{NIR} - \rho_R}{\rho_{NIR} + C_1 \rho_R - C_2 \rho_B + L} \quad [3.1]$$

where, ρ is the atmospherically corrected or partially atmospherically corrected (Rayleigh and ozone absorption) surface reflectance, L is the canopy background adjustment that addresses non-linear, differential NIR and red radiant transfer through a canopy, and C_1 and C_2 are the coefficients of the aerosol resistance term, which uses the blue band to correct for aerosol influences in the red band. The global validated coefficients are L = 1, C_1 = 6, C_2 = 7.5 and G = 2.5, which represents a gain factor (Huete et al. 1994; Huete et al. 1997).

The EVI values thus have an extended sensitivity, which makes them more likely to discriminate between canopy structure differences, such as LAI differences (Justice et al. 1998). The EVI is MODIS-specific and is based on high quality EVI values during the 16-day cycle. A filter to the data is applied, which is based on quality, cloud cover and viewing angle in order to create the high quality EVI values (Huete et al. 2002). The MODIS EVI values range from –2000 to 10000, with a scale factor of 10000, and have a fill value for missing data of -3000. On this scale, water bodies have a negative EVI value or close to zero while canopy cover has positive EVI values up to a maximum of 10000 (dense forest canopy).

3.4.3 Ground Truth and Survey Data

In order to determine the accuracy of image classification at a pixel level, it was necessary to assimilate ground truth data at various locations throughout the study region. This was done by doing 2-3 field trips during the crop-growing season for each year of interest using a handheld global positioning system (GPS) to capture data (Figures 3.5 to 3.11). The sampling strategy consisted of (i) driving on the main and secondary roads of a region as well as in some cases on farm roads, (ii) select large enough paddocks (circa >100ha) to avoid mixed canopy reflectance.

Because of the coarse pixel resolution of MODIS (i.e. 250 m x 250 m) only very large paddocks with homogenous crop canopy cover were captured. This formed the basis of the *region of interest (ROI)* within this study.

To determine the accuracy of the proposed methods (as described below) at shire scale level, it was necessary to have observed shire-scale area planted data. Since no ABS data exist for the period of the study (2003 and 2004), actual data was obtained from ABARE through their farm survey framework for each shire. However, for increased accuracy (as required in this study), a higher sampling rate was undertaken than that traditionally used in ABARE's general farm surveys (ABARE 2005b).

Figure 3.5: Inspection of a barley and wheat crop in full flowering in the Darling Downs region by A Potgieter and A Apan.

Figure 3.6: Showing different fallow practices i.e. zero till (left) and conventional tillage practice (right) for the Darling Down region during 2006.

Figure 3.7: Poor wheat crop paddock during the 2006 drought in south-east Queensland.

Figure 3.8: Winter wheat crop (left) and summer sorghum (right), both ready for harvest at the end of September 2006 north of Emerald in central Queensland. The coincidence of both a summer and a winter crop ready to be harvested is likely a result of farmers adapting to global changes e.g. warmer temperatures and less chance for frost risk (Hammer 1987; Stone et al. 1996a)

Figure 3.9: Well established chickpea crop in central Queensland during 2006.

Figure 3.10: Canopies for a barley crop (left) and a wheat crop (right) both planted at the same time in the Darling Downs region.

Figure 3.11: Irrigated chickpea crop in the Darling Downs region during 2008.

3.4.4 Crop/Feature Classification

The multi-date imagery was trained on selected ground truth data pixels for specific feature classes, while the accuracy was determined using an independent sample set of ground truth data. Ground truth data were collated during field trips undertaken in each year. Locations sampled within the study area were classified according to crop/feature classes (e.g. wheat planted early, wheat planted late, barley, fallow, etc.). All features were identified from ground truth data gathered during field trips except for the vegetation and forest classes, which were identified from the 1999 land use map. The accuracy of the feature classes acquired from the land use layer was high with a minimum mapping unit of 4 hectares (e.g. 200 m x 200 m pixel size) and a minimum attribute accuracy of 80% (Department of Natural Resources and Water 2006). The feature class selections encompass classes of main interest, i.e. wheat, barley, and chickpea.

The ability to discriminate between crops is directly related to the amount of reflectance, specifically in the NIR bandwidth, by the leaf and canopy structures (Campbell 2002). For wheat and barley, these features are very similar. The main

factor contributing to differences in canopy reflectance between wheat and barley relates to canopy architecture and density, which is a function of the number of tillers and rate of growth. Under similar environmental and climatic conditions, early tillering and growth, of barley, are nearly double that of wheat, causing more rapid crop canopy closure (Meinke et al. 1998). This is a significant feature because discriminatory ability is likely to be associated with this attribute. The different crop architecture and phenology of chickpea causes its leaf and canopy structure development to be quite different from wheat and barley (Thomas et al. 1995), thus enabling its discrimination.

Supervised classification on multiple layer inputs (i.e. multiple imagery) was performed via the traditional *maximum likelihood classification* (MLC) algorithm (Richards et al. 1999), which is available as part of the ENVI software. For classification of only one layer or band, as in the case of the PEVI approach, the more appropriate *minimum distance classifier* (MDC) method was used (Richards et al. 1999). The classifiers (i.e. MLC and MDC) were trained using *pure* pixels from the ground truth data sample set, i.e. those pixels that fall completely within a large and homogeneous paddock for a specific feature type.

3.4.5 Assessment and Validation

3.4.5.1 Separability of Crop Feature Classes

The inclusion of crop feature classes or merging of specific classes was determined using separability metrics, such as the *Jeffries-Matusita* (JM) and the *Transformed Divergence* measures. This metric constitutes the separability between two feature classes and is a function of the average distance between the spectral means of two classes. Output values range from 0 to 2.0 and indicate how well the selected feature class pairs are statistically separate. Values greater than 1.9 indicate that the feature class pairs have good separability (Richards et al. 1999).

3.4.5.2 Pixel Scale Accuracy

Pixel accuracy is derived through the calculation of the *error/confusion matrix*. This matrix is made up of rows and columns with the number of observed pixels for each of the corresponding feature classes or categories (e.g. wheat, fallow) in each

cell. The row labels or feature class names (categories) are those given by the operator, while the column names are a result of the classification procedure (Mather 1999). The diagonal cells represent the agreement between ground truth data and the classified image, while the off-diagonal cells represent the disagreement between the classified image and the ground truth data (Mather 1999; Sim et al. 2005).

Overall accuracy is calculated as the ratio of the sum of the diagonal observations to the total number of all observations included in the error matrix. Accuracy for each individual feature class is given as the ratio of the observations from a specific diagonal feature class divided by the corresponding column total for the specific class (Mather 1999). Multiplying these ratios by 100 constituted the *percent correctly classified* (PCC) metric used in this study.

The second statistic used is the *kappa coefficient* (KC). The KC is generally known as a reliability measure since it is expressed as a measure of agreement in the absence of chance (Cohen 1960; Lillesand et al. 2004). Conceptually it can be defined as

$$KC = \frac{observed\ accuracy \quad - \quad chance\ agreement}{1 \quad - \quad chance\ agreement} \qquad [3.2],$$

and is calculated as

$$KC = \frac{N\sum_{i=1}^{r} x_{ii} \quad - \sum_{i=1}^{r}(x_{i+} \times x_{+i})}{N^2 - \sum_{i=1}^{r}(x_{i+} \times x_{+i})} \qquad [3.3],$$

where

r = number of rows in the error matrix

x_{ii} = number of observations in row i and column i (on the major diagonal)

x_{i+} = total observations in row i

x_{+i} = total observations in column i

N = total number of observations included in matrix

In addition, classification results from the approaches in this thesis were tested using the *t*-test statistic of significance (Cohen 1960) and is expressed as follows:

$$Z = \frac{\left|KC_1 - KC_2\right|}{\sqrt{\text{var}_{KC_1} + \text{var}_{KC_2}}} \qquad [3.4]$$

where, var_{KC_i} is the approximate large sample variance of KC, *i* represents the KC values from any two approaches tested, and Z is the standard normal deviate.

3.4.5.3 Shire-scale Accuracy

The accuracy at the aggregated shire and regional scales was determined by comparing derived estimates of total and specific winter crop area with results of extended surveys conducted in the study region for the 2003 and 2004 seasons (ABARE 2005b). The degree of correspondence within a specific season at a shire-scale was measured by calculating the *percent error* (PE), which is defined as follows:

$$PE = \frac{observed_i - predicted_i}{observed_i} \times 100 \qquad [3.4]$$

PE is computed as the percent ratio of the difference between the remotely sensed area estimate (predicted) and the surveyed area estimate (observed) to that of the surveyed area estimate (observed) for each method for each year within a shire.

Chapter 4
Crop Area Estimates Using Multi-Date MODIS Imagery

"By a small sample we may judge of the whole piece"

Don Quixote (1605-15)

4.1 Introduction

The major constraints in the use of medium to high resolution satellite imagery for estimating crop area or yield are aligning the image date with maximum crop canopy-cover, during the crop growth period, and the high costs involved in acquiring such imagery (Section 2.2). This is further confounded by variability in climate, soil and crop practices within a specific region, making crop yield and area estimates less accurate and more tedious to compute. The use of multiple consecutive images spanning the whole calendar year (i.e. January to December) provides a means to overcome this problem. It would allow the capture of crop canopy information before, during, and after the crop growth period.

With a repeat cycle of ~2-days and a spatial resolution of 250 m x 250 m pixel size, MODIS is an ideal platform for capturing crop canopy trajectories throughout the growing season (Justice et al. 2002). This enables measurement of plant canopy response to climate, soil and management practices at a high temporal resolution resulting in a series aligned with the biophysical crop growth profile at pixel scale. Using such high temporal resolution, MODIS imagery would furthermore facilitate measuring the impact (magnitude and timing) that extreme events (e.g. heat waves, frost spells) might have on plant health and ensuing plant canopy architecture. As discussed earlier in Sections 2.2 and 2.3, multi-date low resolution MODIS imagery have been shown to have similar or better accuracy than that of a single-date high resolution Landsat TM when used in determining shire or regional scale crop canopy attributes (Lobell et al. 2003; Price 2003).

The main objective of this chapter was to determine the utility of multi-temporal MODIS satellite imagery in estimating the area of specific and total winter crops at

the end of the cropping season. This was achieved by utilising and comparing four multivariate approaches to analyse time series of enhanced vegetation index (EVI) temporal profiles throughout the cropping period.

4.2 Methods

4.2.1 Overview

The accuracy of four analytical approaches to the multi-temporal data was examined: (i) clustering of *multi-date* MODIS EVI (MEVI) image values, (ii) *Harmonic Analysis of the Time-series* (HANTS) of EVI data, (iii) *principal component analysis* (PCA) of the time series of EVI data, and (iv) *fitting of curves* to the multi-date MODIS imagery (CF). The methods were assessed based on their ability to correctly classify image pixels based on field observations over a period of 2-years (2003 and 2004) and the degree of association with surveyed shire-scale crop area data (ABARE 2005b).

The first multi-temporal approach involves classifying EVI values from the consecutive MODIS imagery during the main winter crop growth period, which spans from early April to late October in this region (see next section for detail). This constitutes the MEVI approach.

The second approach, HANTS, is based on decomposing the time series of EVI data from the imagery into harmonic components or terms. In this study, for each pixel within the study area, the full annual time series encompassing 23 x 16-day MODIS EVI composites in each year was decomposed using a discrete *Fast Fourier Transform* algorithm (DFFT) (Bloomfield 2000) into a set of *amplitude* and *phase* terms at different temporal frequencies. This technique was applied through the use of the Harmonic Analysis of Time Series (HANTS) software (Verhoef et al. 1996).

The third approach, used a traditional multivariate analysis - the *principal component analysis* (PCA) - to reduce the multidimensional complexity in the temporal EVI profile. In this study, principal component analysis (Campbell 2002; Davis 2002; Richards et al. 1999) was used to reduce the EVI time series at each

pixel from the full annual 23-image sequence into a smaller set of transformed variables or principal components (PC), which explained 90% or more of the temporal variability in the series.

Fourthly, two *curve fitting* (CF) methods were used to decompose the full annual EVI time series into a vector of distribution attributes, that related to crop phenology characteristics such as the green-up, flowering, and crop senescence periods, and are intrinsic parameters in defining the shape of the EVI curve. Two different curve fitting procedures were investigated to determine their ability to discriminate between winter crops.

Finally, a benchmark (or control) classification approach was included. This was derived from a single date EVI MODIS image acquired around the peak of the average EVI profile. In the analysis, peak EVI (PEVI) was selected at day-of-year (DOY) 225. The EVI image from this date captures crop canopy growth during the last 2-weeks of September, which usually coincides with flowering and thus peak green-up of the winter crop planted in Queensland. Vegetation index values from this period is known to be highly correlated to final crop yield or total crop biomass (Boken et al. 2002; Smith et al. 1995).

Pixel and shire-scale accuracies were assessed using data for two selected shires in the Darling Downs region, Queensland, Australia (Figure 4.1). For each analysis method, pixel classification was trained based on ground truth data and its accuracy tested on an independent set of ground truth data and on survey data at aggregated shire scale as discussed in Chapter 3.

4.2.2 Decomposition of a Multi-temporal Crop Profile into a Vector of Crop Specific Variables

4.2.2.1 Single-date EVI Value – *The Benchmark*

For any new multi-temporal approach to be useful, it has to perform better than the classification derived from a single-date image. This constitutes *efficacy* as referred to later on in this study.

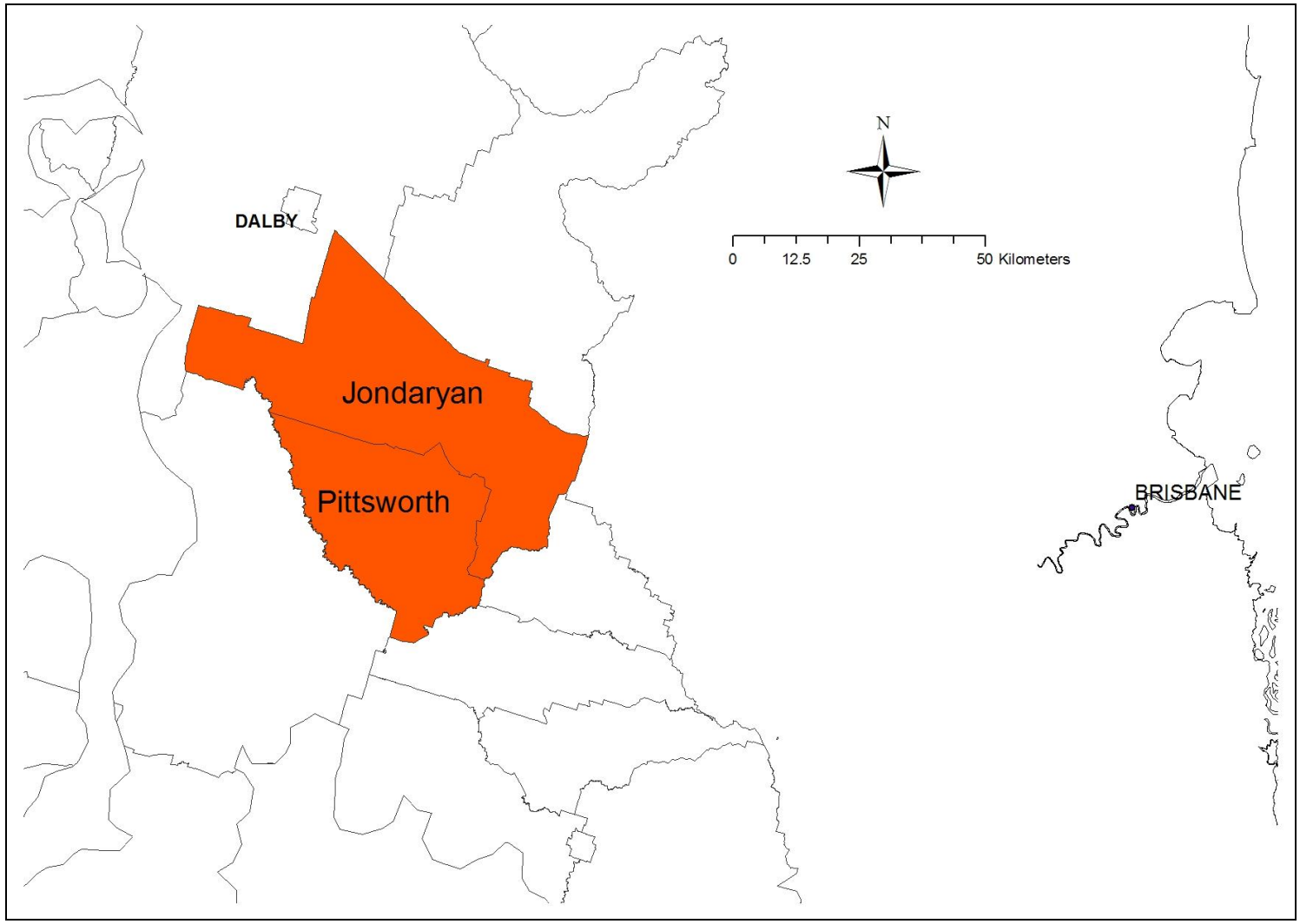

Figure 4.1: Location of the Jondaryan and Pittsworth shires (orange colour) within the southern Queensland, Australia. Shire boundaries are given by black solid lines.

Remote sensing-deduced vegetation index values before or around flowering (usually the period of maximum greenness) have been shown to be highly correlated with end-of-season crop biomass (Aase et al. 1981) and crop yield (Badhwar et al. 1982a). Hence in this study, the image at the date of average peak EVI for wheat and barley within a specific season was used. This method, from here on, is referred to as *peak* EVI (PEVI) and is the *benchmark*, against which all other multi-temporal approaches are contrasted. The image date chosen (around DOY 225) was close to the time of maximum LAI (thus peak green-up) and flowering dates of wheat and barley as shown in Figure 4.2. Associations derived from this single-date approach constituted the *benchmark* accuracy.

4.2.2.2 Multi-date EVI Approach

Traditionally, winter crop is grown from April to October in the north eastern shires of Australia (Figure 4.2).

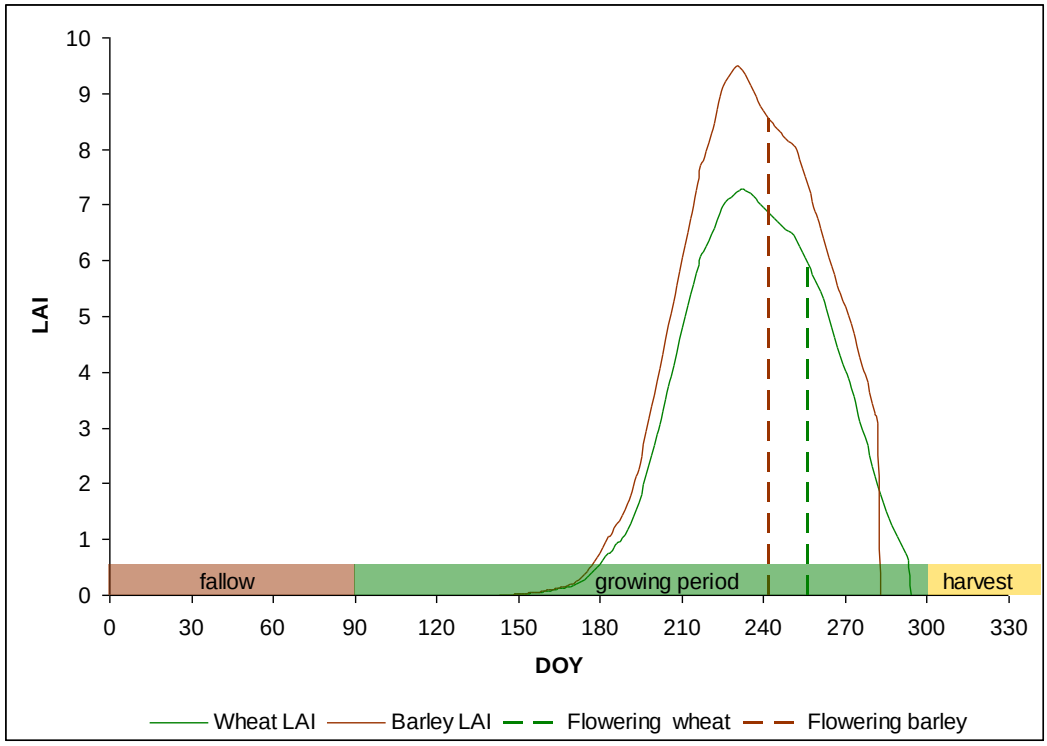

Figure 4.2: Leaf area index (LAI) growth curves for wheat and barley planted on the same day. LAI was simulated using APSIM (Keating et al. 2003) with the same initial soil, plant density parameters and medium growing cultivars. The crop growth period is traditionally from April (DOY 91) to end of October (DOY 304).

It is therefore apt to select imagery during this period to assess the ability of multi-date MODIS imagery to discriminate among winter crops within the crop growth period. This approach uses the EVI values from each 16-day MODIS image between day of year (DOY) 97 (early April) and DOY 305 (end of October) and is abbreviated as MEVI from here onward.

4.2.2.3 Harmonic Analysis of EVI Time-series

Harmonic analysis is based on decomposing a complex sequence of equivalently distributed imagery data through time into harmonic components or terms. In this study, the time series for a single year encompassing 23 x 16-day MODIS EVI composites was decomposed using a discrete Fast Fourier Transform algorithm (DFFT) (Bloomfield 2000) into a set of amplitude and phase components at different temporal frequencies for each pixel within the study area. This technique was applied through the use of the Harmonic Analysis of Time Series (HANTS) software (Verhoef et al. 1996). The Harmonic (*Fourier*) analysis allows a complex curve to be expressed as the sum of a series of *cosine* waves (terms) and an *additive* term, and is given as follows:

$$f(x) = c_0 + \sum c_n \cos\left(\frac{2\pi n x}{L} - \phi_n\right) \qquad [4.1]$$

where, c_0 is the additive term or 0^{th} harmonic term and represents the average of the time series, c_n is the amplitude of the n^{th} harmonic term, ϕ_n is the phase or peak of the n^{th} harmonic term, and L represents the number of 16-day images within the analysis period (Davis 2002).

Each wave is defined by a unique *amplitude* and *phase angle* (Figure 3.3a), where the amplitude is half the height of a wave and the phase angle (or simply phase) defines the offset between the origin and the peak of the wave over the range 0 to 2π. The number of complete cycles completed by a wave is represented by a harmonic term (e.g. second term completes 2-cycles, third term completes 3-cycles etc.) (Figure 4.3b). Adding successive harmonic terms will reproduce the original complex time series (Figure 4.3c) and each component term accounts for a percentage of the total

variance in the original time series data set (similar to principal component analysis) (Jakubauskas et al. 2002).

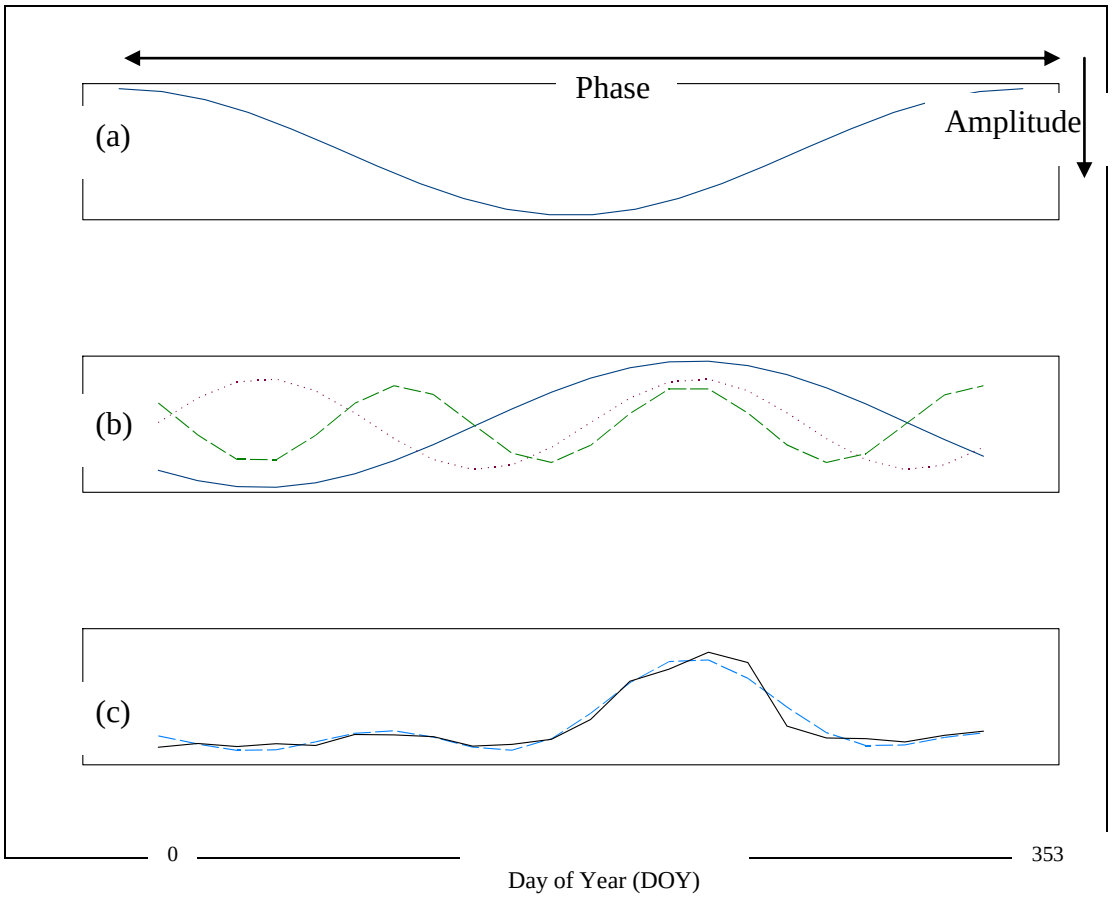

Figure 4.3: (a) Simple cosine curve depicting the amplitude and phase, (b) Curves for harmonic terms 1, 2 and 3 (including the additive term), and (c) Aggregated curve (blue stippled line) produced from addition of first 3 harmonics in Figure 3(b). Black solid line depicts the original EVI time series data.

Fourier analysis has been used previously in digital remote sensing in filtering single date imagery (Richards et al. 1999) for spatial analysis, and more recently it has been used in characterising crop phenology using multi-temporal AVHRR imagery (Jakubauskas et al. 2001, 2002). Although a recent study has contrasted Fourier analysis versus wavelet transforms using MODIS to determine crop phenology of rice in Japan (Sakamoto et al. 2005), no specific studies could be found on the use of multi-temporal MODIS imagery for determining winter crop area estimates for Australia. The development of the HANTS methodology resulted in a more reliable and rigorous way of deriving frequency, amplitude and phase values

than using the traditional Fourier analysis approach (Verhoef et al. 1996). HANTS outputs, such as the *additive* term, *amplitude* and *phase* for each wave up to the 5th harmonic, were extracted on a per pixel basis for the MODIS EVI temporal profile for each year.

4.2.2.4 Principal Component Analysis of EVI Time-series

The third method utilised traditional multivariate analysis to reduce the multidimensional complexity in the temporal EVI profile. In this study, the *principal component analysis* (PCA) (Campbell 2002; Davis 2002; Richards et al. 1999) was used to reduce the sequence of data from the 23-image stack into new transformed variables or principal components (PC). Each PC contributes to the total temporal variance at each pixel, and the final number of PCs selected was based on the variance level at which the contribution of consecutive PC variances was negligible. The linear transformed combination is of the form (Campbell 2002):

$$Y = c_1X_1 + c_2X_2 + c_3X_3 + ... c_nX_n \quad [2]$$

where $X_1,...X_n$ represents the original EVI pixel values measured at each of the n-image acquisition dates, c_i are the associated coefficients or component loadings applied individually to the respective EVI values, that combine to generate Y, which represents the transformed value for the pixel.

A forward rotational PCA algorithm within the ENVI remote sensing software (ITT 2008) was conducted on the EVI data to determine the major underlying *orthogonal* factors representing the temporal variability within the sequence of imagery of each pixel. The incremental proportion of total variance explained was used to determine the number of orthogonal factors to be retained as subsequent PCs contributed less to the overall variance of the original imagery (Richards et al. 1999). Although most of the total variation is explained by the first few principal components, the discriminative ability was further enhanced by omitting PCs that did not significantly increase class separability between winter crops within ENVI (Richards et al. 1999). The final selected rotated principal components contributed significantly to discriminating between crop types and represented the main

determinants (including crop type, canopy health, crop phenology etc.) of spatial variability among the stacked image pixels. The time series of PC scores, which are the transformed image values, represent the temporal variation associated with each principal component.

4.2.2.5 Curve Fitting to EVI Time-series

The final method employed was the fitting of a curve shape function to the temporal profile of EVI values for each pixel. Firstly, an approach, which proved to be successful in predicting the growth stages of small grains (Badhwar 1984; Sharma et al. 1989) and the feature classification of corn and soybeans (Badhwar et al. 1982a) was applied. The aim of applying such a *curve fitting* approach for the purposes of this study was to reduce the multi-dimensional complexity of the multi-date EVI values, which captures the crop growth features like green-up rate (e.g. vegetative stage) and greenness decline (e.g. ripening stage). Such features are intrinsic to the shape of the growth curve and have proved to be significant in discriminating between the crop profile shapes of wheat or barley (Crist et al. 1980) and corn or soybean (Badhwar et al. 1982a) using Landsat imagery at a 30 m x 30 m pixel resolution. The success of this approach is dependent on ability of the greenness measure to discriminate between soil greenness and canopy greenness. From here onward, this approach will be referred to as CF1.

MODIS EVI is an ideal candidate for the application of such a curve fitting approach because of its (i) high temporal acquisition cycle and (ii) EVI's improved capability in capturing canopy structure and vigour, while being less sensitive to soil background noise and atmospheric contamination. A model, which is a function of crop and condition specific parameters (α, β) and timing of crop emergence (t) was fitted. The model form of CF1 is given as follows:

$$\rho(t) = \begin{cases} \rho(t) = \rho; & t < t_0 \\ \rho_s(t_0)(t/t_0)^{\alpha} \exp[\beta(t_0{}^2 + t^2)]; & t \geq t_0 \end{cases} \qquad [4.3]$$

where $\rho(t)$ is the greenness value (measured through the EVI value) at any time t during the growing cycle of the crop, $\rho_s(t_0)$ is the soil greenness value at and before

emergence date t_0, which can be estimated from the original data for each pixel, while α and β are crop specific constants (Badhwar 1980; Badhwar et al. 1981; Sharma et al. 1989).

The crop emergence date t_0 was determined as the time at which crop greenness values were greater than soil greenness values. It was derived as the point at which the first derivative of the EVI curve changed from negative to positive. Or if this condition was not met, the point at which the second derivative changed from negative to positive was used to identify the start of the crop green-up period. The timing of crop emergence was limited to not earlier than 15th March and not later than 30 days before t_{max}. This will account for late planted crops (e.g. double cropping after a summer crop) and fluctuation, in EVI values around anthesis (maximum canopy growth), caused by factors such as water-induced stress. If none of the above criteria was met, crop emergence was assumed to be during the last week in March (Sakamoto et al. 2005).

The end of the growing cycle usually coincides with the harvest date but can also be due to crop failure (e.g. caused by terminal stress) or when haying occurs due to management practices. The end of the crop cycle was determined by estimating the time at which the first derivative changed from positive to negative, or if this criterion was not met, the time at which the second derivative of the EVI curve changed from negative to positive (adapted from (Sakamoto et al. 2005). The first incident occurring before peak greenness in both criteria was used. The end of the crop cycle could not be earlier than 30-days after the maximum greenness (i.e. anthesis). If none of these criteria were met, the cessation time was set as the last week in November. The use of two discriminative points (first and second derivatives) for determining the start and end of the crop cycle will enable the detection of small changes in crop growth, especially during these periods when crop reflectance is known to be small in comparison with reflectance during other phenological periods. Furthermore, limiting the beginning and end of the growing period to ±30 days around peak greenness ensures a crop growth length of at least 5 images (including time of peak greenness).

This approach captures the period in which there is a significant increase in canopy cover, which reflects the start of the growing season; and the period when crop growth has completely stopped, which reflects the end of the growing period. The soil greenness value is the EVI value at time t_0. The starting values for the shape parameters α and β were calculated through differentiation and assuming that peak greenness (or maximum canopy cover) occurred at the point where the first derivative $\frac{d\rho}{dt} = 0$. Solving this differential equation resulted in an estimate of the time at which maximum ground cover was reached ($t_{\max}$), and is given by the equation (see Appendix A for detail):

$$t_{\max} = \sqrt{\frac{\alpha}{2\beta}} \qquad [4.4].$$

Substituting equation 4.4 back into equation 3 for $t = t_{\max}$, initial estimates for α [5] and β [6] were defined as:

$$\alpha = \frac{\log(\rho_{\max})}{\log\left[\frac{t_{\max}}{t_0}\right] + \left[\frac{t_0^2 + t_{\max}^2}{2t_{\max}^2}\right]} \qquad [4.5]$$

$$\beta = \frac{\alpha}{2t_{\max}^2} \qquad [4.6]$$

where $\rho_{\max}$ represents the maximum greenness at time $t_{\max}$ (Figure 4.4).

The second curve fitting approach (CF2), was a piece-wise sigmoidal curve fitting procedure, which is forced through the peak of the EVI profile and is a function of the vegetative rate (i.e. green-up) and the senescence rate (i.e. greenness decline) around this maximum greenness point (Figure 4.4). This is calculated as follows (Crist et al. 1980):

$$\rho(t) = \begin{cases} a * \exp^{b_1 (t - t_\rho)^2} . & t < t_\rho \\ a * \exp^{b_2 (t - t_\rho)^2} . & t >= t_\rho \end{cases} \quad [4.7]$$

Peak greenness is a prominent feature of all crop growth profiles and is therefore much easier to calculate than time of crop emergence. In this model, a represents the peak or maximum greenness value, at time t_{max}, which ensures continuity between the two segments in Equation [4.7]. The model has two crop specific parameters b_1 and b_2, which quantify the green-up and greenness decline or senescence rates (Crist et al. 1980).

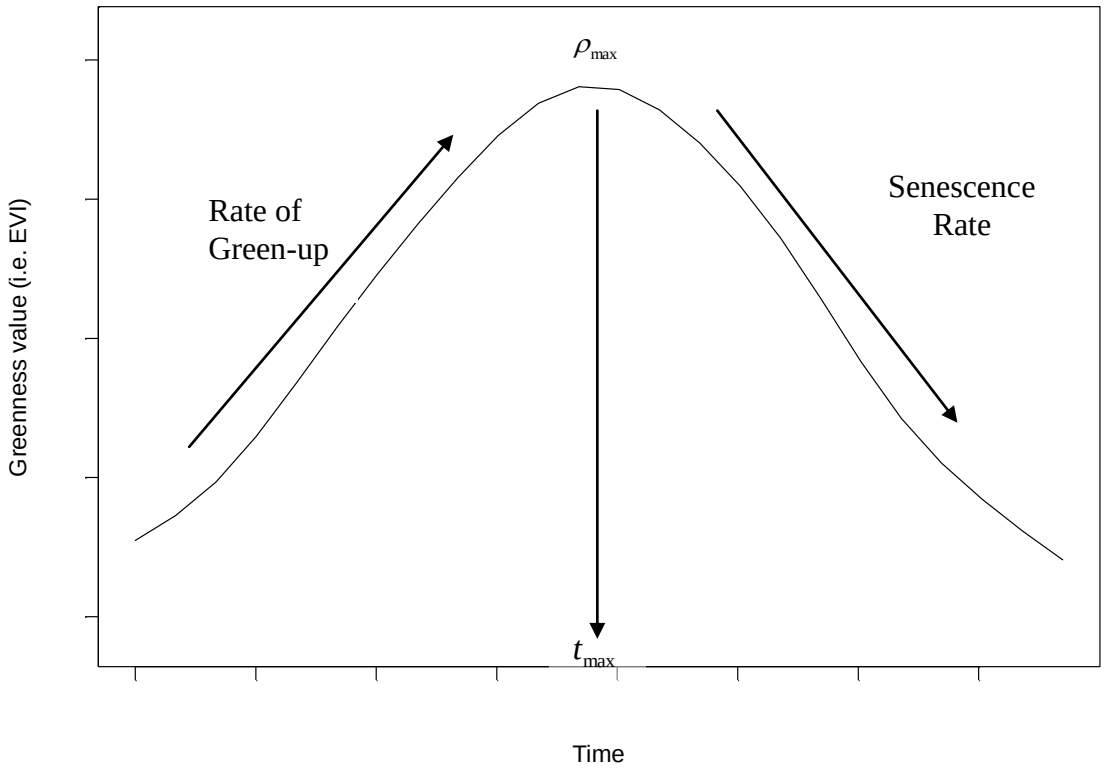

Figure 4.4: Curve depicting the profile features of rate of green-up and rate of senescence rate for EVI values during a crop growth cycle (adapted from Crist and Malila, 1980).

4.2.2.6 Crop/image Feature Classes and Pixel Classification

For each analysis method, the multi-date image classification was trained on selected ground truth data and its accuracy validated using an independent set of ground truth data. Ground truth data was collated during field trips undertaken in each year. In total, 1,302 (wheat = 252; barley = 96; chickpea = 36; other = 918) and 1,365 (wheat = 243; barley = 45; chickpea = 9; other = 1,068) sampling points were selected from the ground truth data for the 2003 and 2004 season, respectively. These points were used to train the classification on. Locations sampled within the study area were classified according to crop/feature classes (i.e. wheat planted early, wheat planted late, barley, etc.) given in Table 4.1. The multi-date image was classified using *supervised* classification via the *maximum likelihood* classification algorithm, while the single-date image was classified using the *minimum distance classifier* (MDC) algorithm (as discussed in Section 3.9).

Table 4.1: Feature classes and data collating method used in the first level of classification for 2003 and 2004 seasons. *(Double cropped represents cropping in consecutive summer and winter seasons; fed off is traditionally hayed or grazed; late plantings are usually plantings occurring at the end or after the close of the traditional wheat planting window; na - represents no available data.)*

Feature Class	2003	2004
Barley	Field trip	Field trip
Barley double cropped	Field trip	na
Barley fed off	Field trip	na
Chickpeas	Field trip	Field trip
Grazing & natural vegetation	Field trip & Land use map	Field trip & Land use map
Natural forest	Land use map	Land use map
Production forest	Land use map	Land use map
Stubble & soil	Field trip	Field trip
Wheat	Field trip	Field trip
Wheat late plantings	Field trip	na

4.2.2.7 Independent Validation and Accuracy Assessment

The accuracy of classification was assessed by contrasting the classified image (as described in the previous section) with independent randomly selected sub-samples from the ground truthing collated through field trips. This was done to reduce artificial accuracy, i.e. minimise classification bias. In total, 316 and 344 random ground truth pixels were selected. These points were independent from the training sampling points and used to calculate the image classification accuracy for the 2003 and 2004 seasons, respectively. This represented approximately 25% of the total

ground truth samples in each year. The statistic *percent correctly classified* (PCC) was used (Section 3.4.5) to determine the overall and between-crop accuracies for each classification approach (Richards and Jia 1999). Statistical significance was tested using the *z*-values as derived in Section 3.4.5. The results allowed inferences about the comparative discriminatory ability of the multi-temporal decomposition approaches used in this study.

The accuracy at the aggregate shire-scale was determined by comparing the derived estimates of total and specific winter crop area with the results of extended farm surveys conducted in the study region for the 2003 and 2004 seasons (ABARE 2005). The degree of correspondence within a specific season at a shire-scale was measured by calculating the *percent error* (PE). The average of the absolute PE was calculated to determine the accuracy across seasons and shires (MAPE).

4.3 Results and Discussion

4.3.1 Feature Class Selection

Feature class selection was determined by calculating the separability between feature classes using the layer stacked imagery data from May to October. The separability between class means of wheat and wheat late plantings was only moderate (JM = 1.6, Section 3.4.5 for detail on the JM measure) when the distance measures were compared (see Appendix B, Table B1 for detail). Hence, all wheat samples were merged into one feature class with 252 and 243 sampling points in 2003 and 2004, respectively. Although good separability was evident between barley and barley double cropped (JM = 1.99) and barley and barley fed off (JM = 1.99), both barley double cropped and barley fed-off were excluded from the final classification. Both these classes represent less common practice and resulted in few sampling points for ground truthing. This resulted in 96 and 45 sampling points for barley in 2003 and 2004, respectively. Very few chickpea sites were observed and selected in either season, mainly because very little area was sown to chickpea, especially in the 2004 season. Although, this is likely to result in unrealistically high PCC (e.g. 100%), and therefore should be interpreted with caution when applied to a real world scenario, such crop types (e.g. very small sample sizes) where kept as a separate

category to determine its separability from the other crop types rather than specific accuracy.

The average EVI crop profiles measured at 16-day intervals through the calendar year for each of the feature class ground truth samples for the 2003 and 2004 (Figure 4.5a and b) seasons showed a range of distinctive features. Overall, all classes had much higher average EVI crop values for the 2003 season than for the 2004 season. This was expected as the 2004 season was classified as an El Niño year (Potgieter et al. 2005a), which resulted in below average rainfall within the study area for that season (Figure 4.6).

The winter crop temporal EVI profiles for wheat (filled and open square symbols), barley (filled and open triangles) and chickpea (open circle) are uni-modal with a peak around DOY 225 (image 15) for both seasons. Barley double cropped (solid line) and barley fed-off (triangle) have bi-modal EVI profile trajectories showing a peak in early summer (e.g. before image 1) and a peak at DOY 225. This suggested that pixels belonging to those classes had been cropped during the preceding summer. The stubble-and-soil (x – symbol, Figure 4.5) temporal EVI profile shows a uni-modal trajectory with the peak at DOY 33 (image 3, early February) and low values during the winter period. Natural forest (filled diamond), production forest (open diamond) and grazing (brown circle) have flat average EVI crop profiles throughout the calendar year.

Although there are few sampling points for chickpea (36 in 2003 and 9 in 2004) it was retained as a separate class to assess the discriminatory ability of the proposed methods between the two main winter crops (i.e. wheat and barley), and the less important winter crop (i.e. chickpea). The separability between barley and chickpea is larger than that between wheat and chickpea. For simplicity, all other features (e.g. vegetation, natural forest, bare fallow etc.) are combined to form one feature class with 918 and 1068 sampling points for both seasons. In total, four main feature classes (i.e. wheat, barley, chickpea and non-cropping) were formed for further analysis and classification.

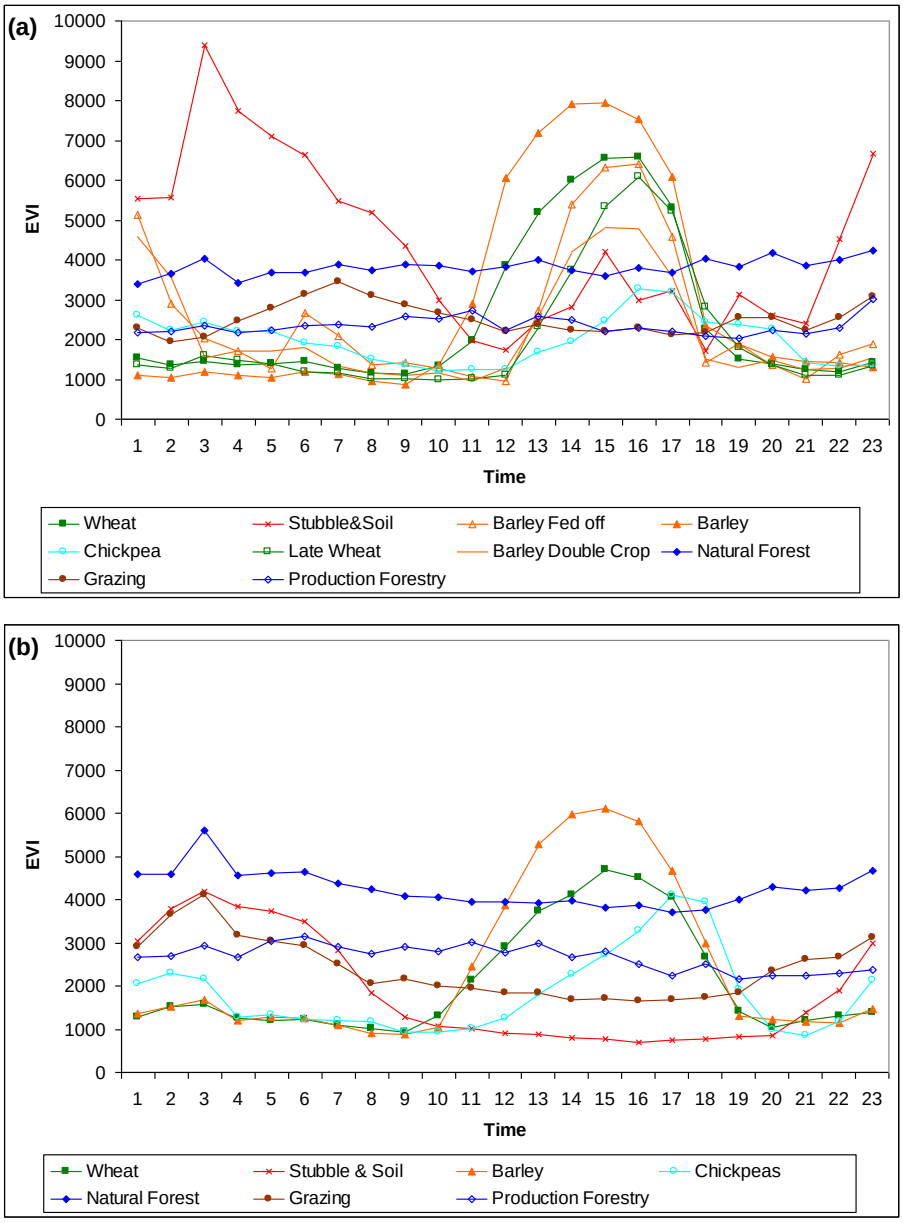

Figure 4.5: Average EVI crop profiles of all feature classes for the (a) 2003 and (b) 2004 seasons.

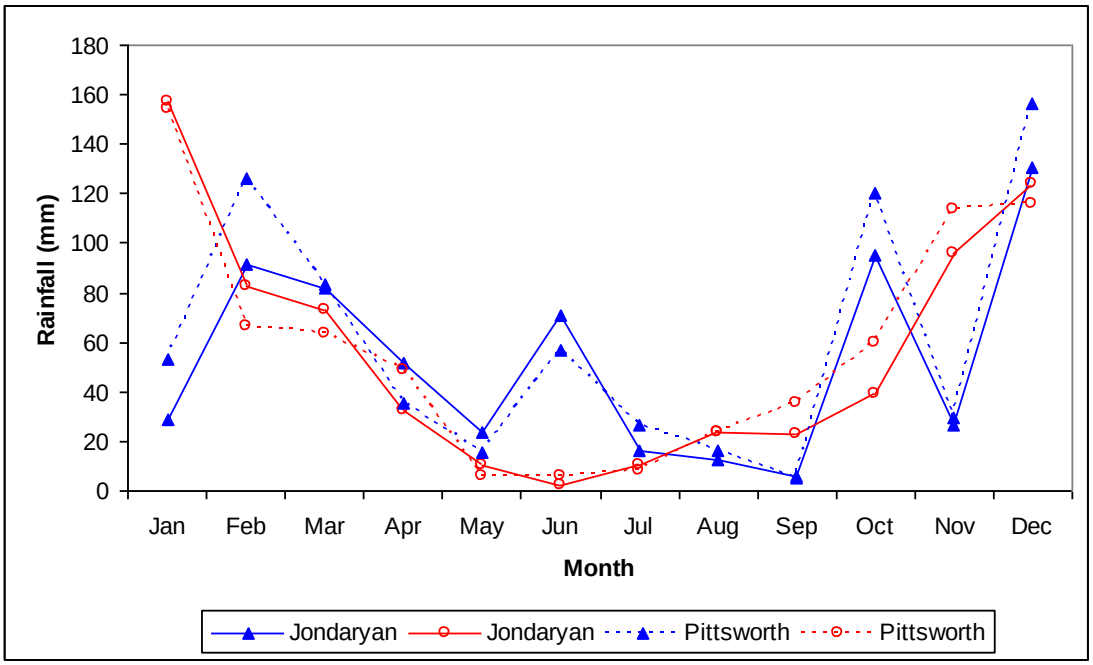

Figure 4.6: Average aggregated monthly rainfall for Jondaryan (solid triangle) and Pittsworth (open circle) for the 2003 (blue) and 2004 (red) seasons. Note the much lower rainfall during the planting months of May to July for 2004 compared to the higher values specifically during June for 2003. This resulted in much less planting opportunities and therefore small sampling numbers for 2004 than that of 2003.

4.3.2 Temporal Crop EVI Profiles

The average temporal EVI profiles throughout each growing season showed distinct differences for wheat, barley and chickpea (Figure 4.7a and b). The profiles represent the temporal plant canopy responses to soil, plant and water regime combinations within the study area for each season. The differences among crops in slope of the spectral profiles from emergence (i.e. EVI >2000 after image 9) to anthesis (i.e. flowering around peak EVI at image 15) are more evident during 2003 than in 2004. The period from crop emergence to anthesis is known as the green-up period while the period after anthesis to crop harvest is known as the senescence period. The temporal profiles for barley and wheat suggest a very similar planting date as crop emergence is around the same time in both seasons for both shires (Figure 4.7a and b). The average crop emergence date of chickpea is at least 2 months after that of wheat and barley, which suggests a later average planting date in both seasons within the study area and/or a slower rate of green-up, which is what happens

with chickpea. This result concurs with ABARE statistics, which indicate an average planting period of May to June during both years for the two shires (ABARE 2005b).

The average EVI temporal profile for barley was higher than that of wheat in both seasons. In addition, the green-up rate for barley was quicker than that of wheat in both seasons, which is mainly a consequence of the greater (i.e. nearly double) tillering and early leaf area growth rate of barley (Meinke et al. 1998). There are, however, some instances where the green-up rate of wheat is similar to that of barley. This can possibly be ascribed to differences in soil temperatures, increased nitrogen levels or no water limitations (e.g. irrigated) (Meinke et al. 1997). Conversely, chickpea has much lower average EVI values than that of wheat and barley in both seasons. Chickpea has very small leaves and a much slower rate of canopy development than the cereal crops (Thomas et al. 1995).

The differences in average peak EVI values were not as great in the 2004 season. Although there is some overlap in the temporal profile distributions between crops, the differences in the shapes of the profiles for wheat, barley and chickpea were apparent in both seasons. The much lower EVI peaks for wheat and barley during the 2004 season were mainly caused by the significantly below average rainfall recorded during 2004 (http://www.bom.gov.au) that resulted in a reduction in biomass and crop growth.

During periods of severe moisture stress such as in 2004, the reflectance of crops in the visible (blue, green and red) bands increases (due to less absorption by chlorophyll), while reflectance in the near-infrared band decreases, resulting in smaller band ratio values and ensuing EVI values. The presumed overlaps in EVI temporal profile distributions for wheat, barley and chickpea indicate that there will be some confusion in separating these crops. Consequently, some pixels will likely be wrongly classified.

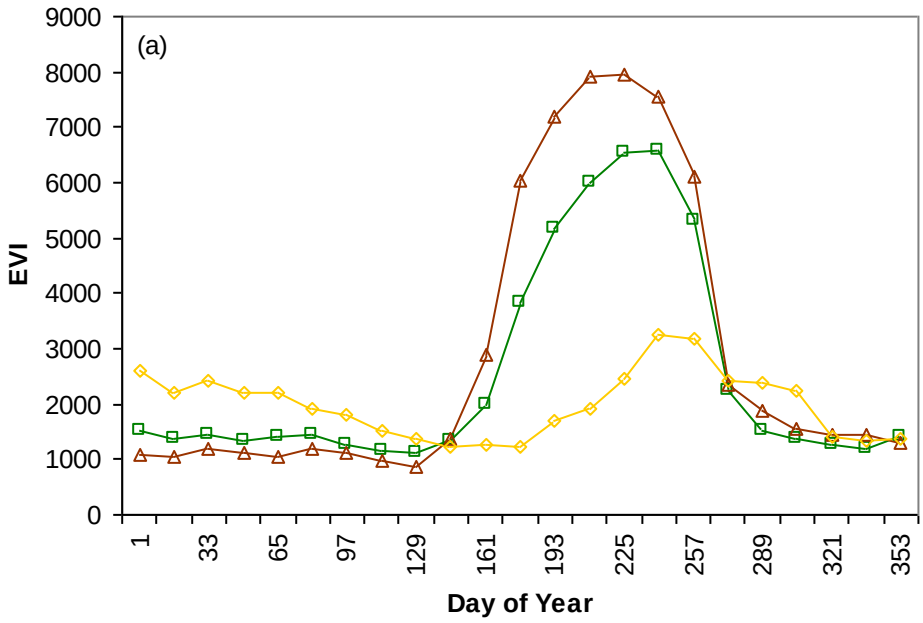

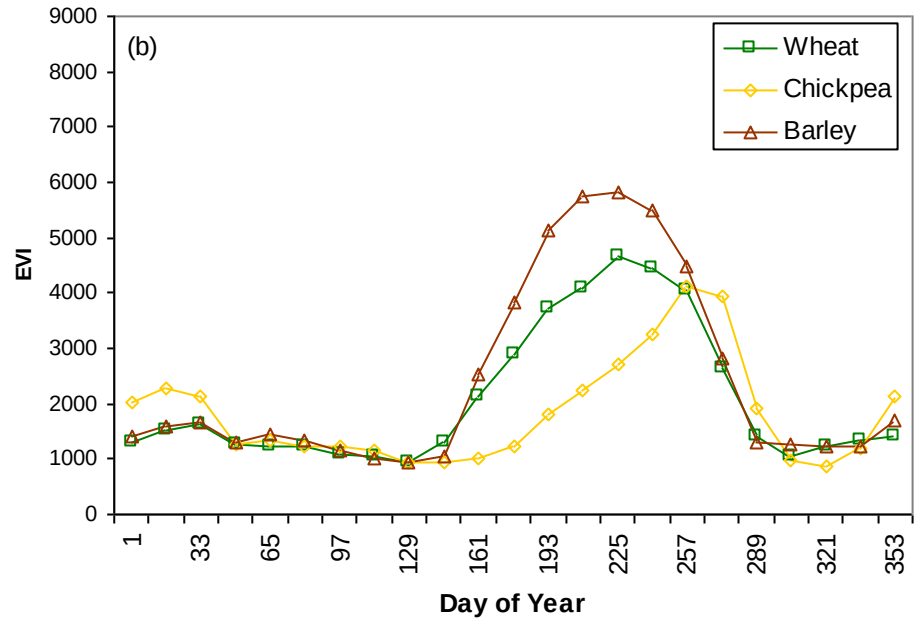

Figure 4.7: Average temporal EVI profile of the main winter crops throughout the growing season for wheat (green, square), barley (brown, triangle) and chickpea (yellow, diamond) for the 2003 winter crop season (a) and the 2004 winter crop season (b).

4.3.3 Image Classification

Once each method was trained on ground truth data, the classification of all pixels on the image was done by applying the standard maximum likelihood classifier for the multi date EVI data (from DOY 97 to 305) and the derived PCA and HANTS data. The minimum distance classifier was used to classify the *benchmark* peak EVI approach at DOY 225 (PEVI). For the PCA approach, 11 principal components were retained, which explained more than 90% of the total temporal variability in the time series derived from the 23-images (Figure 4.8). The factor scores (reconstructed from the derived principal components) for wheat, barley and chickpea showed diminishing differences beyond the first few PCs, while the scores were very similar for the last few PCs. The retention of 11 PCs resulted in explaining 90% of the total temporal variability of the 23-image series, and a reduction of more than 50% in input data.

For the HANTS approach, three harmonic terms (each term consists of a phase and amplitude value) and the zero amplitude were used in the final classification. This included the EVI average (0^{th} harmonic), first, second and third harmonics (amplitude and phase for each harmonic). The three harmonics, including the average, explained more than 90% of the temporal variability, similar to the results obtained for the PCA approach. Figure 4.9 shows the classified images using the PEVI (a, b) and HANTS (c, d) approaches for the 2003 and the 2004 seasons, respectively. In general, the two seasons differ significantly in the amount of total winter crops planted. Independent of the classification approach, more winter crop is evident in 2003 than in 2004.

This relates mainly to the poor rainfall recorded during 2004 and the lack of sowing opportunities during the winter crop planting window (i.e. May to June) as mentioned earlier. The PEVI approach overestimated the chickpea occurrence in both seasons with much of the non-cropping pixels classified as chickpea in both 2003 and 2004 (a, b). The HANTS approach shows substantially better discriminatory ability between wheat, barley, chickpea and non-cropping than the PEVI approach in both seasons.

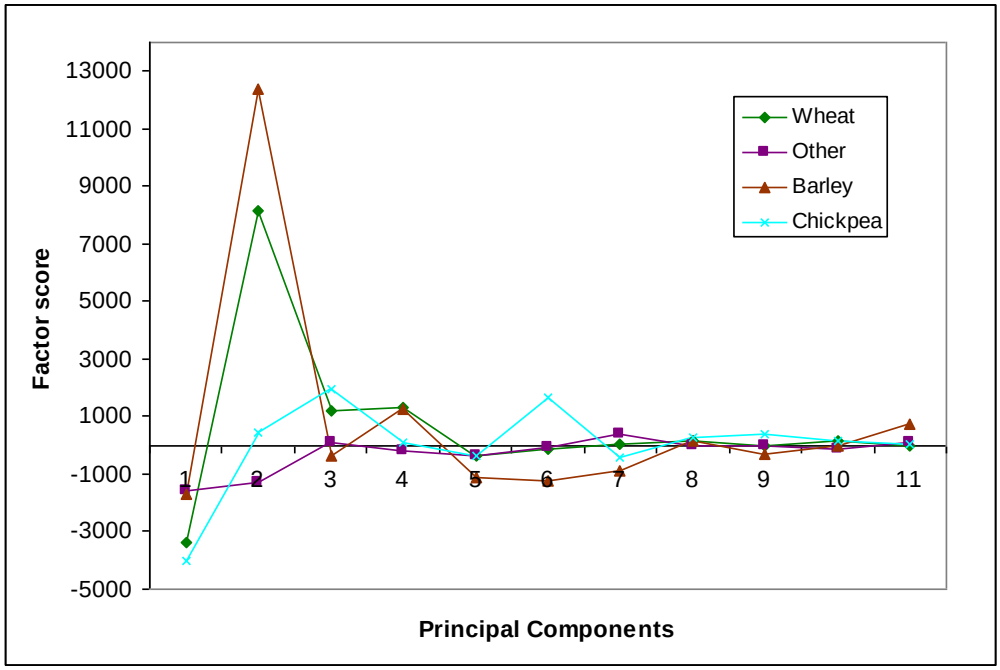

Figure 4.8: Factor scores of the first 11 principal components on the time-series of EVI data.

This is due to the ability of the HANTS method to capture measured differences in the temporal EVI trajectories throughout the growing period, while the single-date approach captures likely crop canopy differences at a single point in time, making it less accurate at a pixel scale (Table 4.2). Similar results to that for the HANTS approach were found for the MEVI, PCA and CF data reduction methods (see Appendix C, Figures C1(a, b), C2(a, b), C3(a, b), C4(a, b)). However, the CF approaches had less discriminatory ability between non-crop and chickpea and non-crop and wheat, resulting in an overclassification of chickpea and an underclassification of non-cropping areas (see Appendix C, Figures C3 (a, b) and C4 (a, b)).

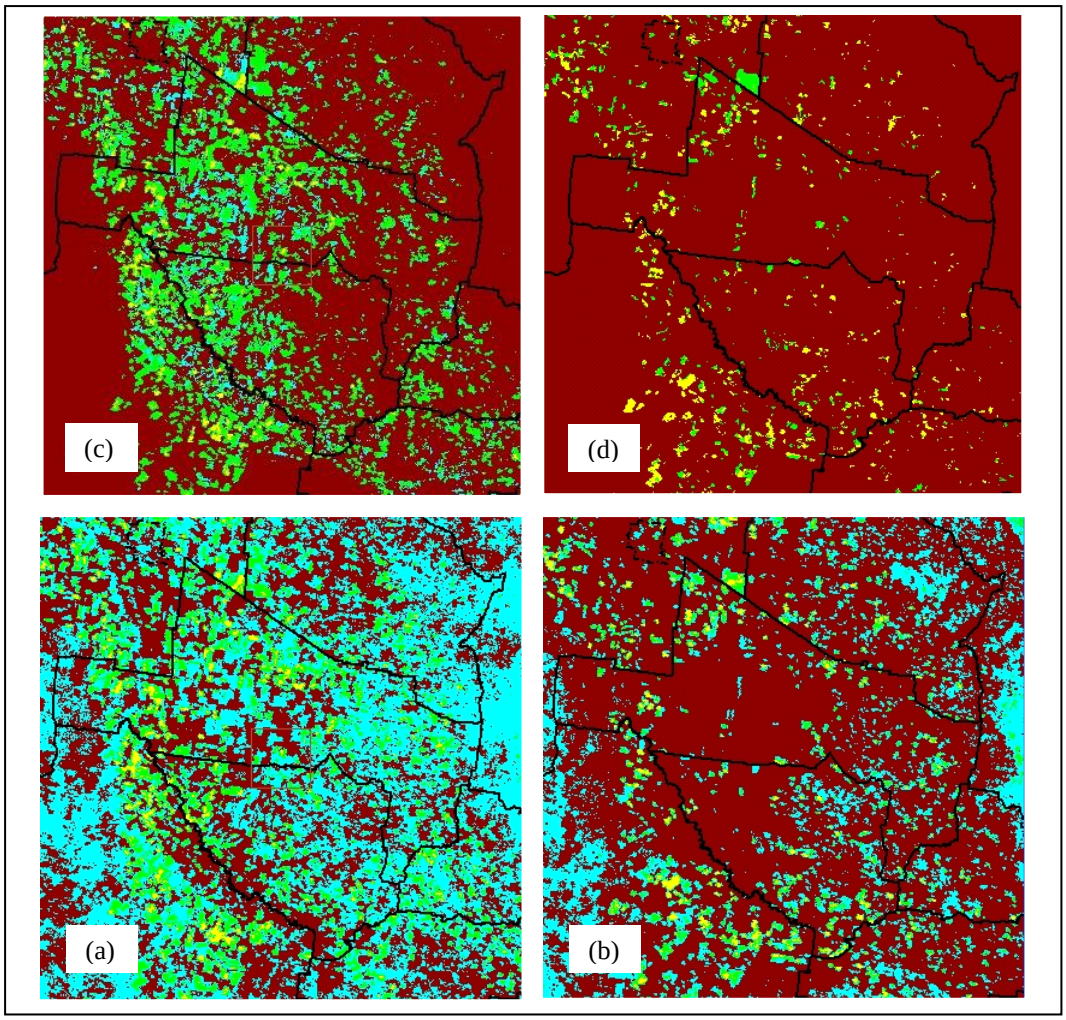

Figure 4.9: Classified images using the PEVI classification for the 2003 and 2004 seasons (a, b) and classified images using the HANTS approach for 2003 and 2004 seasons (c, d). Wheat is coloured in green, barley in yellow, chickpea in cyan and non crop (e.g. natural and production forest, vegetation, stubble, bare soil, etc.) in brown.

4.3.4 Independent Validation and Accuracy Assessment

The percent of pixels correctly classified (PCC) for each of the four methods is given in Table 4.2. The overall accuracy among the methods ranged from only 56% to 98%. The single date approach (PEVI) had most pixels incorrectly classified with an overall accuracy of 56% and 61% for 2003 and 2004 seasons, respectively. Most of this error came from misclassifying wheat and non-cropping classes during both seasons.

The overall PCC values for the multi-temporal approaches are all very high with the highest accuracies produced in 2004. All multi-temporal approaches classified the

non-cropping pixels correctly (100%). This is significant because it means that such approaches can be effectively used to discriminate crops from non-cropping land use areas in future studies. All multi-temporal approaches achieved much higher overall accuracy compared with the single date method for both the 2003 and 2004 seasons. This is mainly a result of the better ability in discriminating between wheat, barley, chickpea and non-cropping in both seasons by utilising the temporal canopy signatures derived from the entire crop growth period. Although, the CF approaches have the highest ability to discriminate wheat from the other two winter crops for the 2004 season, their ability to separate non-cropping areas from cropping areas was the lowest of the multi-temporal methods. This will probably limit the use of such CF approaches when determining winter crop area estimates at a regional scale.

Table 4.2: Accuracy (%) across all classes (i.e. wheat, barley, chickpea and non-cropping) for each image classification method for the 2003 and 2004 seasons. ***Kappa coefficients*** **of overall accuracies are in closed brackets.**

	Percent Correctly Classified (%)				
2003	**Overall**	**Wheat**	**Barley**	**Chickpea**	**Non-cropping**
Single-date	56	57	90	80	51
Multi-date	94	76	76	93	100
PCA	93	60	86	93	100
HANTS	93	56	95	86	100
CF1	87	58	90	100	92
CF2	85	58	86	100	89
2004					
Single-date	61 (0.36)	74	85	100	56
Multi-date	97 (0.93)	89	100	25	100
PCA	98 (0.96)	92	93	0	100
HANTS	95 (0.86)	85	71	0	100
CF1	95 (0.86)	92	71	50	97
CF2	92 (0.80)	89	100	25	93

When comparing the *kappa coefficients* (KC) of each approach with one another in both seasons (Table 4.3), the PEVI approach was significantly different from all multi-temporal approaches while the time-series approaches in general showed no significant differences in their KC values from each other. This strengthens the superior ability of multi-date approaches to that of a single image approach in estimating crop area.

Table 4.3: Z statistic for testing the hypothesis that the *kappa coefficient* (KC) values of one classification approach differs from another. Values of $Z \geq 1.96$ are significant at the 95% level *(highlighted in bold)*.

2003	PEVI	MEVI	PCA	HANTS	CF1	CF2
Single date (PEVI)		**10.27**	**9.16**	**8.92**	**6.72**	**5.95**
Multi date (MEVI)			0.81	0.97	**2.78**	**3.46**
PCA				0.16	1.96	**2.63**
HANTS					1.79	**2.46**
CF1						0.66
CF2						
2004	**PEVI**	**MEVI**	**PCA**	**HANTS**	**CF1**	**CF2**
Single date (PEVI)		**11.39**	**12.60**	**9.27**	**9.30**	**7.69**
Multi date (MEVI)			0.99	1.49	1.55	**2.79**
PCA				2.40	**2.48**	**3.68**
HANTS					0.04	1.27
CF1						1.25
CF2						

Table 4.4 shows the comparison of total winter crop area estimates (i.e. wheat, barley and chickpea) to surveyed shire-scale area estimates as collated by ABARE through their annual farm surveys (Section 3.). It should be noted that the ABARE farm survey data showed root mean square errors of between 20 to 60% during these two years for the study area (ABARE 2005b). So any estimates within this range should be regarded as "correct". This emphasises the imperativeness of investigating the ability of remote sensing approaches in determining crop area estimates that are near-real time, objective, accurate and cost effective.

The HANTS method produced the smallest error (i.e. highest accuracy) for total winter crop estimates within the Jondaryan shire for both seasons (Table 4.4). It has an average mean absolute percent error (MAPE) of 26% (PE of 18% and -35% for each season, respectively). The MAPE across both shires was 27%. All other methods showed MAPE greater than 63% for the Jondaryan shire and 97% across both shires for both seasons (data not shown). The single-date method had the smallest PE for total wheat area, estimated at 5% and 9% for the Jondaryan shire for 2003 and 2004, respectively (Table 4.4). This result, however, is fortuitous because of the very poor overall and within-class pixel accuracies (Table 4.2). This artificial accuracy of the single-date approach is further confirmed by the very poor total winter crop shire-scale accuracy within 2003 (182%), 2004 (268%) and overall (225%) (Table 4.5). It

is likely that most of the error for the PEVI approach came from the misclassification of non-cropping areas as crops, and vice versa, explained by the low pixel scale accuracy of non-cropping and particularly wheat. This caused a fortuitous bias correction, which resulted in small PE values by classifying non-cropping areas as mainly chickpea for Jondaryan shire in both seasons. The high accuracy for the single-date wheat classification at an aggregated shire scale is therefore spurious because of compensating errors when aggregating. Further, the single-date approach must confront the issue of the best date to use, which cannot be readily determined until after the season. Therefore the single date approach cannot be recommended as an acceptable method in determining winter crop area at a regional scale.

The CF mutli-temporal approaches, i.e. CF1 and CF2, show MAPE of 129% and 159%, respectively for the Jondaryan shire across both seasons. The MAPE for the CF1 and CF2 methods are 197% and 233%, respectively for total winter crop estimates across shires and seasons (Table 4.5). This low accuracy is likely related to the poorer ability such approaches have in discriminating between non-crop and other crops (specifically wheat and chickpea) (Table 4.2). This misclassification of non-cropping areas as either wheat or chickpea can be addressed by introducing another layer of information, which delineates the cropping from the non-cropping areas. This can be done using either the latest land use map showing non-cropping classes or the broad non-cropping class derived from the multi-temporal approaches i.e. HANTS, MEVI or PCA. Employing an approach of masking the cropped area when using the CF methods, could improve the accuracy of winter crop area estimates at a regional scale.

The HANTS approach showed moderate to high within-season accuracy for total winter crop area estimates, with MAPE values of 33% and 21% for the 2003 and 2004 seasons, respectively (Table 4.5). All multi-temporal approaches showed significantly higher accuracy at the aggregated shire-scale level within and across seasons compared to the accuracy of the single-date approach. The HANTS method had the highest overall accuracy (27%) when determining total winter crop area estimates across seasons within the study area.

Table 4.4: Total shire-scale area estimates for each classification method and ABARE surveyed (actual) data for all feature classes (i.e. wheat, barley, chickpea and other) for the 2003 and 2004 seasons within the Jondaryan shire. The accuracy is given in the percentage error (PE (%)) column as the difference between the estimated and actual. *(Estimate and Actual values to the nearest 100)*

Jondaryan	2003 Season			2004 Season		
Single Date	**Estimate**	**Actual**	**PE (%)**	**Estimate**	**Actual**	**PE (%)**
Wheat	28,500	27,300	5	5,900	5,400	9
Barley	4,500	10,700	-58	1,800	2,700	-32
Chickpea	87,100	7,700	1023	18,000	1,600	993
Winter Crop	120,200	45,900	162	25,800	9,800	163
Multi-date	**Estimate**	**Actual**	**PE (%)**	**Estimate**	**Actual**	**PE (%)**
Wheat	74,500	27,300	172	12,400	5,400	128
Barley	2,800	10,700	-73	7,200	2,700	167
Chickpea	14,300	7,700	85	0	1,600	-100
Winter Crop	91,600	45,900	100	19,600	9,800	101
PCA	**Estimate**	**Actual**	**PE (%)**	**Estimate**	**Actual**	**PE (%)**
Wheat	72,500	27,300	165	8,900	5,400	65
Barley	2,800	10,700	-73	5,500	2,700	103
Chickpea	6,800	7,700	-11	0	1,600	-100
Winter Crop	82,300	45,900	79	14,400	9,800	48
HANTS	**Estimate**	**Actual**	**PE (%)**	**Estimate**	**Actual**	**PE (%)**
Wheat	37,800	27,300	38	4,900	5,400	-10
Barley	2,600	10,700	-75	1,500	2,700	-44
Chickpea	13,800	7,700	78	0	1,600	-100
Winter Crop	54,300	45,900	18	6,400	9,800	-35
CF1	**Estimate**	**Actual**	**PE (%)**	**Estimate**	**Actual**	**PE (%)**
Wheat	48,100	27,300	76	16,400	5,400	202
Barley	4,500	10,700	-58	6,600	2,700	146
Chickpea	49,600	7,700	540	100	1,600	-94
Winter Crop	102,400	45,900	123	23,200	9,800	137
CF2	**Estimate**	**Actual**	**PE (%)**	**Estimate**	**Actual**	**PE (%)**
Wheat	35,300	27,300	29	21,300	5,400	293
Barley	5,200	10,700	-51	5,900	2,700	118
Chickpea	64,100	7,700	727	1,200	1,600	-25
Winter Crop	104,700	45,900	128	28,500	9,800	191

Table 4.5: Aggregate mean absolute percent error (MAPE%) for each of the remote sensing analysis approaches for both shires in the study area for each of the two years (2003 and 2004) and over both years (All).

	2003	2004	All
	Single Date		
Wheat	4	37	20
Barley	63	21	42
Chickpea	2645	1971	2308
Winter Crop	182	268	225
	Multi Date		
Wheat	175	201	188
Barley	76	240	158
Chickpea	509	100	304
Winter Crop	128	172	150
	PCA		
Wheat	165	116	140
Barley	68	145	106
Chickpea	171	100	135
Winter Crop	99	95	97
HANTS	**HANTS**		
Wheat	43	15	29
Barley	81	33	57
Chickpea	366	100	233
Winter Crop	33	21	27
	CF1		
Wheat	78	329	203
Barley	64	187	126
Chickpea	1941	86	1013
Winter Crop	168	226	197
	CF2		
Wheat	31	454	242
Barley	55	159	107
Chickpea	2250	47	1149
Winter Crop	166	300	233

Although the HANTS approach showed overall pixel accuracy similar to that of the other multi-temporal approaches, it had the smallest error across both seasons for determining total winter crop area and is thus likely to be more reliable than any of the other analysis approaches. The shire-scale accuracy of HANTS can be further increased by including ground truth data on areas that have been double cropped with barley (i.e. cropping barley immediately after a summer crop). The degree of discrimination between wheat and barley relates to how similar/dissimilar the temporal profile trajectories are within the cropping window (Figure 4.2). The

discriminatory ability of the HANTS approach, at shire scale, seemed to be weaker during the wetter seasons of 2003 and stronger during the drier season of 2004 (Figure 4.6). This weaker discriminatory ability in the more heavily cropped wet year is likely to be related to an increase in spatial variability of rainfall and soil types, as well as more spatially variable crop management practices, such as plant density rates, fertilizer application rates or a combination of these. During 2004, which was classified as an El Niño year, there was less classification error (at pixel scale) between wheat and barley crops, resulting in more accurate area estimates at the shire-scale. In addition, almost all of the area that could be planted was planted to wheat and barley, which resulted in very few ground truth fields for chickpea during the 2004 season. This restricted the capacity to develop good discriminatory ability for chickpea. Thus, future studies will need more or stratified ground truth sampling points to enable rigorous discriminatory ability of chickpea from other winter crops.

Discrepancies between the error determined at pixel scale (PCC) and the error determined at shire/regional scale (PE) are mainly due to the ability or lack thereof of the sampling data at pixel and surveyed data at shire scale to be representative of all likely temporal EVI crop canopy profile possibilities when extrapolated across a large area. If such complete enumeration can be assumed at pixel scale, then a likely way forward is to revise the total area estimates for crop types using the output from the confusion matrix (Congalton et al. 2009). However, this was not within the scope of this study.

The temporal profile trajectory represents the crop life cycle (e.g. emergence, anthesis, maturity, etc.) at a specific location and incorporates canopy reflectance responses to immediate environmental conditions (i.e. temperature, soil, moisture, light, etc.). Thus, applying these multi-temporal approaches to other geographical regions with soils and climate regimes not captured within the study area needs further investigation.

4.4 Conclusion

Using the temporal profile of EVI data throughout the growing period has shown enhanced efficacy over the traditional single image approach in classifying crops at the pixel as well as the shire scale. Although the single date approach showed poor accuracy at the pixel scale, it showed high accuracy at the shire scale for determining wheat and barley area estimates. This occurred due to a fortuitous compensation of misclassification errors when aggregating from pixel to shire-scale for the single-date approach. Most of the contradiction in accuracy of the single date approach can likely be attributed to the pass-over date of the satellite image, which highly depends on how close the acquisition date of the image is to the flowering date of the crop. The closer these two dates are to each other, the better the discriminative ability between crops might be. This, however, was not always the case for the single-date classification as suggested by the contradicting accuracies at the different spatial scales.

All multi-temporal classification approaches showed high accuracy during both seasons, when comparing the classified imagery with independent ground truth samples at pixel scale. The overall discriminative ability of these methods was higher during the drier season of 2004, than during the wetter season of 2003. This year effect was also evident for discrimination between wheat and barley. The discrimination of chickpea was moderate during the 2003 season, while the 2004 season showed poor classification of chickpea crops at a pixel scale. This was mainly a result of the small sample size for chickpea during the 2004 season. The HANTS, MEVI and PCA methods showed high accuracy in classifying non-cropped.

Extrapolating these methods to a shire/regional-scale showed high accuracy in estimating crop area, with the HANTS method being most accurate across regions and seasons. In contrast, the curve fitting procedures (CF1 and CF2) had the lowest accuracy for shire scale winter crop estimates. This could be mainly attributed to their inability to correctly classify non-cropped areas, resulting in an overestimation of wheat and chickpea crops across regions and seasons.

The multi-temporal approaches showed significant ability to discriminate between winter crops and estimate their area at a shire scale at the end of the cropping season.

This is well in advance of any estimates disseminated by ABS or ABARE through their surveys, which traditionally are published 1 to 2 years after the cropping season. This multi-temporal remote sensing (MTRS) approach also improves the spatial detail with which crop statistics are captured. End-of-season crop area estimates for wheat and barley are important to industry for generating accurate production estimates to aid transport logistics and marketing decisions. The value of this multi-temporal remote sensing approach would be enhanced if accurate crop area estimates could be produced earlier in the season. This issue was addressed in Chapter 5.

Chapter 5

Early-season Crop Area Estimates for Winter Crops in NE Australia using MODIS Satellite Imagery

"Prediction is very difficult, especially about the future"

Niels Bohr (1885 - 1962)

5.1 Introduction

In Chapter 4, the efficacy of using different multi-temporal approaches to estimate end-of-season crop area was investigated. Appreciably high accuracy was found at pixel and shire-scales. However, there remains a need within the grains industry (e.g. feed grain, fertilizer companies etc.) to have crop production estimates well in advance of harvest. Although end-of-season area estimates are used to balance final supply and demand figures, such information lacks the ability to assist industry in tactical decision-making processes (e.g. forward buying or selling). This is mainly a result of the lateness of the end-of-season crop area estimates.

Accuracy and timing of the forecast are important aspects in assisting decision-makers to adjust their management decisions accordingly. Forecasts are valuable when a change in decision (e.g. forward buying) leads to a desirable change in the outcome (e.g. increased profitability), which can allow the decision-maker to move from a point of passive acceptance of the forecast, to a point of active response, to the forecast (Hammer et al. 2001). The earlier the forecast is issued, even with less accuracy than end-of-season estimates (Potgieter et al. 2003), the more time the decision-maker has to respond to the likely impact of the forecast. The issue of "*how early and with what accuracy*" crop area estimates can be determined using the multi-temporal approach derived in Chapter 4 is investigated in this chapter.

Various studies have investigated the relationships between accumulated monthly vegetation indices (e.g. NDVI), biomass/LAI through the growing period, and ensuing final end-of-season crop yield or production (Dubey et al. 1991; Labus et al.

2002; Tucker et al. 1980, 1981; Zang et al. 2005). These studies found that the period around peak anthesis was highly correlated with final production figures at different spatial scales, thus enabling the prediction of crop yield/production between flowering and harvest with varying degrees of accuracy. These approaches mainly applied complex multiple regression metrics between accumulated NDVI over various crop growth stages, crop growth curve parameters and final yield figures. Such approaches can only be used at the end of the crop growth season to determine crop area. They did not focus specifically on early-season crop area estimates. Thus, the purpose of this study was to develop and evaluate a relatively simple but accurate method for estimating crop area well before harvest for winter crops in north-eastern (NE) Australia.

5.2 Methods

5.2.1 Overview

The contiguous Pittsworth and Jondaryan shires, as described in Sections 3.3 and 4.2.1 (Figure 4.2), were selected as the study region for deriving and validating an approach to early-season crop area estimation. A simple metric was developed and used to determine the rate of crop green-up before flowering. This metric is a surrogate for measuring winter crop canopy vigour or growth. The pixel classification image was trained, based on ground truth data, and its accuracy tested on an independent set of ground truth data and on survey data at aggregated shire scale as discussed in Chapter 3. This was done for both the 2003 and 2004 seasons. In this chapter, the temporal extrapolability of the methodology was tested by comparing estimates for the 2000, 2001 and 2002 winter cropping seasons with actual shire crop area information. The *percent correctly classified* (PCC) and *kappa coefficients* (KC) (Section 3.4.5) were used to assess the accuracy at pixel scale, while shire scale accuracy was assessed through linear regression.

5.2.2 Early-season Metric

Crop canopy vigour was estimated using a relatively simple measure based on the summation of the differential EVI between three consecutive MODIS images, acquired at 16-day intervals, and derived at monthly periods from April (DOY 97) to September (DOY 257). The summation of the EVI differences is referred to here as

$\sum \Delta EVI$. The green-up period (crop emergence to peak EVI) of all main feature classes (Chapter 4, Figure 4.5 & 4.6) occurred over at least five (~80 to 90 days) consecutive 16-day images, which makes three images a suitable number in capturing the crop growth vigour during green-up. Three different $\sum \Delta EVI$ thresholds, ranging from 250 to 750 at increments of 250 (i.e. >250, >500 and >750) were examined for discriminatory ability. These thresholds were selected because values smaller than 250 indicate a relatively flat profile and are likely to be classified as non-cropping, while large values (i.e. >1000) are likely to exclude crop types like chickpea and water stressed wheat crops, especially during drier seasons like 2004 (Chapter 4, Figure 4.5 a & b). The screening of the thresholds was done using the band math functionality in ENVI and applying the following equation:

$$(b_1\text{-}b_2) + (b_2\text{-}b_3) > T \qquad [5.1]$$

where, T represent the threshold cut-off and $b_{(1)}$, $b_{(2)}$ and $b_{(3)}$ represent the appropriate MODIS images. These differential EVI threshold cut-offs are abbreviated as $\sum \Delta EVI_{T250}$, $\sum \Delta EVI_{T500}$ and $\sum \Delta EVI_{T750}$ from here on. This resulted in six images (at monthly periods from April to September) for each threshold for 2003 and 2004 seasons (Figure 5.1).

The ability to discriminate among wheat, barley and chickpea crops increases through the growing season, with the poorest ability around sowing and crop emergence (April to June) and the best ability at the end of the crop growth period (November/December) (Figure 5.2). The discriminative ability improves significantly from around the time of flowering (August/September). A similar result occurred for the 2004 season (data not shown). Because of the poor ability to discriminate crops (i.e. separating wheat from barley) before flowering, only early-season estimates for combined total winter crop area were attempted.

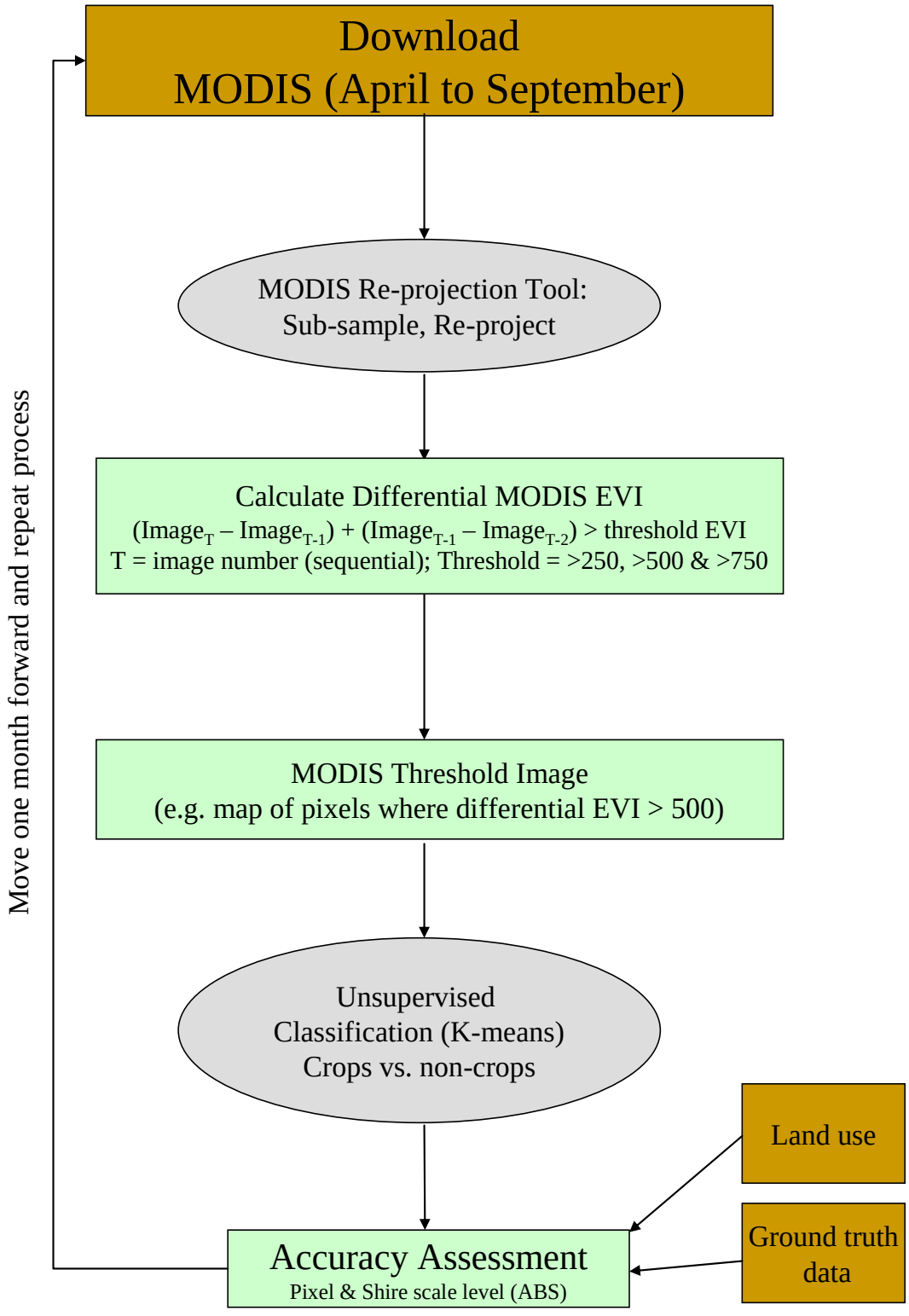

Figure 5.1: Diagram showing the steps involved in determining the early-season crop area estimates for the 2003 and 2004 seasons.

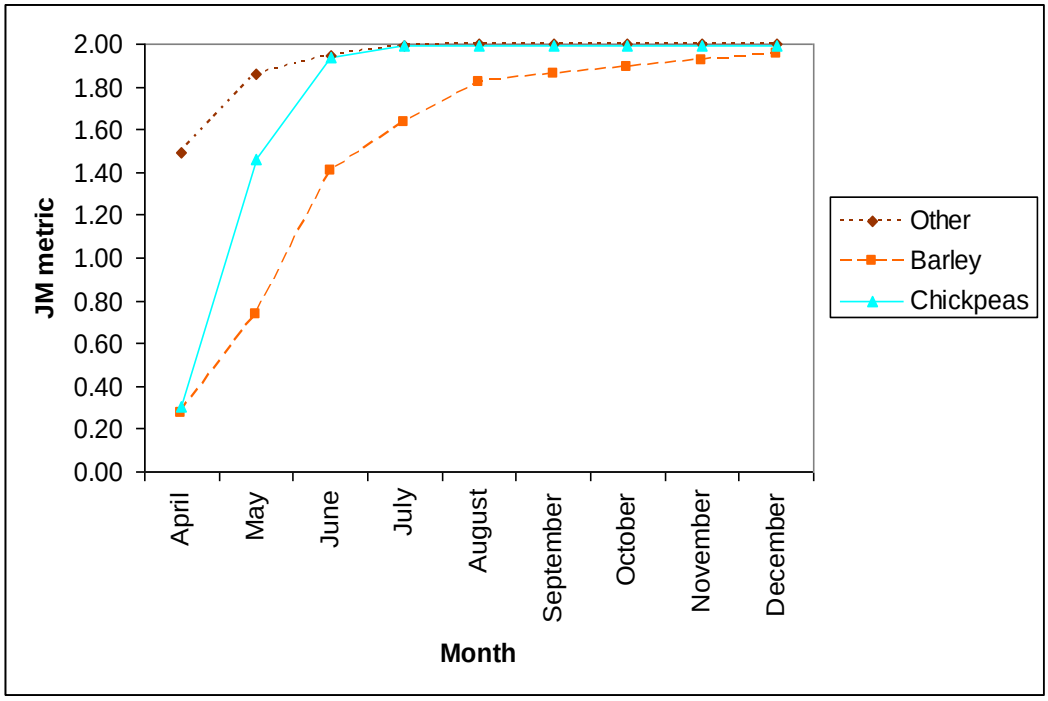

Figure 5.2: Temporal EVI separability of wheat from other (dotted line), barley (broken line) and chickpea (solid line) crops throughout the 2003 season, as measured using the JM-metric as defined in Section 3.4.4.

5.2.3 Feature Classification and Validation

Each specific $\sum \Delta EVI$ image (i.e. year, threshold value, months) was classified into two classes, crops and non-crops, by applying the unsupervised *K*-means clustering algorithm in ENVI limited to two clusters/groupings. Ground truth data from all crop and non-crop types was merged into 384 and 297 crop sampling points for 2003 and 2004, respectively. Sampling points for non-cropping land use areas equated to 918 and 1365 for 2003 and 2004, respectively. This data was used to determine the accuracy at pixel scale by calculating the PCC and KC metrics (Section 3.4.5). This constituted the *pixel scale accuracy*.

The accuracy of area estimates at shire scale was only calculated for the $\sum \Delta EVI$ approach with the highest pixel-scale accuracy, each month through the season, by contrasting area estimates with the actual shire-scale data (ABARE 2005a; ABS 2004). A simple root means square error (RMSE) was calculated between predicted area and actual area for the period 2000 to 2004 (excluding 2002, which was not available at shire level from ABS) for both shires combined. Combining data of all

years (2000, 2001, 2003, and 2004) for both shires (4-years x 2-shires) had enough degrees of freedom to ensure statistical rigour when calculating the RMSE.

5.3 Results and Discussion

5.3.1 Efficacy of Early-season Metrics

The threshold images ($\sum \Delta EVI$) were generated for each set of three consecutive images from DOY 97 (i.e. early April) through to DOY 257 (i.e. early October) for each of the 2003 and 2004 seasons. Figure 5.3 and 5.4 depict the threshold image of T500 for early July for 2003 and 2004, respectively. The red to green pixels represent high values while the blue pixels represent low values. White represents no green-up. To predict crop area, each threshold image was classified into two classes i.e. green-up (i.e. crops) or no green-up (i.e. non-crops). Figures 5.5 and 5.6 show the classifications of the $\sum \Delta EVI_{T500}$ images in figures 5.3 and 5.4.

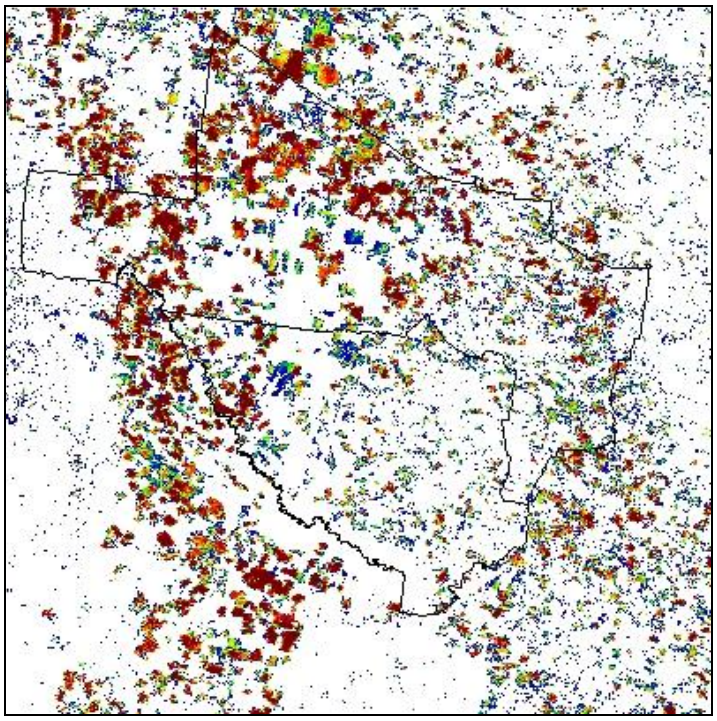

Figure 5.3: The $\sum \Delta EVI_{T500}$ image for early July for 2003. The blue colour represents low differential EVI values while the red to green represents higher values.

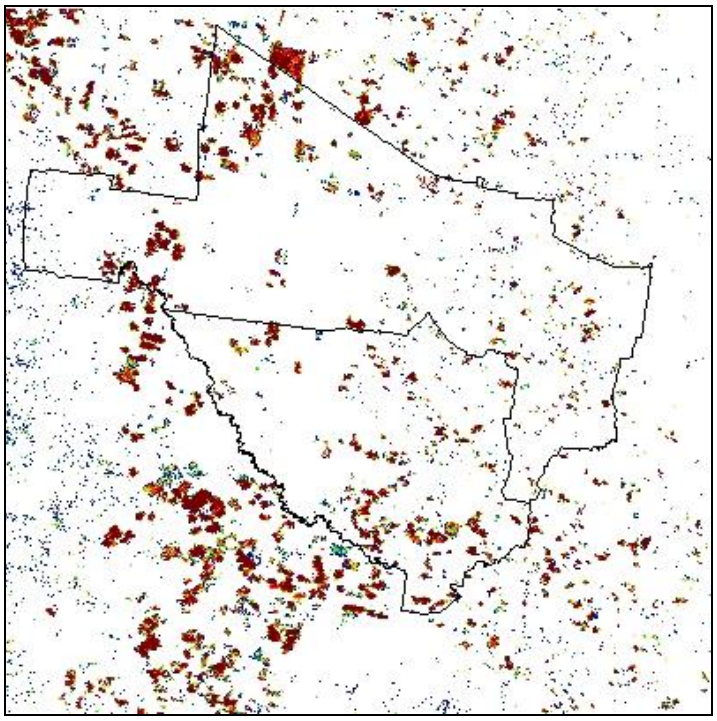

Figure 5.4: The $\sum \Delta EVI_{T500}$ image for early July for 2004. The blue colour represents low differential EVI values while the red to green represents higher values.

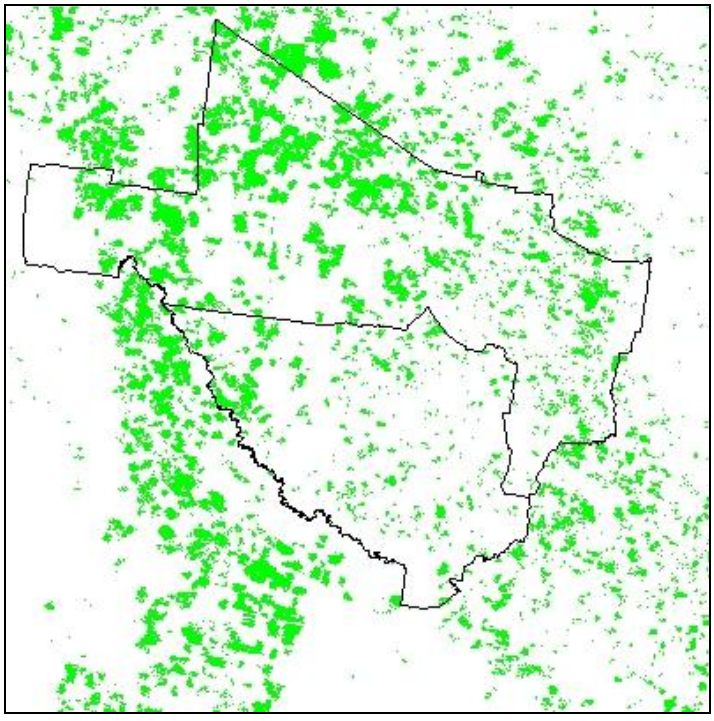

Figure 5.5: Classified image for the 2003 season, derived from the $\sum \Delta EVI_{T500}$ image using unsupervised *K*-means classification. Green = crops and white = non-crops.

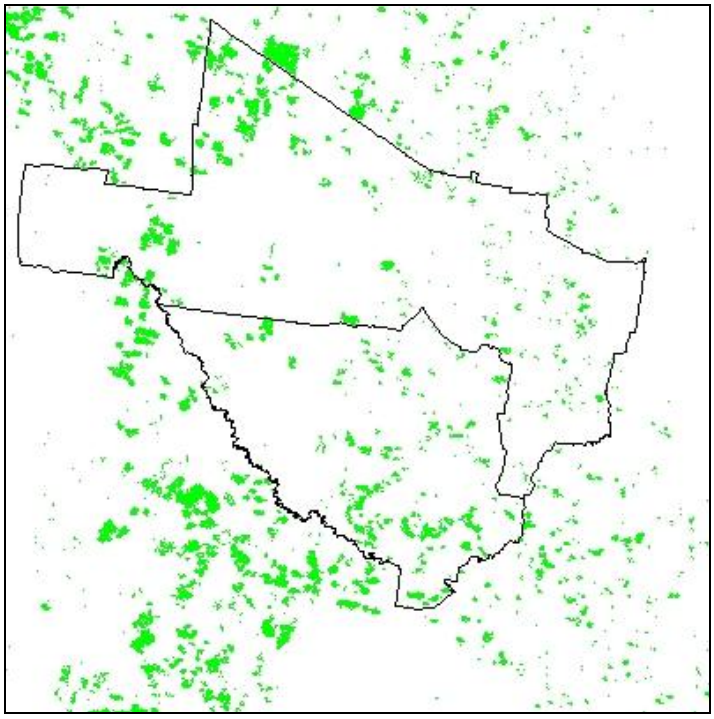

Figure 5.6: Classified image for the 2004 season, derived from the $\sum \Delta EVI_{T500}$ image using unsupervised *K*-means classification. Green = crops and white = non-crops.

More pixels were classified as crop in 2003 than 2004. The reduced winter crop area for 2004 was due to the very dry conditions experienced during that season due to an El Niño, as discussed in Chapter 4.

Discriminatory ability at pixel scale was high and peaked in July for all $\sum \Delta EVI$ approaches both seasons (Figure 5.7 & 5.8). The $\sum \Delta EVI_{T250}$ and $\sum \Delta EVI_{T500}$ approaches had slightly better PCC values than the $\sum \Delta EVI_{T750}$ throughout the growing season during both years. Although there was little difference in the PPC values of the $\sum \Delta EVI_{T250}$ and the $\sum \Delta EVI_{T500}$ approaches, the $\sum \Delta EVI_{T750}$ approach showed less accuracy in general. In order to avoid small fluctuations in green-up, which can be caused by crop regrowth or spurts in weed growth (Pratley 2003), being misclassified as winter crop, it was decided to use the $\sum \Delta EVI_{T500}$ approach as the most suitable threshold cut-off for estimating total winter crop area.

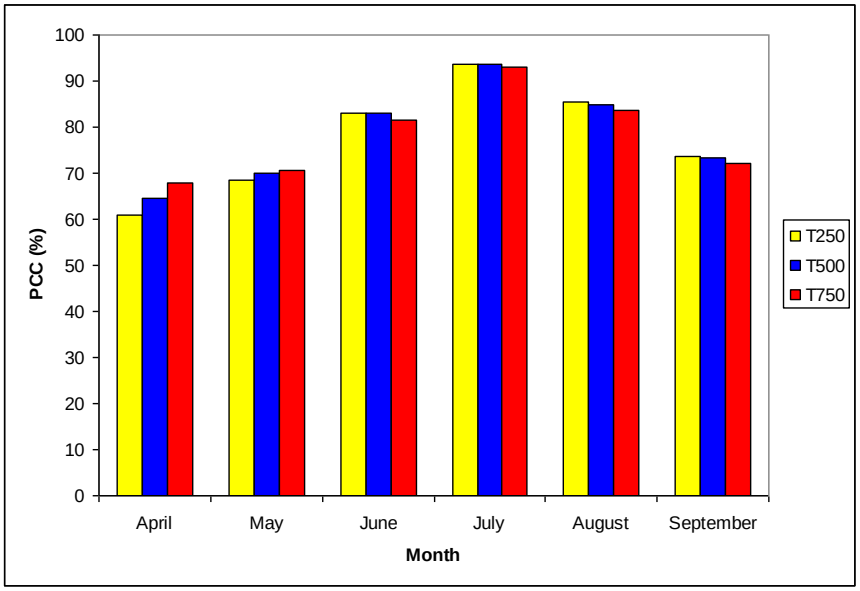

Figure 5.7: Percent correctly classified (%) for the T250, T500 and T750 thresholds for each month during the 2003 season.

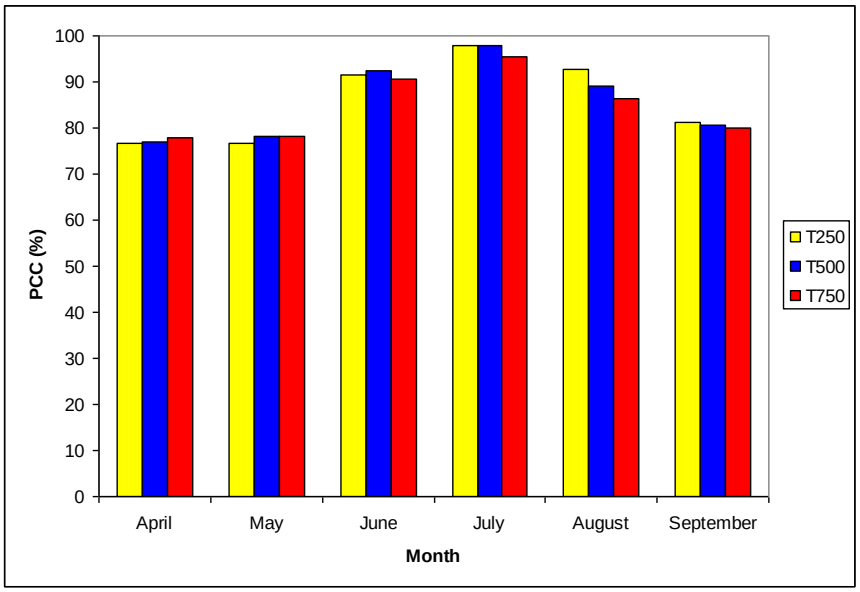

Figure 5.8: Percent correctly classified (%) for the T250, T500 and T750 thresholds for each month during the 2004 season.

The *kappa coefficient* for the $\sum \Delta EVI_{T500}$ approach for July was significantly different from June and August (Table 5.1) at the 95% level with statistical Z-values

of 9.58 and 8.30, respectively (see Section.3.4.5 for detail on statistic). As expected, KC values of June, August and September did not significantly differ from one another. Similar results were found for comparing the other approaches among months and years (data not shown). This confirms the accuracy of the $\sum \Delta EVI_{T500}$ approach for July to be significantly different from other threshold approaches used at other months. The period of maximum accuracy (i.e. July) might however change when this methodology is extrapolated to other regions and season mainly because of the variability in planting dates across large areas within a specific season.

Table 5.1: Kappa coefficients (KC) for each threshold approach for June to September for 2003 and 2004.

		2003		
Threshold	**June**	**July**	**August**	**September**
T250	0.51	0.83	0.60	0.16
T500	0.51	0.83	0.57	0.13
T750	0.45	0.82	0.53	0.08
		2004		
Threshold	**June**	**July**	**August**	**September**
T250	0.74	0.94	0.76	0.20
T500	0.74	0.94	0.61	0.66
T750	0.67	0.85	0.48	0.11

5.3.2 Accurate Shire Scale Crop Area Estimates based on In-season Metrics

The aggregated shire scale area estimates peaked in early August for both seasons and shires (Table 5.1). The July and August estimates of 40,078 ha and 45,102 ha, respectively, for the Jondaryan shire, were the closest to the actual estimate of 46,359 ha. This suggested a peak in green-up during August associated with a planting period in May, which takes into account that maximum canopy cover is reached at around 65 to 75 days after crop emergence (Chapter 4, Figure 4.2). This concurs with an average observed sowing date in May for 2003 for Jondaryan shire. Similar results were found for the 2004 season for Jondaryan.

For the Pittsworth shire, August (31,398 ha) and September (18,736 ha) were the closest to the actual area estimate of 21,951 ha for 2003, whereas the estimate in July (9907 ha) was considerably below the actual. This suggested a planting time around middle May, which concurred with the actual observed average planting time of May

for the 2003 season (ABARE 2005a). The poor estimate in July was likely related to the delay in green-up associated with this later planting. During 2004, maximum peak green-up was in September, which suggested a likely shift to an even later (one month) planting time for the Pittsworth shire in that year. This one-month shift in peak estimates for Pittsworth can be partly explained by the fact that 94% of the wheat plantings (i.e. main winter crop) occurred at the end of June during the 2004 season (ABARE 2005a). July and August area estimates of 6,336 ha and 8,481 ha, respectively, were the closest to the actual area estimate of 6,822 ha.

Thus, to capture peak EVI as early as possible, while accounting for effects associated with the spread of planting times, the average of July and August was used to calculate the early-season prediction for total winter crop area in both shires. The actual and predicted (in brackets) total winter crop area sown for Jondaryan and Pittsworth (in closed brackets) were 46,359 ha (42,590 ha), 21,951 ha (20,652 ha) for 2003, respectively, and 12,336 ha (10,020 ha) and 6,822 ha (7,409 ha) for 2004, respectively (Table 5.2). This resulted in percent differences (%Diff column in Table 5.2), which ranged from -19% to 9% across seasons and shires. The 2003 season estimates had the smallest average difference from the actual, while the 2004 season estimates were the largest for both shires. This suggested a larger percentage error in crop area estimates during the dryer 2004 year, when crop area planted was reduced, than the wetter 2003 season. However, this inference needs to be tested in other regions and seasons to determine its general applicability. Furthermore, it should be noted that the actual data figures in Table 5.2 include surveyed values for areas sown to wheat, barley and chickpea (ABARE 2005a). The actual harvested area for these crops is always likely to be equal to or less than the sown area and will differ from region to region and season to season due to climate (failed crops due to water stress) and crop management practices (hayed or fed off). If crop emergence rates are poor, the predicted area will be closer to the area harvested than the area planted.

Table 5.2: Predicted area estimates using the T500 approach throughout the growing season for each year and each shire. "Actual" is the ABARE surveyed and census figures, while "Average" represents the mean of July and August.

	Year	Area	June	July	August	September	Actual	Average	% Diff
	2003	**%**	5.42	20.98	23.61	11.38			
Jondaryan		**ha**	10354	40078	45102	21739	46359	42590	-8
	2004	**%**	3.28	4.48	6.01	4.99			
		ha	6266	8558	11481	9532	12336	10020	-19
	2003	**%**	2.91	9.1	28.84	17.21			
Pittsworth		**ha**	3168	9907	31398	18736	21951	20652	-6
	2004	**%**	4.22	5.82	7.79	8.157			
		ha	4594	6336	8481	8880	6822	7409	9

To test extrapolability, total winter crop area estimates were calculated for the 2000 and 2001 seasons for both shires by applying the $\sum \Delta EVI_{T500}$ approach to derive the average for July and August predictions. The 2002 season was omitted since no actual shire scale ABS data was available for this year. Further, the area estimates for these additional years (i.e. 2000, 2001) from ABS only included wheat and barley values (i.e. not chickpea). Figure 5.9 shows the total winter crop area estimates of the predicted (dotted line) and the observed (solid line) for the 2000 to 2004 period for both shires. The predicted area estimates were slightly higher than the actual data especially in the Jondaryan shire. This slight over prediction of area can mainly be attributed to the fact that area sown to chickpea was not included in the ABS crop area estimates. The average area sown to chickpea was 15% and 6% of the total area sown to winter crop during the 2003 and 2004 seasons for Jondaryan and Pittsworth shires, respectively. The average over-prediction in 2000 and 2001 was 24% and 3% for Jondaryan and Pittsworth shires, respectively, which approximates the average observed area shown for these shires. The 2002 prediction for both shires was the lowest during the 5-year period. Although no estimates of actual area were available, anecdotal evidence supports this estimate as 2002 was classified as an El Niño year (as was 2004) and very little winter crop was planted during that season.

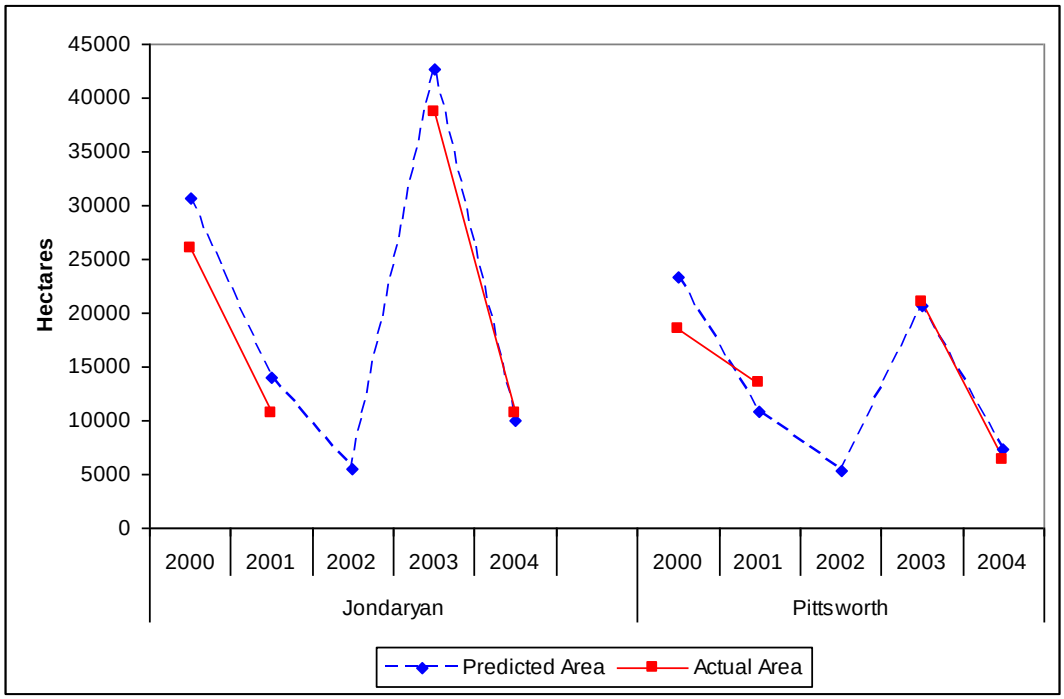

Figure 5.9: Total winter crop (excluding chickpea) area figures of predicted and actual for the 2000 to 2004 period for the Jondaryan and Pittsworth shires.

The total winter crop area (excluding chickpea) averaged 18,149 ha each year (over both Jondaryan and Pittsworth shires) during the 4-year period. At a regional scale (i.e. combining data from both shires) the error in the prediction of wheat and barley area equated to 3,157 ha (RMSE) on average over the 4-year period. Given the inclusion of chickpea in the predicted values and some error in the ABS and ABARE survey estimates, this is an acceptable level of error. Overall, the predicted area was highly correlated with the actual area and is significantly different from a 1:1 relationship ($p=0.00002$) (Figure 5.10). This was mainly caused by the significance in the slope ($p=0.00001$) rather than the intercept, which did not differ from zero ($p=0.48$). The significance in slope was a result of the over-prediction of actual production for years that have productions above 20,000 tons (i.e. 2003 for Jondaryan and 2000 for Pittsworth, Figure 5.9).

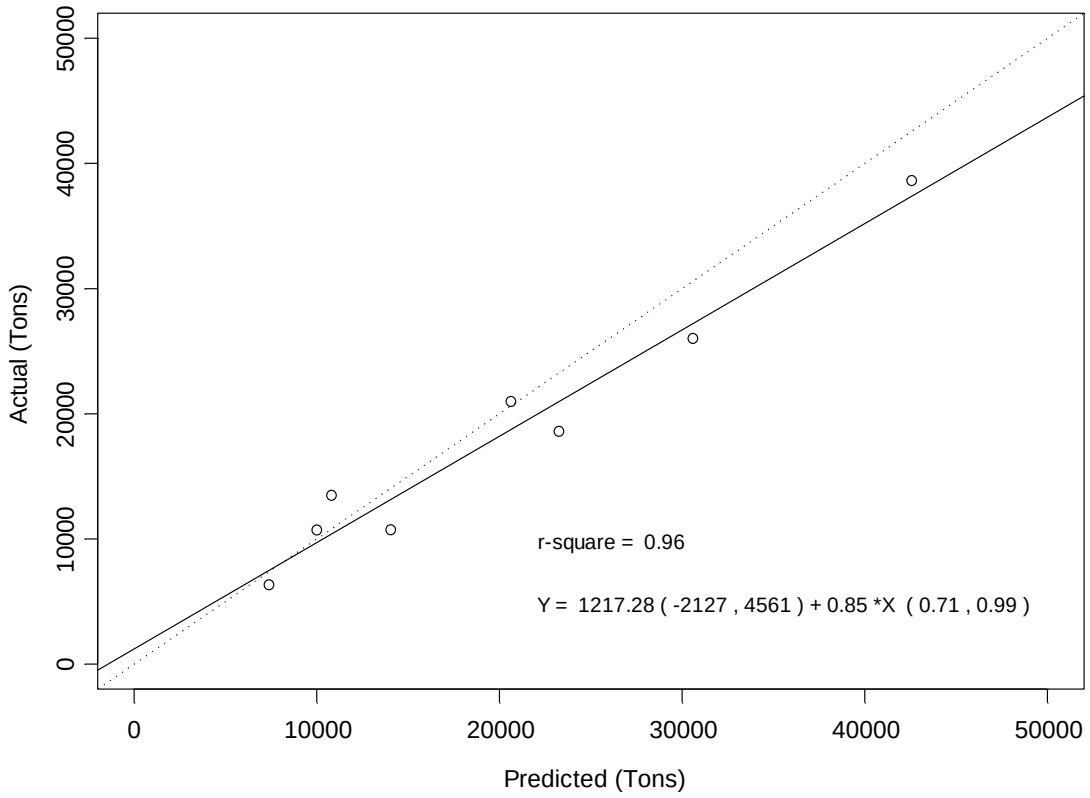

Figure 5.10: Scatter plot of predicted (using $\sum \Delta EVI_{T500}$) actual total winter crop area (excluding chickpea) values for the 2000, 2001, 2003 and 2004 seasons for the Jondaryan and Pittsworth shires. The portion of variance explained is given as the r-square. Lower (ll) and upper (ul) 95% confidence intervals (CI) are included in brackets for each coefficient in the equation: Y = a (llCI, ulCI) + b*X (llCI, ulCI). The 1:1 line is shown as a stippled line, while the solid black line is the fitted regression line.

5.3.3 Early Season Area Estimates are Critical in Bridging the 'Information Gap'

Advance knowledge of crop yield and production has become increasingly sought by industry and government agencies over the last decade (Hammer et al. 2001). While effective systems have been developed to deliver advance knowledge of yield likelihood (Potgieter et al. 2005a; Potgieter et al. 2006) it has not been possible to derive associated production estimates due to the absence of accurate and timely estimates of crop area. Such estimates have been available only at the end of the cropping season or even later depending on the source. In-house sources, such as agronomists and agents within the specific agri-businesses or government agencies, generate qualitative estimates during the season. Official agency sources like ABS generate estimates via survey and data collating exercises, but they only become

available long after harvest. The availability of precise crop area estimates was seriously diminished by the cessation of the annual ABS census. In addition, the scale at which such information is available is limited to region or state level due to the lack in accuracy at the shire scale. All of this contributes to the widening of the *information gap*, which currently exists in Australia. There is no accurate, objective, and near-real time crop area and ensuing crop production estimates available at shire scale to support industry decisions.

Internationally, specifically in the U.S., through the USDA and World Agricultural Outlook Board (WAOB), crop forecasts are issued every month for nearly every country-crop pair in the world (Crutchfield 2008). Final estimates are discussed in a round table exercise including all agricultural forecasting agencies within the USDA. For the U.S., remote sensing derived information from Landsat is used with relatively high accuracies (Mueller 2008), compared to detailed ground truth data from farm surveys (NASS 2006; Vogel et al. 1999), at the end-of the growing season. The dissemination of remotely sensed data for crop area only became operational during the 2008 season in the U.S. (Mueller 2008). It is anticipated that the application of early-season crop estimates, as derived in this Chapter, if available in *other countries*, will increase the accuracy and objectivity of crop information utilised in the WAOB round table crop forecasting discussions. Furthermore, it is likely that such remotely sensed derived crop area estimates, well before harvest, will have similar accuracies to that of a survey/census, as found in this chapter, but at much lower anticipated cost than in the U.S..

The availability of early-season (as discussed in this chapter) and ensuing end-of-season crop (Chapter 4) area estimates at shire scale, when combined with similar yield estimates (Potgieter 2008), provides the means to bridge this *information gap*. Reliable, timely and detailed production estimates underpin industry decisions on commodity handling logistics and commodity marketing. Furthermore, they provide a transparent basis for government decisions in relation to exceptional circumstances policy associated with extreme events or potential supply shortfalls to industry. However, further research is necessary to determine the applicability of the approach to other regions and states with Australia.

5.4 Conclusion

This study shows that accurate, early-season estimates of crop area can be generated using change in MODIS EVI values through the season associated with crop green-up. Area estimates can be obtained as early as the 1st week in July with a relatively high accuracy. However, the issue of spatial variability in sowing dates (early or late plantings) from region to region may delay availability of accurate estimates by requiring averaging of values from early July and early August. The approach requires further investigation to test its applicability in other regions. Nonetheless, for the study area, this research has shown that accurate early-season winter crop area estimates are possible at least two months before harvest. Such advance knowledge of crop area and production is of high value to agri-industry and government in supporting business and policy decisions. In addition, government agencies like ABARE acquire such information to update their quarterly commodity estimates.

Chapter 6

Estimating Winter Crop Area across Seasons and Regions Using Time Series MODIS Imagery

"One swallow does not make a summer"

Aristotle, *Nichomachean Ethics* (384 BC - 322 BC)

6.1 Introduction

Wheat is the second largest agricultural export commodity after beef, in Australia, with a total value of $3.5 billion per annum. Of the total 23 Mt of wheat production on average, Western Australia and New South Wales contribute 39% and 36% to the national total, respectively (ABARE 2007) South Australia, Victoria and Queensland contribute 12%, 9% and 6%, respectively. Although Queensland has the lowest production, it usually produces high quality grain, which is highly sought in international markets. Furthermore, the close proximity of Queensland to the fast growing economies of Asia, which have an increasing demand for food, adds impetus to Queensland grain industries. World demand for feed grains (including barley and wheat) is expected to continue to rise, providing opportunity for an increase in Australian grain exports (Anthony et al. 2007; Penm 2006). There is also an increasing domestic demand for feed grain from the feedlot industry, a heightened importance of grains for industrial purposes, such as ethanol and biodiesel production. All of these influences indicate a strong future demand for grain, resulting in an increased need for timely production estimates.

Chapters 4 and 5 focussed on the development and application of multi-temporal remote sensing approaches for early-season, as well as end-of-season, winter crop area estimation using two contiguous shires in southeast Queensland. It was shown that such technology could be utilised to estimate shire-scale total and specific winter crop area with acceptable accuracy. In this chapter, the ability of these multi-temporal approaches in estimating winter crop area over large areas was investigated. Such estimates are necessary to generate accurate, objective and near-real time production

estimates for winter crops across large regions. Information on the spatial distribution of production estimates is sought by agri-industry to support critical resource management and financial decisions (e.g. shifting of resources, bulk handling crops, forward buying or selling, etc.), particularly in the background of a highly variable climate.

Deriving large scale crop area estimates usually involves the use of exhaustive sampling approaches (e.g. area frame sampling) or sampling approaches combined with moderate resolution imagery (e.g. Landsat TM) (Cotter et al. 1994; Dadhwal et al. 1991; Fecso et al. 1986; MacDonald et al. 1980). However, those approaches are labour-intensive and expensive. The advent of MODIS satellite imagery has enhanced the capability of remote sensing to estimate crop area over large areas with acceptable accuracy and cost. This is mainly due to the high temporal resolution (~2 days) of the imagery, as well as the use of suitable spectral bands, which target specific biophysical attributes of crop canopies at relatively fine spatial resolution (i.e. 250 m x 250 m pixel scale).

The main objective of this chapter was to test the temporal and spatial extrapolability of the remote sensing approaches derived in chapters 4 and 5. Specifically, the study aimed to assess the ability of multi-temporal remote sensing approaches (as derived in previous chapters) for (i) early-season total winter crop area estimation for Queensland and (ii) end-of-season crop area estimation for total and specific winter crops (i.e. wheat, barley and chickpea) for Queensland.

6.2 Methods

6.2.1 *Study Area*

The study area encompasses the broad cropping region of Queensland and lies between latitudes 21^{o} South and 29.5 ^{o} South on the north-eastern side of the Australian continent (Figure 6.1). The total broad agricultural production zone is approximately 15.88 million ha, of which 18% is specifically used for dryland and irrigated agricultural or plantation production (DNR&W 2006).

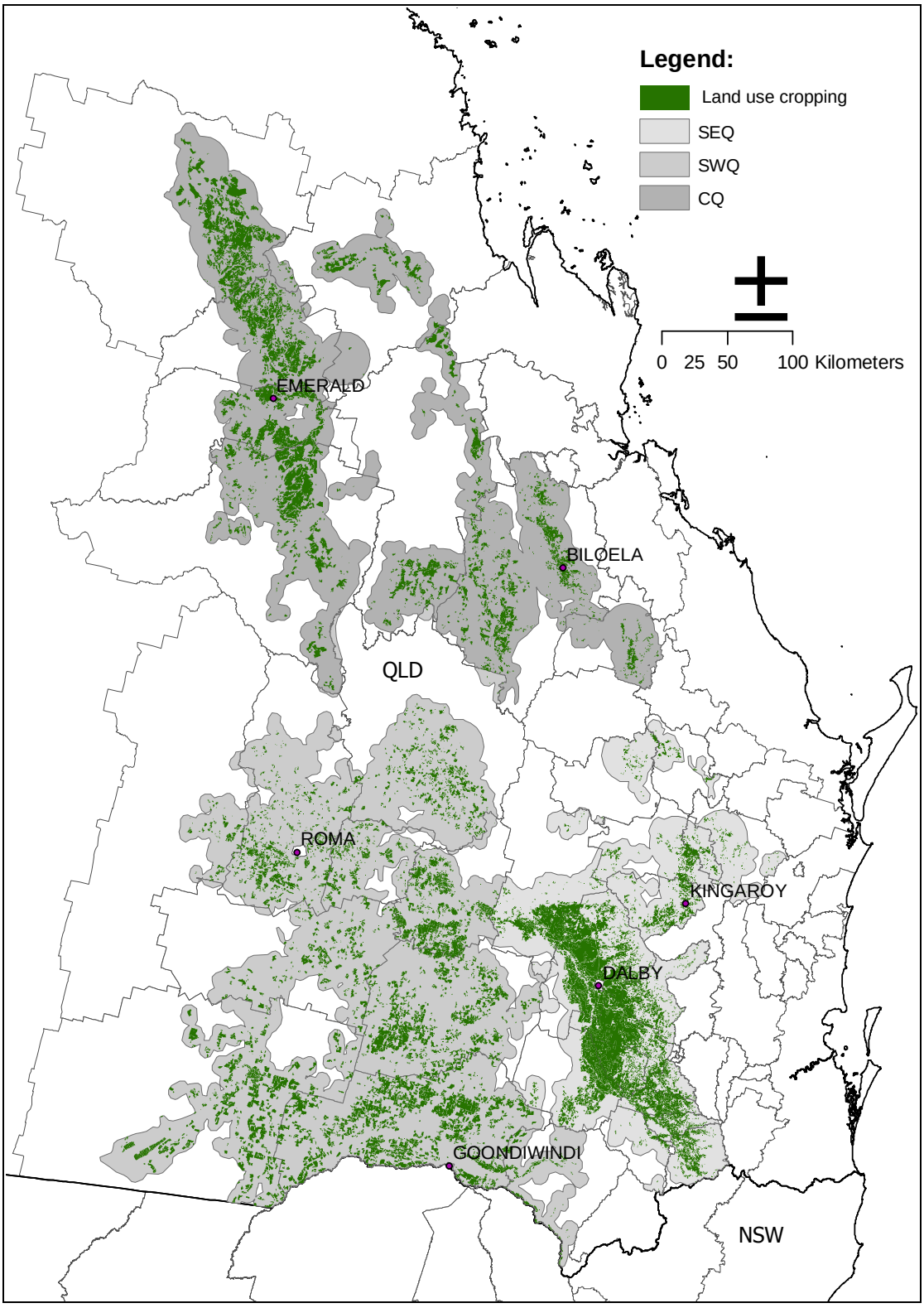

Figure 6.1: Map of the broad cropping area within Queensland (shaded). The sub-regions are shown in shades of grey. Specific areas with agricultural land use (i.e. dry land and irrigated cropping), as derived in 1999, are indicated in green.

Traditionally, and also for the purposes of this study, the Queensland cropping region was divided into sub regions. These regions are central Queensland (CQ), southwest Queensland (SWQ) and southeast Queensland (SEQ) (Figure 6.1). The average wheat area and total production for CQ, SEQ and SWQ for the period 1975 to 2000 were 162,000 ha and 246,000 tons, 162,000 ha and 295,000 tons and 453,000 ha and 585,000 tons, respectively. Although SWQ had the highest production on average, it had the lowest crop yield per unit area of the three regions at 1.22 tons/ha. SEQ had the highest average wheat yield of 1.75 tons/ha with CQ intermediate at 1.37 tons/ha (ABS 2004).

6.2.2 *Early-season Prediction of Crop Area*

Prediction of crop area early in the season was done using the *T500* measure detailed earlier in Chapter 5. In this simple measure, the summation of the differential in EVI between three consecutive MODIS images ($\sum \Delta EVI_{T500}$) for two specific monthly periods was calculated. This captured the green-up rate before and around flowering preceding and including DOY 193 (July) and DOY 225 (August). The accuracy of the derived $\sum \Delta EVI_{T500}$ image for end of July, August, Average (i.e. average area estimates of July and August) as well as the combined (union) image of the $\sum \Delta EVI_{T500}$ images from both periods (i.e. July & August) were tested at a pixel scale using ground truth data. These procedures were applied to the 2005 and 2006 winter cropping seasons across the entire Queensland cropping region. The land use polygon boundaries determined in 1999 (DNR&W 2006) were used as primary mask for land use areas when calculating the preliminary (or early-season) total winter crop area estimates. Figure 6.2 sets out an overview of the procedures involved in deriving crop area estimates before flowering and at the end of the season.

6.2.3 *End-of-season Prediction of Crop Area*

Prediction of the end-of-season crop areas was done using the HANTS approach as derived in Chapter 4 of this study. The HANTS method was applied to discriminate between crop areas for wheat, barley, chickpea and non-crop across all sub-regions for the 2005 and 2006 seasons.

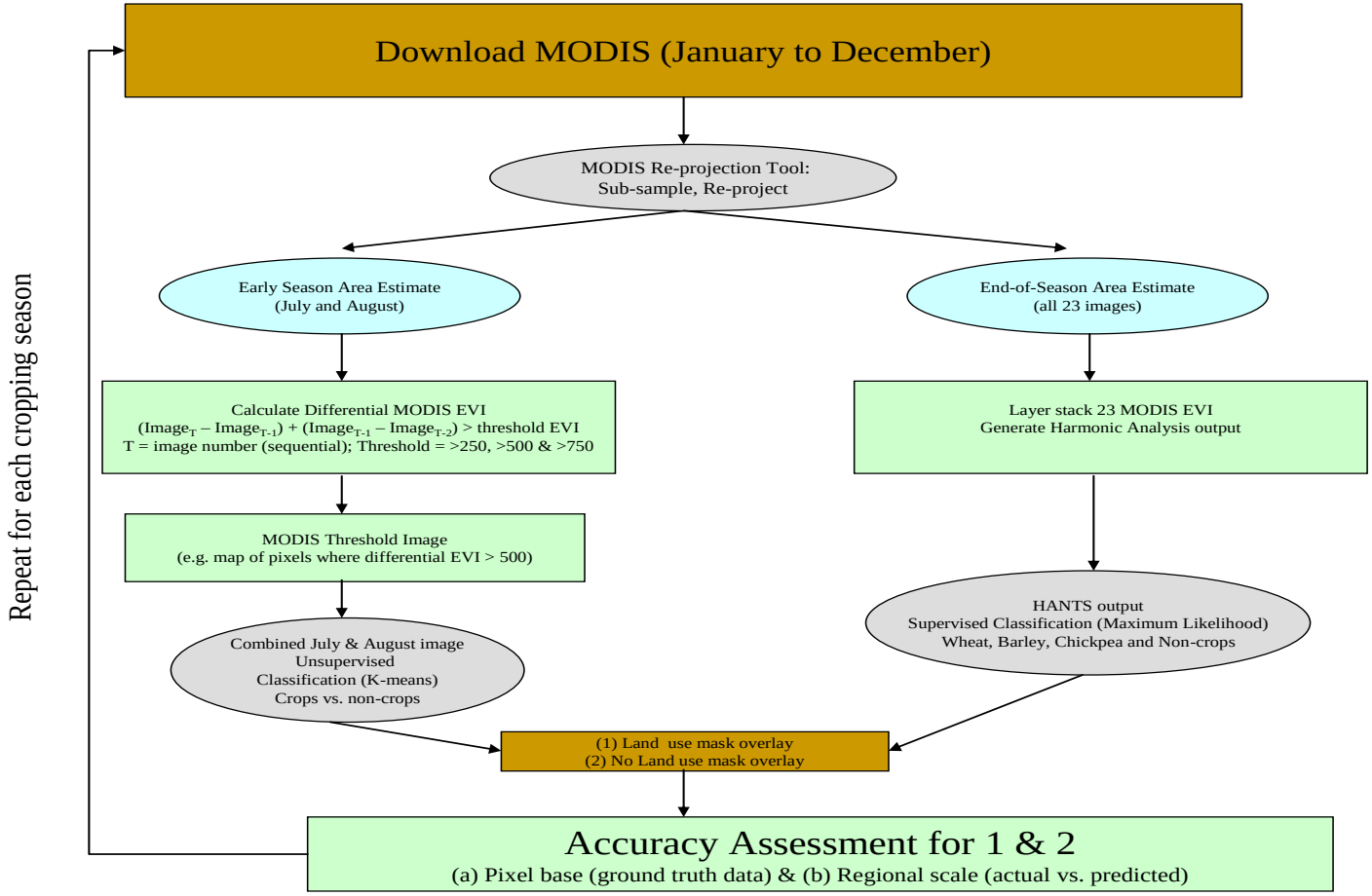

Figure 6.2: Procedures involved in assessing the ability of MODIS multi-temporal approaches for early-season and end-of season crop area estimates. Accuracy was assessed at pixel as well as regional scales and with and without land use masking.

6.2.4 *Ground Truth Data*

Ground truth data was collected via targeted field trips and from paddock identification information received from public and/or private agronomists and industry agents for both the 2005 and 2006 seasons across the three sub-regions (i.e. CQ, SWQ and SEQ) within the entire QLD cropping region.

Table 6.1: Ground truth sampling points collated at pixel scale for each sub-region and entire Queensland region for each feature class for 2005 and 2006. This was used to classify the images. R denotes the independent sampling points used to test the classification approach. "na" was assigned to feature classes when no data for that class was observed.

Region	Feature	2005	2006
SWQ	Wheat	294	252
SWQ	Barley	76	25
SWQ	Chickpea	43	33
SWQ	R Wheat	73	60
SWQ	R Barley	18	7
SWQ	R Chickpea	8	13
CQ	Wheat	315	626
CQ	Barley	na	na
CQ	Chickpea	19	48
CQ	R Wheat	65	115
CQ	R Barley	na	na
CQ	R Chickpea	6	14
SEQ	Wheat	21	37
SEQ	Barley	24	na
SEQ	Chickpea	na	na
SEQ	R Wheat	6	12
SEQ	R Barley	6	na
SEQ	R Chickpea	na	na
QLD	Non-crop	33179	38632
QLD	R non-crop	6131	7281
QLD	Crop	792	1021
QLD	R Crop	182	221

This specific crop type information for both seasons, was assimilated at pixel scale for each crop feature class (e.g. wheat, barley, chickpea, fallowed) for each sub-region (i.e. CQ, SWQ, SEQ) using the region of interest (ROI) functionality in the

ENVI software (ITT 2008) (Table 6.1). Fallowed area classes (i.e. areas not cropped during winter) were season-specific while other classes like forest and pasture were kept the same in both seasons.

6.2.5 *Feature Classification and Validation*

6.2.5.1 Pixel-scale Accuracy

The accuracy at pixel scale was measured using the *percent correctly classified* (PCC, Section 3.4.5.1) metric calculated between crop and non-crop for early-season prediction. For end-of-season area estimates, the discriminatory ability for specific crop classes (wheat, barley, chickpea and the non-crop class) was also determined using the PCC. In addition, the *Kappa coefficient* (Section 3.4.5.1), which is also known as a *measure of reliability* (Cohen 1960; Sim et al. 2005) was calculated and used in assessing comparative accuracy in this study.

These statistics were created from the *error/confusion matrix* contrasting independent randomly selected ground truth points (i.e. class labels preceded by R in Table 6.1) against the classified image trained on main feature classes (i.e. wheat, barley, chickpea, non-crop) using the end-of-season HANTS classification. For early-season prediction accuracy was determined using the statistics generated from the error matrix for the each merged feature class level, i.e. dividing the image into areas that are winter cropped (crop feature class including mainly wheat, barley and chickpea) and those that are not cropped (non-crop class including fallow, vegetation, forest etc.) (Figure 6.2).

6.2.5.2 Regional Scale Accuracy

Regional scale accuracy was determined by contrasting total state level area estimates for wheat, barley and chickpea with actual ABARE statistics (Lawrance 2007) for 2005 and 2006. Actual shire-scale data was only available for the 2005 season. This was contrasted against the predicted shire scale area estimates to create spatial regressions of total winter crop, wheat, barley and chickpea. Thus, accuracy across all shires was assessed through the R^2 metric, calculated from the simple linear regression of actual data (ABS 2008) and estimated area data (using HANTS) for 2005.

The rigorousness of the 1999 land use data (DNR&W 2006) was assessed using the pixel accuracy of the HANTS approach with and without land use mask.

6.3 Results and Discussion

6.3.1 *Observed Field Training Sampling Paddocks*

Collating of ground truth data resulted in 792 and 1021 sampling points within the cropped area and 33,179 and 38,632 non-crop sampling pixels for the 2005 and 2006 seasons, respectively (Table 6.1). More non-crop sampling points were collated (based on randomly selected field data points) during the 2006 season mainly because of the drier conditions in SEQ, which resulted in large fallowed areas observed for that region within the feature class. The increase in crop training samples for the 2006 season, compared to 2005, mainly came from the improved wheat conditions in CQ for that season (increase from 315 to 621 for 2005 to 2006 season). In addition, paddock sizes in CQ tend to be much larger than southern Queensland, thus resulting in more pixels per paddock selected. No barley paddocks were observed during the field trips for CQ in both seasons, while no chickpea paddocks were observed in SEQ during both seasons. In addition, no barley crops could be located during the field trips in SEQ for 2006.

The low number of independent training pixels is of some concern, particularly in the case of the R Chickpea classes of all sub-regions and seasons, and the R Wheat and R Barley classes for SEQ during both seasons. Such crop classes were however included (and not merged) in order to get a more accurate indication of the ability to discriminate wheat areas from barley areas within each sub-region. The collating of data through field work for 2005 and 2006 seasons represented what was practically possible. However, to address the issue of artificial accuracy due to low number of independent training samples for some crop classes, more emphasis needs to be placed on accuracy in the absence of chance calculated using the KC. The KC serves as an indicator of the extent to which the PCC values of an error matrix are due to *true* agreement versus *chance* agreement (Lillesand et al. 2004).

6.3.2 *Crop Classification at Pixel Scale*

6.3.2.1 Early-season Prediction of Crop Area

The early-season $\sum \Delta EVI_{T500}$ approach showed good ability to capture crop canopy vigour across the entire QLD cropping region. In addition, spatial (i.e. between sub-regions) as well as temporal (i.e. July and August) differences in green-up extent between July and August for 2005 and 2006 were well captured using this approach.

Figures 6.3 and 6.4 show areas (at each pixel) where the $\sum \Delta EVI_{T500}$ values are greater or equal than 500, while Figures 6.5 and 6.6 depict the classified maps (crop vs. non-crop) for July and August, respectively, for the 2005 season.

The red pixels indicate higher $\sum \Delta EVI_{T500}$ values (Figure 6.3 and 6.4), while blue represents lower values. In both seasons, the derived images indicate low $\sum \Delta EVI_{T500}$ values (blue) outside the cropping region (grey boundary lines). Most of these pixels get classified with non-crop (white) when applying the unsupervised *k*-means classifier (Figures 6.5 and 6.6). The classified image for July 2005 (Figure 6.5) indicates more areas classified as winter crop than what was evident during August 2005 (Figure 6.6), specifically in CQ. This was likely due to an earlier planting regime for that area (Routley 2006).

The unsupervised classification approach used here seems to be able to handle spurious low EVI pixel values reasonably well. For example, an area of low $\sum \Delta EVI_{T500}$ values (blue colour) for August was clearly visible in the centre of the image (Figure 6.4 and Figure 6.8), and when applying the classifier to this image, the feature mostly disappears as it is classified as non-crop (Figure 6.6 and Figure 6.10). This feature was likely a result of the composition process, which involves selecting pixels with the highest quality vegetation index after filtering on view zenith angles and cloud cover during the 16-day period (TBRS 2007). However, this artificial feature was mainly outside the 1999 agricultural land use region and the classifier corrected it to some degree, thus allowing further analysis.

Comparison of the $\sum \Delta EVI_{T500}$ imagery for July (Figures 6.7 and 6.8) with August (Figure 6.9 and 6.10) of 2006 showed an increase in the likely winter crop area in CQ over that for southern Queensland during July. For August however, the green-up areas were more evident in the Far South West Queensland's cropping

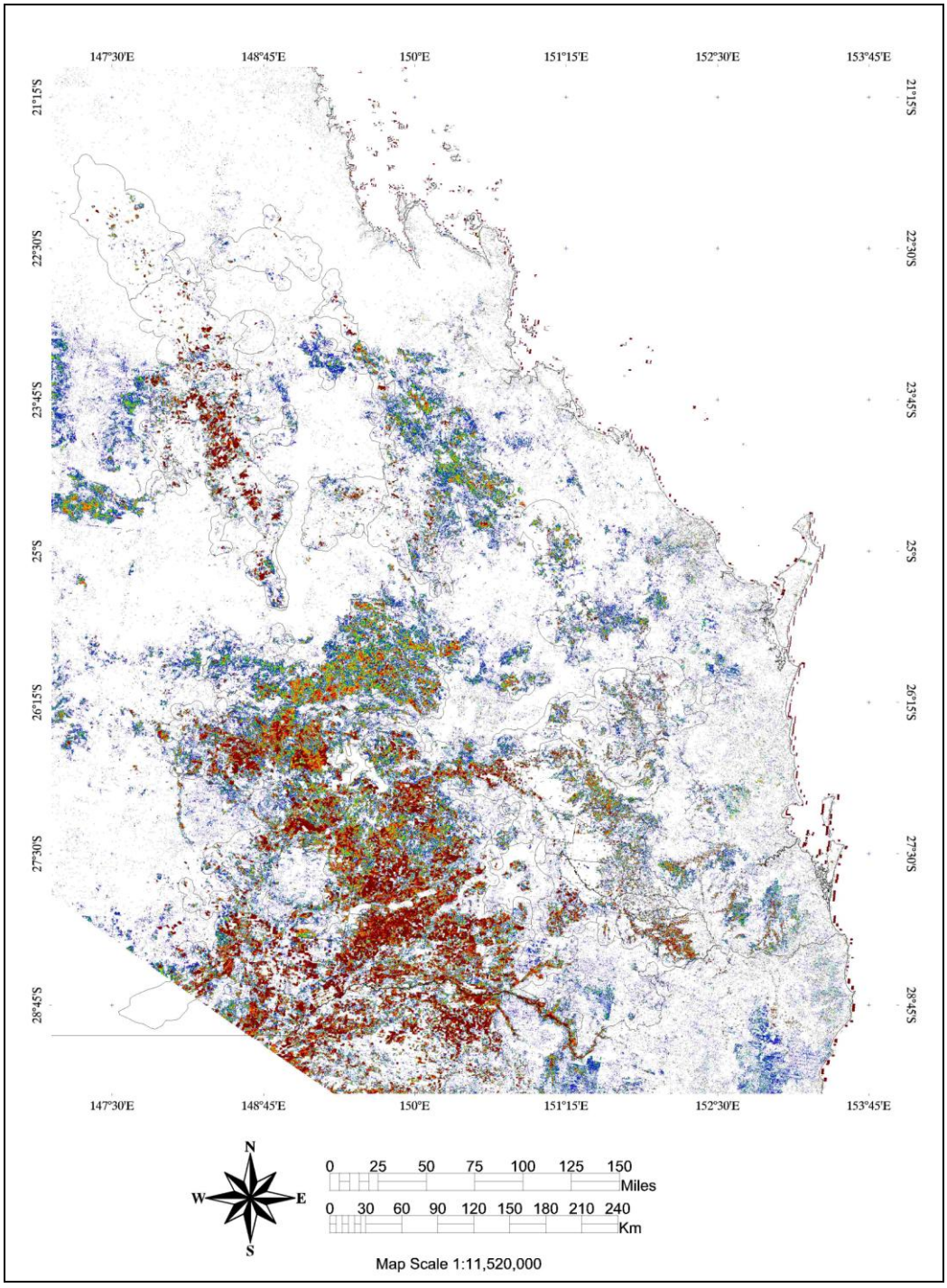

Figure 6.3: Image as derived from $\sum \Delta EVI_{T500}$ approach for July for 2005 season. No land use mask overlayed.

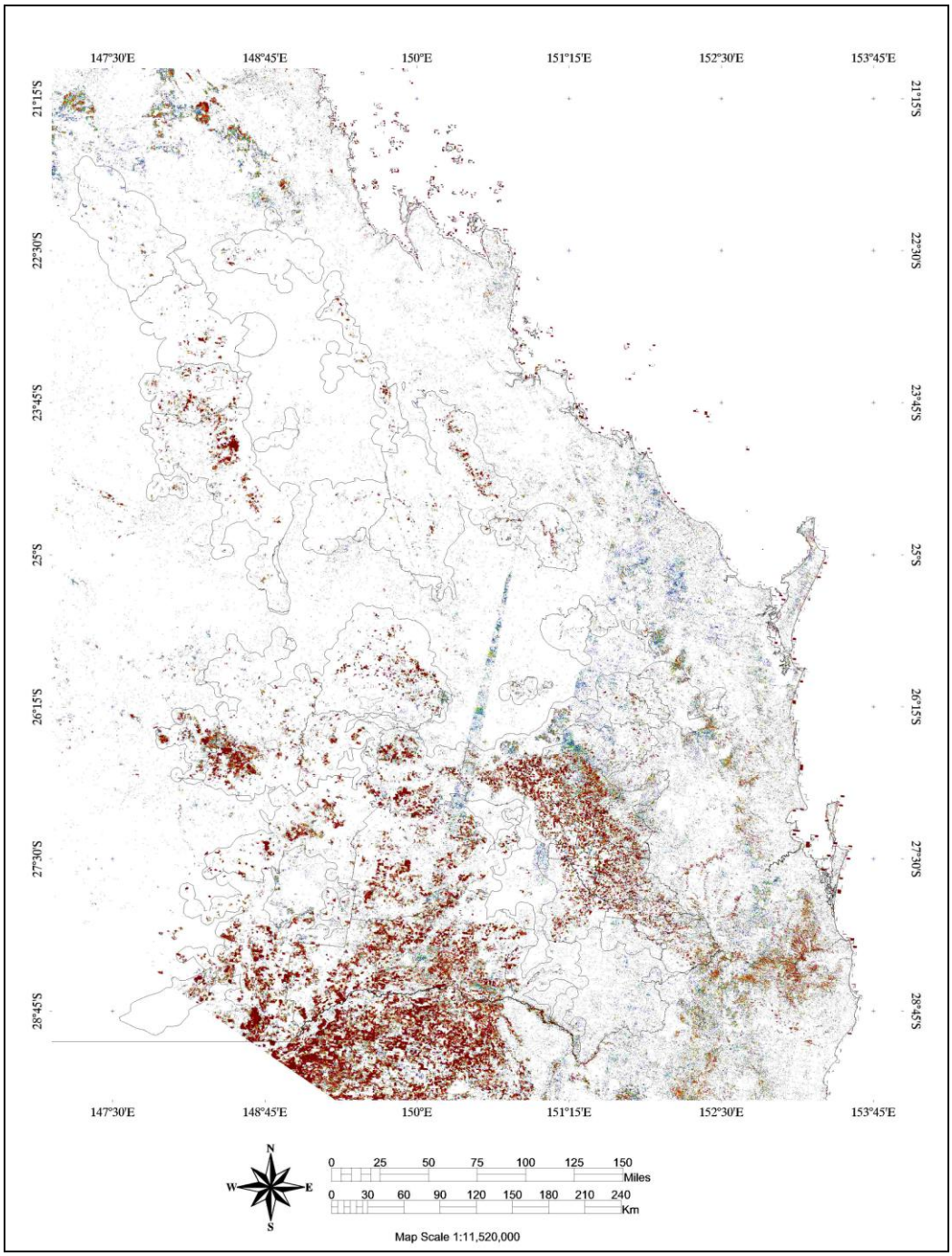

Figure 6.4: Image as derived from $\sum \Delta EVI_{T500}$ approach for August for 2005. No land use mask overlayed.

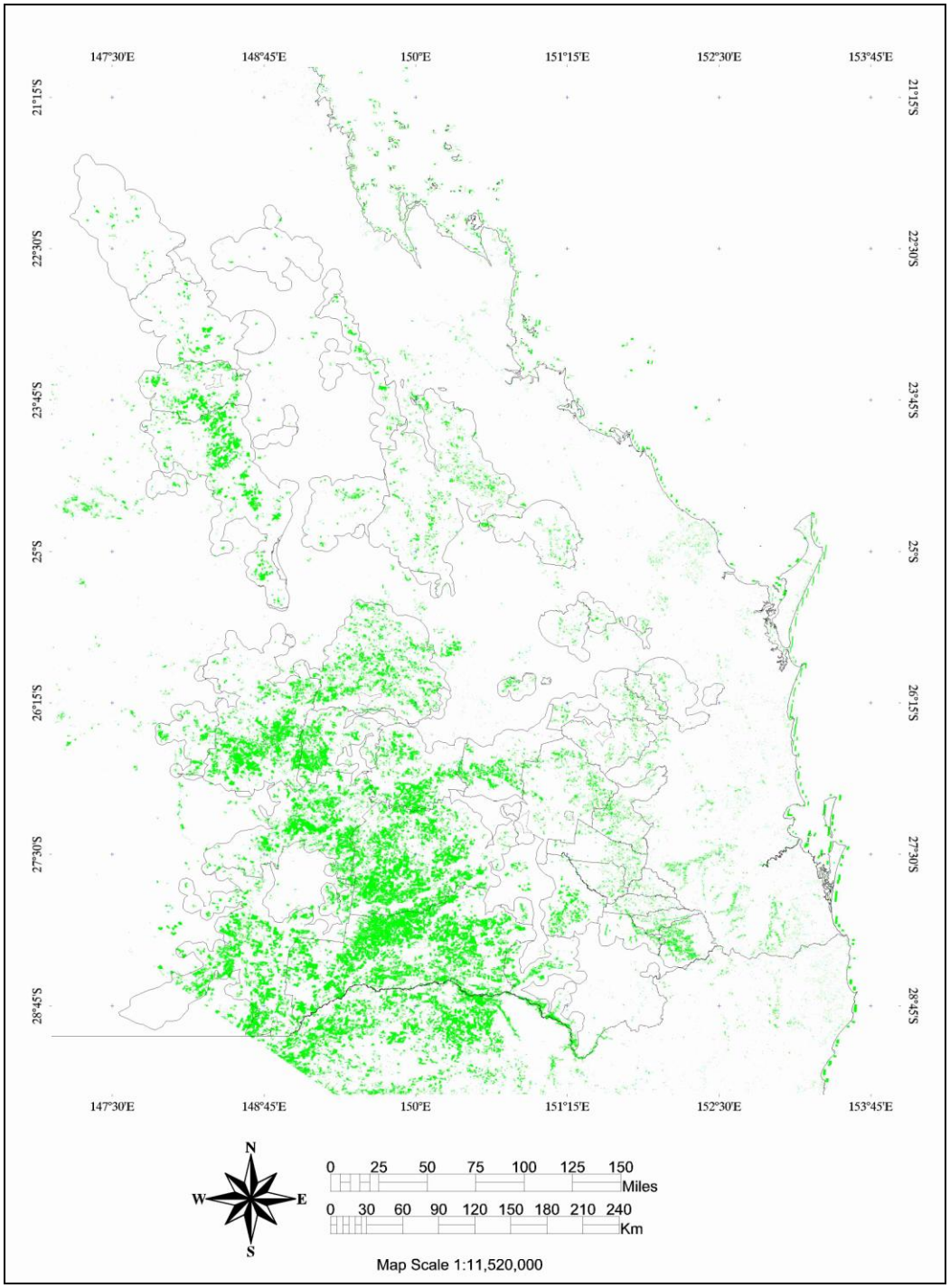

Figure 6.5: The classified image for the $\sum \Delta EVI_{T500}$ image for July for 2005 season. No land use mask overlayed.

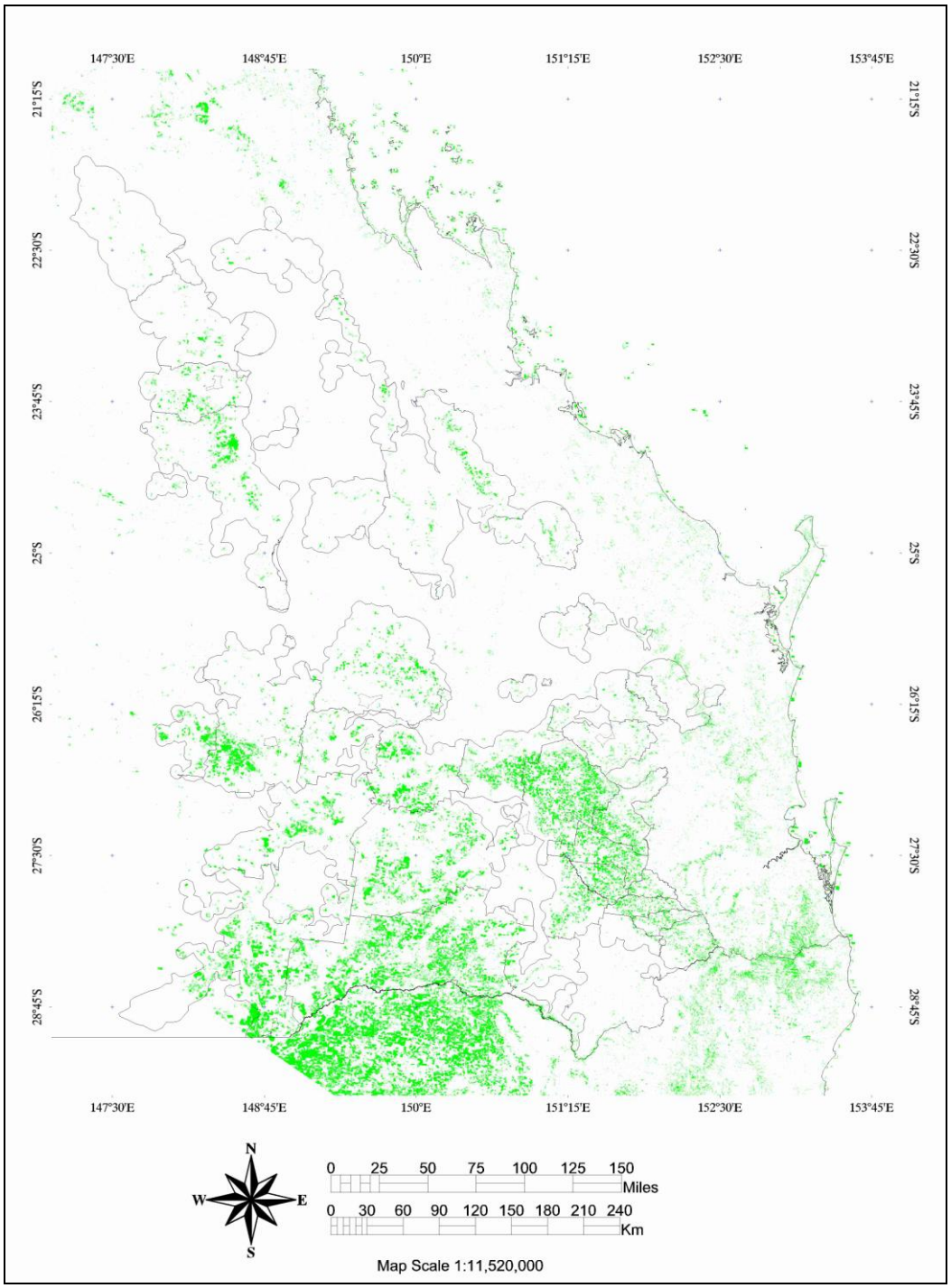

Figure 6.6: The classified image for the $\sum \Delta EVI_{T500}$ image for August for 2005 season. No land use mask overlayed.

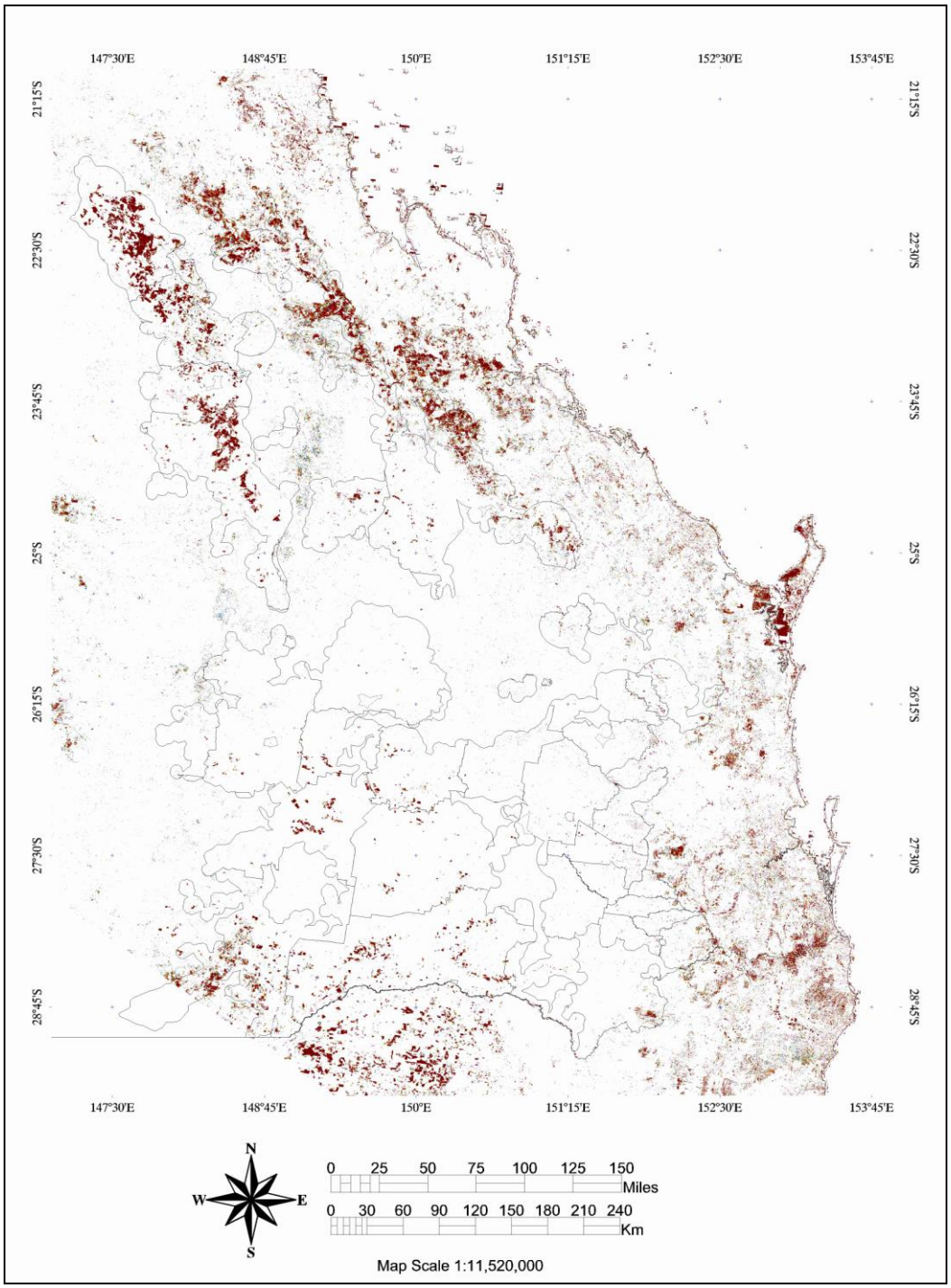

Figure 6.7: Image as derived from $\sum \Delta EVI_{T500}$ approach for July for 2006 season. No land use mask overlayed.

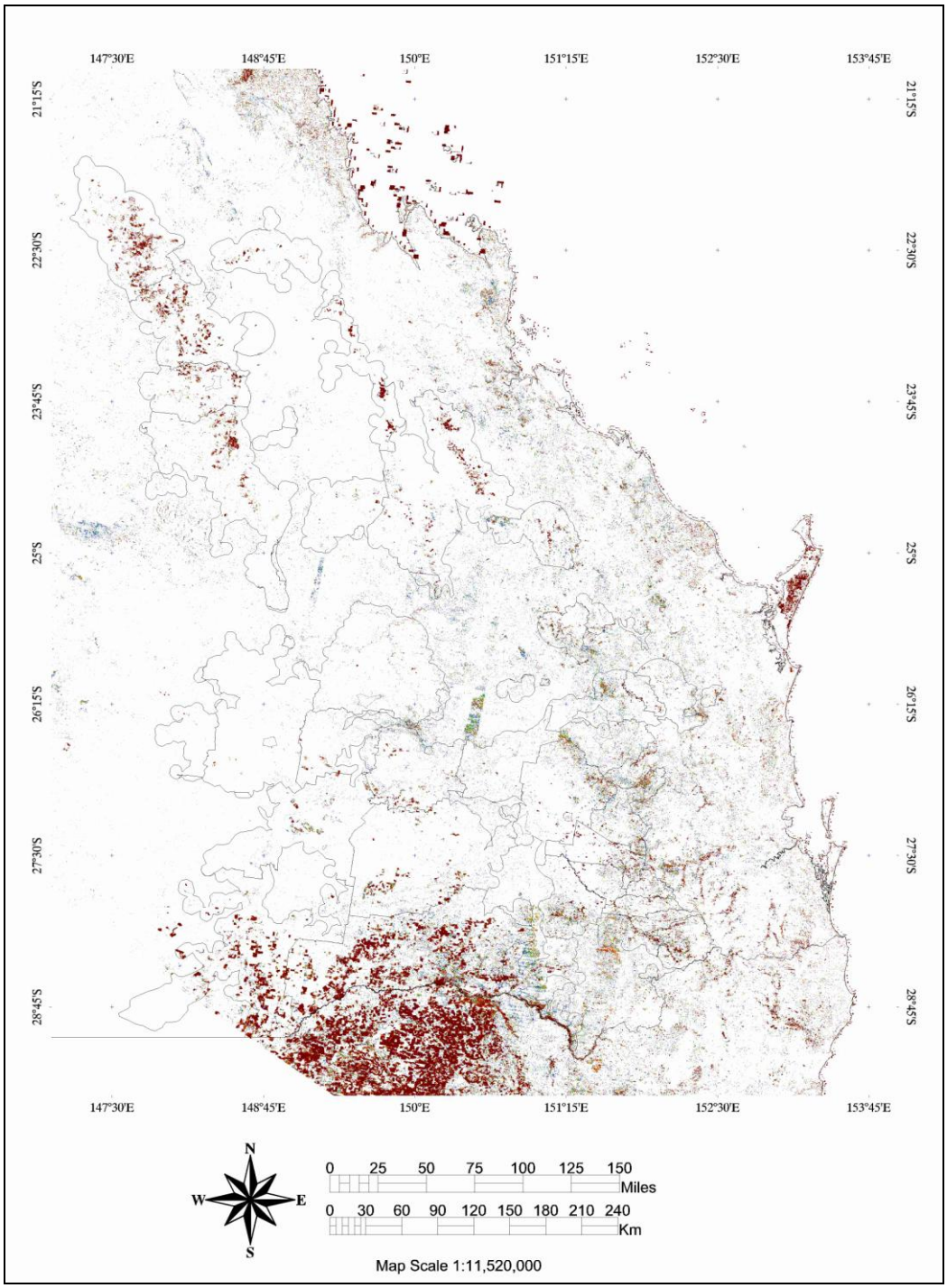

Figure 6.8: Image as derived from $\sum \Delta EVI_{T500}$ approach for August for 2006 season. No land use mask overlayed.

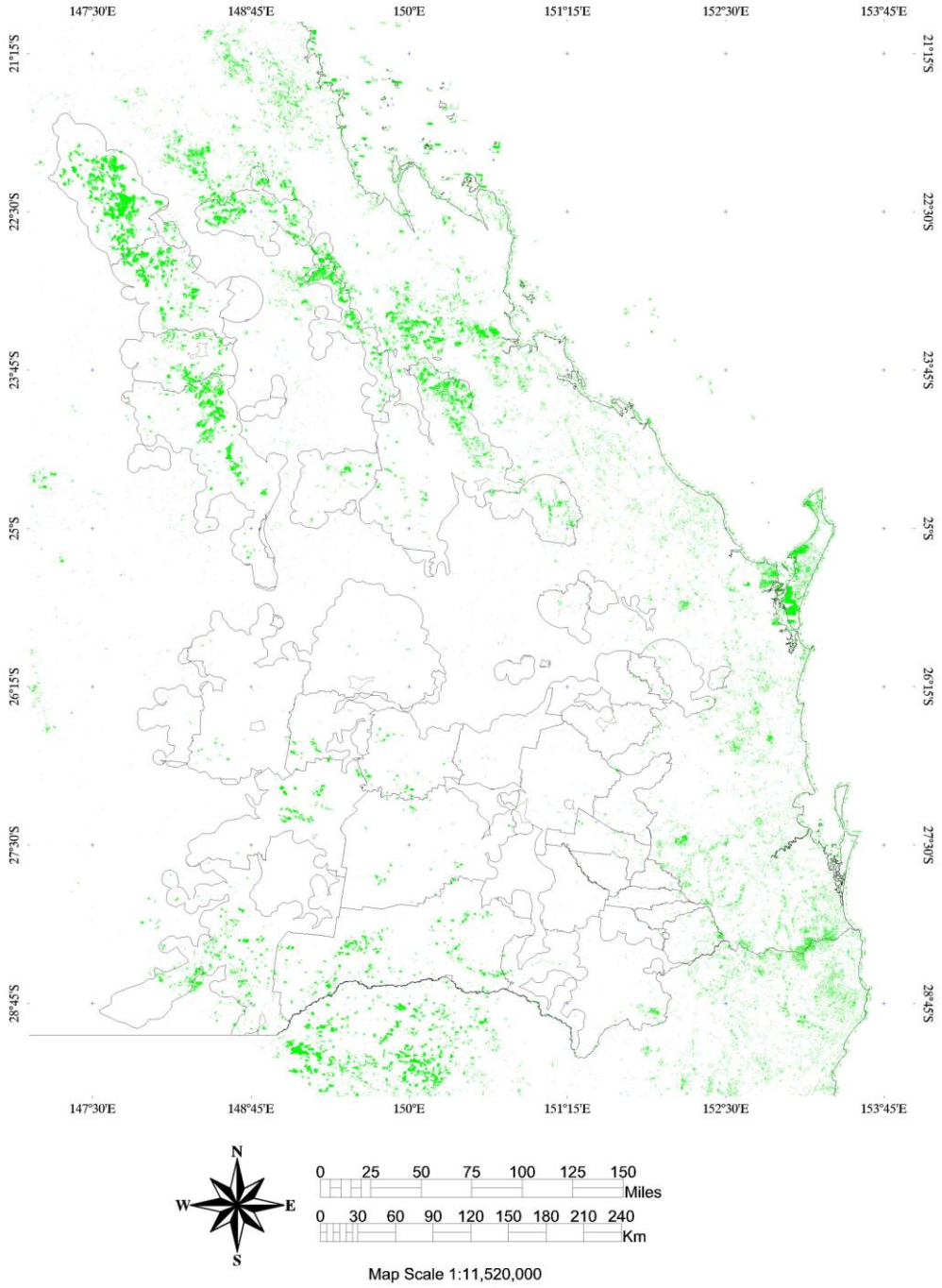

Figure 6.9: Classified image as derived from $\sum \Delta EVI_{T500}$ image for July for 2006 season. No land use mask overlayed.

region than areas of CQ. This suggested an early start to the winter cropping season in CQ due to earlier plantings in that region, while most of the winter crop in southern Queensland was planted later than in CQ. This concurred with findings in QDPI&F's crop outlook report for that season, which concluded an earlier start to the crop

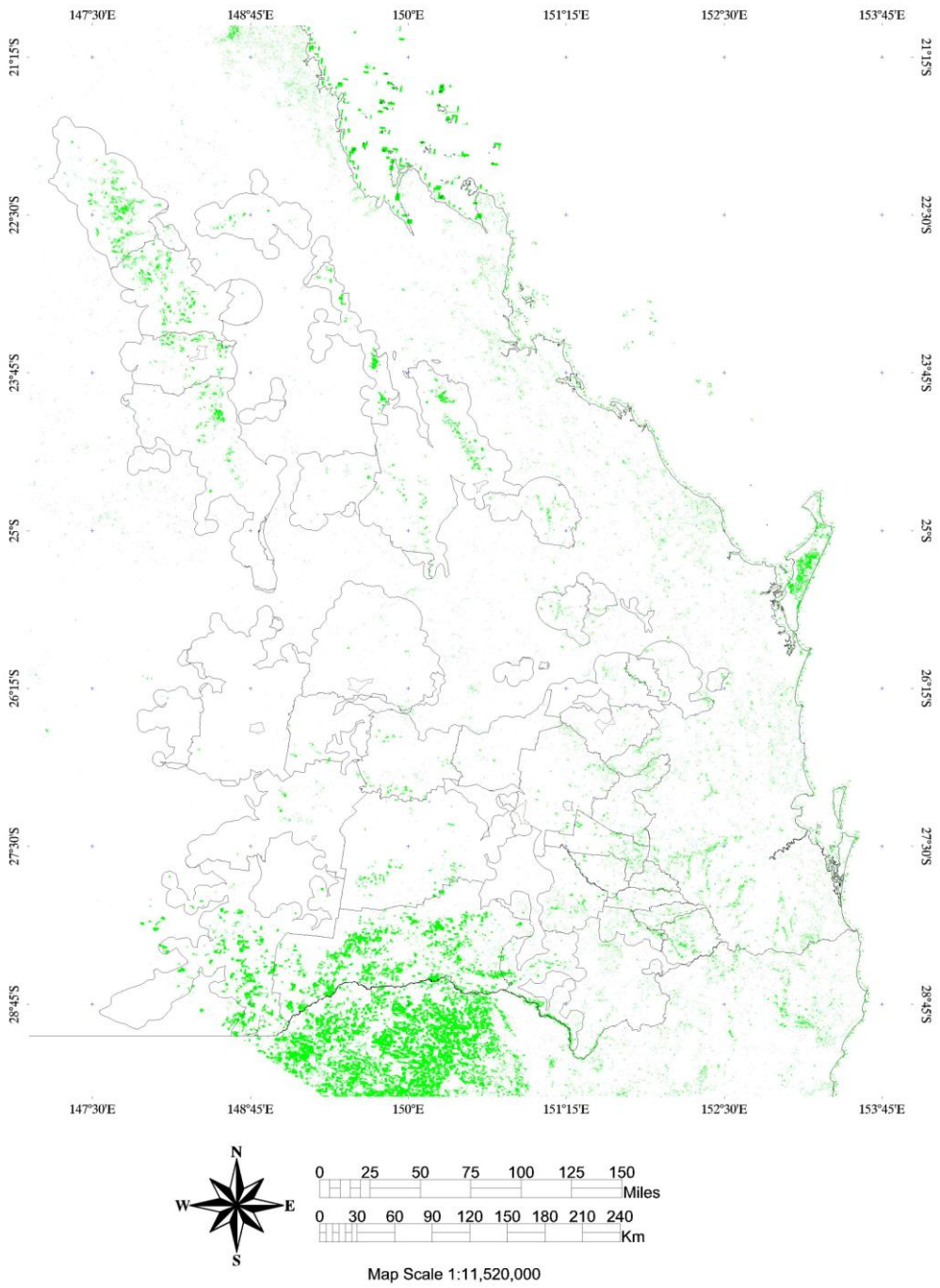

Figure 6.10: The classified image for the $\sum \Delta EVI_{T500}$ image for August for 2006 season. No land use mask overlayed.

growing season that was mainly triggered by good planting rainfall (www.dpi.qld.gov.au/fieldcrops).

6.3.2.2 Accuracy of Predicting Total Winter Crop at Pixel Scale

High accuracies were evident in predicting total winter crop area for July and August for both seasons. However, the highest accuracy was measured when combining/merging the classified crop area maps of July and August for each season. The PCC and the KC values are shown in Table 6.2. These statistics were derived after classification of the $\sum \Delta EVI_{T500}$ imagery into classified images encompassing only two classes i.e. crop and non-crop. Although the PCC was high across all periods (July and August), the merged classified $\sum \Delta EVI_{T500}$ image of July and August had the highest accuracy, with PCC values equal to 99.96% and 99.76% for 2005 and 2006, respectively. This was also the case when calculating the KC with the highest values of 0.99 and 0.78 found for the combined approach in 2005 and 2006 seasons, respectively.

The lower accuracy during the 2006 season is likely attributed to the fact that it was a much drier season in southern Queensland, which resulted in fewer training pixels (Table 6.1) for SEQ and SWQ (i.e. southern Queensland) than in CQ. This created heterogeneous cropping condition between sub-regions, which resulted in different temporal EVI crop profiles between CQ and southern Queensland for 2006. In addition, it suggested likely erroneous classification of crop and non-crop when applying training pixels grouped together from all sub-regions within the Queensland cropping region

Table 6.2: Pixel accuracy and kappa coefficient for the T500 classified imagery for July, August, Average of July and August, and the combined image of July and August for both the 2005 and 2006 seasons.

	PCC%			
	July	**August**	**Avg**	**Combined**
2005	99.72	98.85	99.29	99.96
2006	98.26	98.47	98.37	98.74
	Kappa			
2005	0.93	0.67	0.80	0.99
2006	0.66	0.59	0.63	0.78

Kappa coefficients (KC) for July, August and the combined approach (Table 6.2.) differed significantly at the 95% level (data not shown). Although the PPC values

were high and very similar for all periods and approaches, the real accuracy measured through the KC value (in the absence of chance) was the highest for the combined approach in both seasons. Hence, the combined approach was the most appropriate in determining early-season crop area estimates across regions and seasons.

6.3.3 *End-of-season Area Estimates*

6.3.3.1 Reconstructing the MODIS EVI Time Series Using the HANTS Approach

The multi-temporal HANTS approach showed good ability in mimicking the original EVI data profiles at pixel scale for the 2005 and 2006 seasons. The first three harmonics and the additive or average term (harmonic 0) were used to determine the ability of this approach to discriminate between different winter crops. Figures 6.11 (a & b) show the reconstructed (stippled line, through the HANTS approach) and the original time (solid line, observed 16-day EVI) series for a randomly selected wheat pixel for the 2005 and 2006 season, respectively. It is evident that the reduction in data from 23-images to 7-images (by applying the HANTS approach) numerically mimics the original data time series. Reconstruction of the original time series using the HANTS approach with the first four harmonics resulted in a relatively smooth EVI curve profile. However, the recreated temporal EVI profile had attributes of peak greenness, time of peak greenness and variance similar to that of the original profile. Therefore, this was not regarded as a constraint in this study since (i) 95% of the information of the original time series is accounted for using these three attributes (Lillesand et al. 2004) and (ii) the aim of this study was to discriminate between different crop canopy EVI trajectories/profiles rather than focus on differences in troughs or peaks at certain time periods during the crop growth period.

Figures 6.12 (a & b) show the average temporal EVI profile of each crop type for each sub-region for 2005 and 2006, respectively. No training samples were observed for barley in CQ and chickpea in SEQ for 2005 season, while barley for CQ and SEQ and chickpea for SEQ were not observed during fieldtrips for the 2006 season (Table 6.1). The temporal EVI profiles for barley in SWQ and SEQ were very similar for 2005 season. In addition, chickpea growth, for the training paddocks, was very similar in CQ and SWQ. Conversely, wheat canopy vigour was remarkably different from CQ, SWQ and SEQ for the 2005 season (Figure 6.12a).

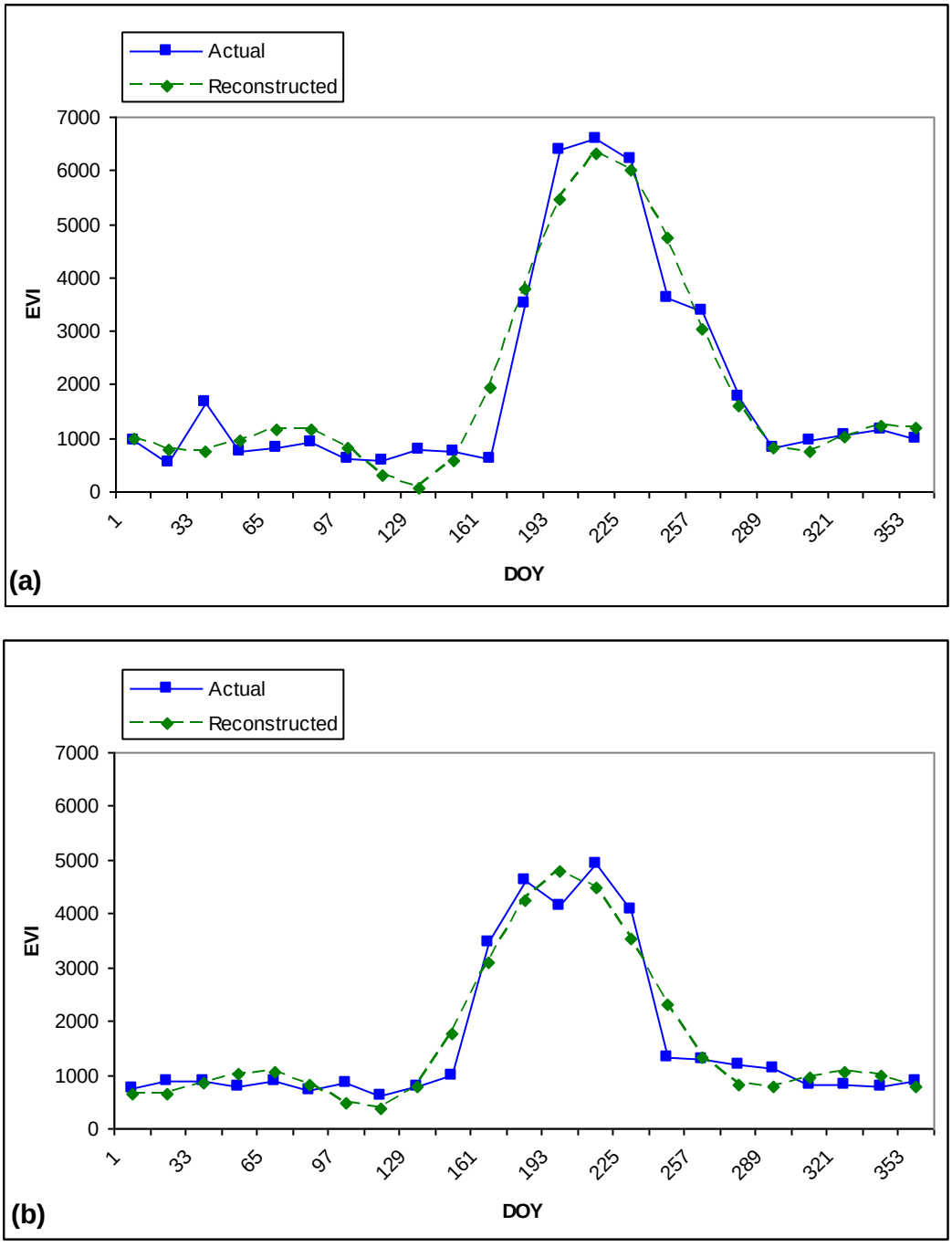

Figure 6.11: Time series of actual EVI (solid line) and reconstructed EVI (stippled line) using the HANTS multi-temporal approach for one wheat pixel for 2005 (a) and 2006 (b) seasons, respectively.

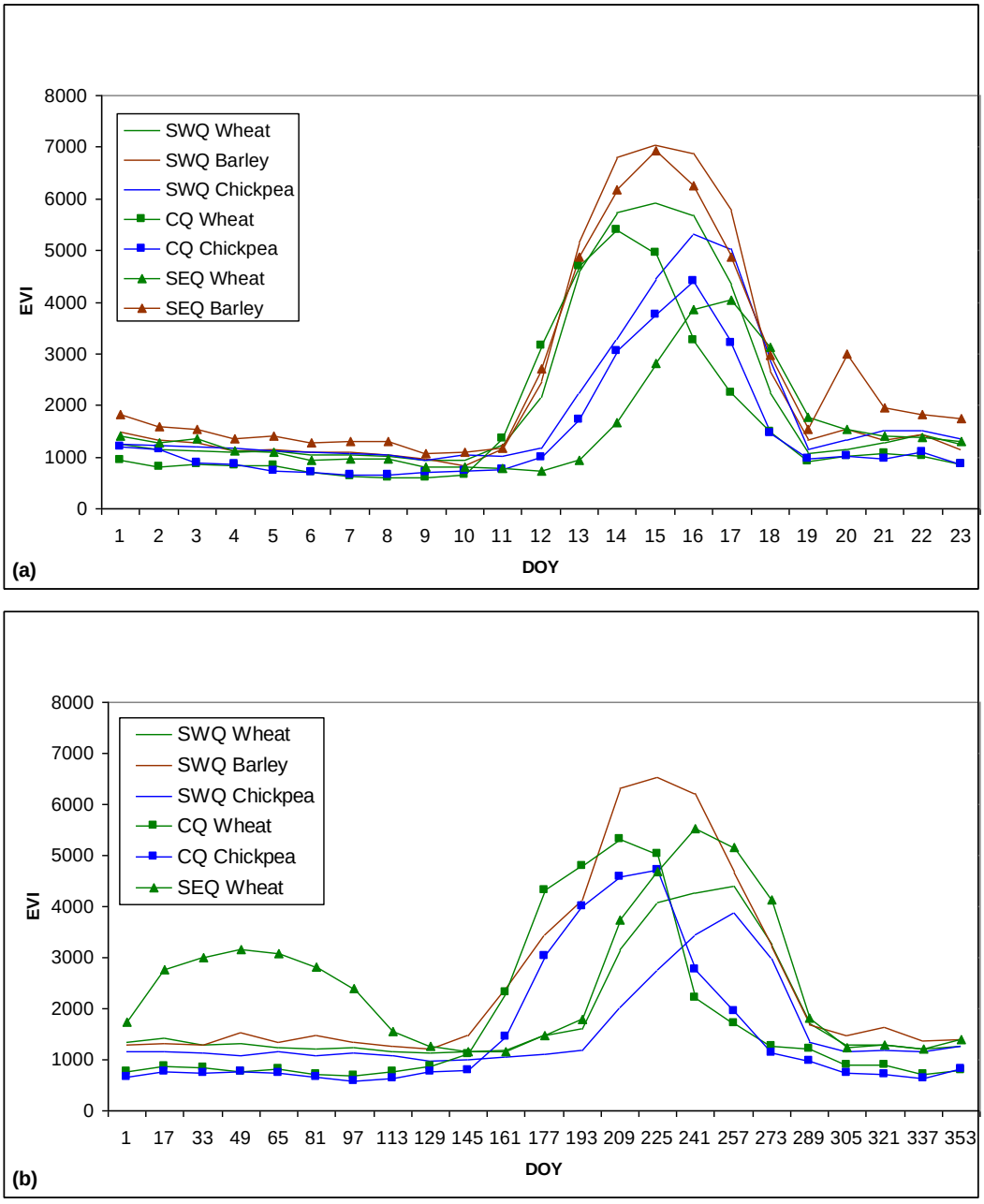

Figure 6.12: Mean temporal EVI profiles for training samples collated for SWQ (solid lines), CQ (square symbol) and SEQ (triangular symbol) for the main winter crops for 2005 (a) and 2006 (b) seasons, respectively. Wheat is displayed in green, barley in brown and chickpea in blue.

Temporal EVI profiles for the crop types for the 2006 season (Figure 6.12b) differ from the EVI crop profiles in the 2005 season (Figure 6.12b), mainly in timing and magnitude of maximum crop canopy growth. In general, crop (wheat and chickpea) emergence was at least one month earlier (DOY 161) in CQ than in SWQ (DOY 193) (Figure 6.11b). Barley was only observed in SWQ, while only wheat was observed for the SEQ region during that season. The mixed crop canopy patterns were mainly

due to the spatial variability in rainfall amount and timing within each sub-region. It also emphasises the importance of capturing sufficiently large samples of training points within each sub-region.

6.3.3.2 Pixel-scale Accuracy at the End-of-season

6.3.3.2.1 Accuracy at the Whole of Queensland Level

The accuracy when using all training samples to discriminate between pixels classified as wheat, barley, chickpea or non-crop for the entire cropping region was substantially high with PCC values of 99% and 98% for 2005 and 2006 seasons, respectively (Table 6.3). Although these PCC values were relatively high, the *kappa coefficients* were moderately lower with values of 0.87 and 0.79 for 2005 and 2006 seasons, respectively. The KC values suggested a slight chance of misclassification of some crop types, which is to be expected. The reduction in accuracy is likely to mainly come from the misclassification of wheat, which showed lower PCC values of 70% and 62% for 2005 and 2006, respectively. Conversely, the accuracies (PPC) for barley and chickpea were 96% and 93% for 2005 and 85% and 93% for 2006.

6.3.3.2.2 Accuracy at Sub-regional Level

Limiting the use of ground truth training data to within sub-region, substantially improved the accuracy levels across sub-regions, and within seasons. Specifically, the accuracy for correctly classifying observed wheat pixels, using the maximum likelihood classifier on the HANTS derived data, improved from 70% to 95% for the 2005 season and from 62% to 82%, for the 2006 season.

PCC values close to 100% (Table 6.3) are likely to be an over estimation of the real accuracy for these crop categories. Although all the random independent observed samples were correctly classified this was largely a result of the small sample size (~ 6) (Table 6.1). The *true* classification accuracy for these crops is closer to 85% given that the ground truth sample sizes for training the classifier (i.e. HANTS) was greater than 20 samples (Mather 1999; Van Genderen et al. 1978).

Table 6.3: PCC for all winter crops and non-crop (Other) for Queensland, SWQ, CQ and SEQ regions. The kappa coefficient is given in closed brackets.

	QLD	SWQ	CQ	SEQ
		2005		
Wheat	70	88	97	100
Barley	96	94	na	100
Chickpea	93	100	83	na
Other	100			
Overall	99	(0.87)		
		2006		
Wheat	62	74	71	100
Barley	85	86	na	na
Chickpea	93	92	86	na
Other	100			
Overall	98	(0.79)		

6.3.3.3 Merging of Sub-region Classified Images to Create Whole of Queensland Image

Merging the classified images for each sub-region resulted in improved crop discrimination at the sub-region level. Figures 6.13a and 6.13b show the final classified areas for wheat, barley, chickpea and non-crop when merging the final classified images for each sub-region for 2005 (Figure 6.13a) and 2006 (Figure 6.13b), respectively. More pixels were classified as winter crop during the 2005 season than the 2006 season. This was mainly because the 2006 recorded below average rainfall, especially in the southern parts of Queensland's cropping region. This season was classified as an El Niño year by the Bureau of Meteorology (www.bom.gov.au) early in the 2006 season. El Niño years usually coincide with below average rainfall in most of eastern parts of Australia (Allan 2000), and thus poor winter cropping seasons (Potgieter et al. 2002; Potgieter et al. 2005b). Overall, more barley was evident during the 2005 season in the southern region of Queensland than in CQ. During the 2006 season, more pixels were classified as chickpea in CQ than was evident in the southern parts of Queensland.

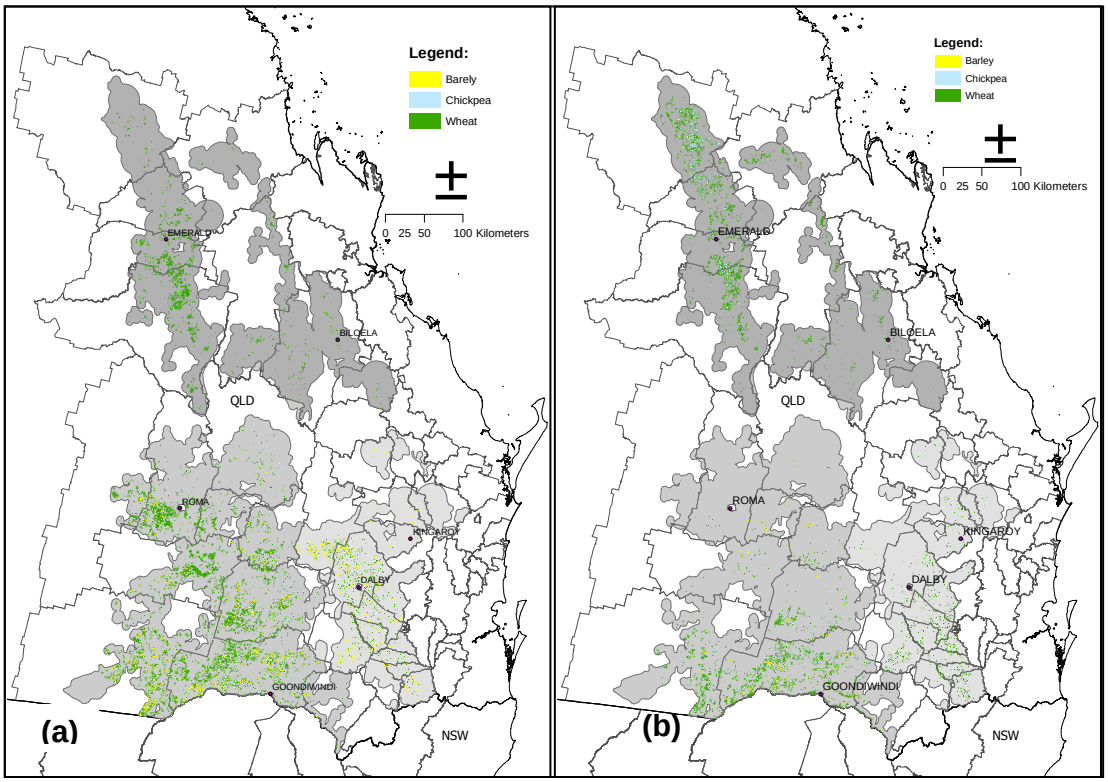

Figure 6.13: Final classified areas for wheat, barley, chickpea and non-crop (grey) when merging the final classified images for each sub-region (SEQ – light grey, SWQ – medium grey and CQ – dark grey) for 2005 (a) and 2006 (b), respectively.

6.3.4 *Feature Classification and Validation at Regional Scales*

6.3.4.1 Early-season method

6.3.4.1.1 Total Crop Area Prediction

State level area estimate data for wheat, barley and chickpea for the 2005 and 2006 seasons were published by ABARE in their quarterly commodity forecast reports (Table 6.4). Predictions derived from the $\sum \Delta EVI_{T500}$ early season approach were contrasted against the ABARE data for the 2005 and 2006 seasons. The ABARE data was generated from surveyed values from industry as well as expert knowledge for areas harvested to wheat, barley and chickpea and total winter area. The total winter crop area estimated by ABARE equates to ~1 million hectares for the 2005 season and ~0.7 million hectares (Ha) for the 2006 season with an error of between 20% to 50% (Lawrance 2007).

Table 6.4: Total winter crop and specific winter crop area figures for Queensland as published by ABARE for the 2000 to 2006 seasons (Lawrance 2007).

Year	Wheat (000 Ha)	Chickpea (000 Ha)	Barley (000 Ha)	Total (mHa)
2000	885	71	112	1.1
2001	604	46	96	0.8
2002	514	111	108	0.7
2003	790	76	151	1.0
2004	711	41	97	0.9
2005	799	36	146	1.0
2006	550	41	90	0.7

Early-season prediction of total winter crop area estimates from MODIS imagery are given in Table 6.5. These predictions were summed within the land use mask of 1999. This was done to limit the green-up areas to only those areas known to be used for cropping, since some pastures/fodder or forest areas are also likely to show green-up in canopy vigour during winter. This partially avoids an over-estimation of crop area planted.

The estimates for total winter crop area ranged from 715,000 ha to as high as 1.28 million ha for the 2005 season (Table 6.5). Although the average area of July and August was the closest to the ABARE figure of 1 mHa, it is likely to be spurious, since the pixel accuracy (i.e. *kappa coefficient*) was the highest for the combined early-season approach (Table 6.2).

Table 6.5: Total winter crop predictions using the early-season $\sum \Delta EVI_{T500}$ approach as described in Chapter 5. These estimates were accumulated within the land use polygons of 1999.

Season	July	August	Average	Combined
2005	1284345	715113	999729	913962
2006	319234	278773	299003	515483

The prediction using the combined approach was 8.6% below the total winter crop area estimate of ABARE for 2005 (Figure 6.14). Early-season predictions for the 2006 season ranged from 278,000 ha to 515,000 ha. The combined approach prediction of 515,000 ha had the smallest error of 184,000 ha (i.e. 26%), below the ABARE figure of 700,000 ha, of all early-season approaches, which was consistent

with the higher pixel accuracy of this approach (Table 6.2). The use of the combined approach showed high overall accuracy both at pixel (reference data) as well as regional (ABARE estimates) scales. A bias towards under estimating the ABARE data was noticeable for almost all early-season approaches (Figure 6.14). This was likely a result of the 1999 land use mask overlay, which had less area that could be cropped than what is currently classified as dryland cropping. This is discussed later in more detail (Section 6.3.4.2.2). Finally, it is envisaged that the derived early-season approach could also be applied to improve on total winter crop area estimates or fill-in the *gaps* for years when ABS agricultural census data was not available as was elucidated in Chapter 5.

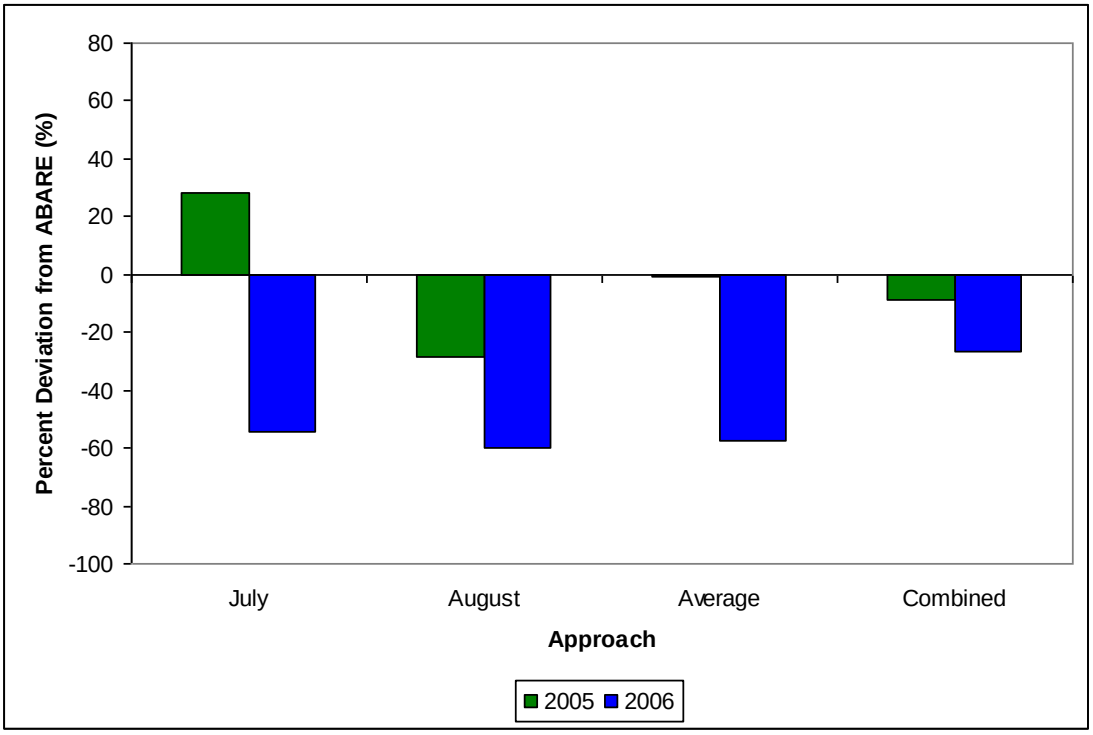

Figure 6.14: Percent deviation of total winter crop predictions from the actual ABARE data for both seasons. The early-season $\sum \Delta EVI_{T500}$ approach (for July, August, Average and Combined) as described in Chapter 5 was used. These estimates were accumulated within the land use polygons of 1999.

6.3.4.2 End-of-season Method

6.3.4.2.1 Total Crop Area Estimates

Crop area estimates from the HANTS approach were also compared with ABARE survey data. Total winter crop area estimates were calculated merging data from each sub-region, which were classified using only training samples from within that sub-

region (i.e. *sub-regional approach*), with no land use mask (Table 6.6c and 6.7c). This resulted in total winter crop area estimates of 1057,000 ha (+5.7%) and 621,000 ha (-11%) compared to the ABARE figures of 1 mHa and 0.7 mHa for Queensland for 2005 and 2006, respectively. Using all ground truth observations to classify the entire Queensland cropping area with no land use mask generated discrepancies of 43% and 29% for 2005 and 2006, respectively (Table 6.6a and 6.7a). While part of this error can be attributed to error in the ABARE data as mentioned in the previous section. The result highlights the need for classification at the subregion level.

Tables 6.6 and 6.7 (a) and (b) give the crop area estimates derived by training the HANTS images on observed sampling points across the entire Queensland region, while (c) and (d) are the estimates derived when the HANTS imagery was classified at sub-region level (i.e. sub-regional approach). The results derived when no land use mask was applied is given in (a) and (c), while the results when the land use mask was applied are shown in (b) and (d). Detail aggregated shire level area estimates are given in Appendix B, in Tables 5 to 12.

6.3.4.2.2 Crop Area Estimates Using Land Use as Primary Mask

Large discrepancies from ABARE estimates were evident in the final total Queensland area estimates when the end-of-season HANTS approach area estimate was derived either with or without a land use mask. The difference was 635,070 ha in 2005 when no land use mask was used (Table 6.6 and 6.7) and training of pixel classification was based on all Queensland (QLD) ground truth sampling points (QLD method in Table 6.6a and b, region = Queensland). When the sub-regional approach to pixel classification was used, this difference was reduced to 411,000 ha (Table 6.6c and d, region = QLD). For the 2006 season, these differences between using no land use mask and using the land use mask were 317,000 ha (for the all QLD training method) (Table 6.7a and b, region = QLD) and 182,000 ha (for the sub-regional training method) (Table 6.7c and d, region = QLD). Thus, the land use mask introduces a bias towards under estimating the total and specific winter crop area within a specific season. These differences in area estimates can mainly be attributed to a change in land use patterns since 1999, specifically in the south western parts of the QLD cropping region (Figure 6.15a and b).

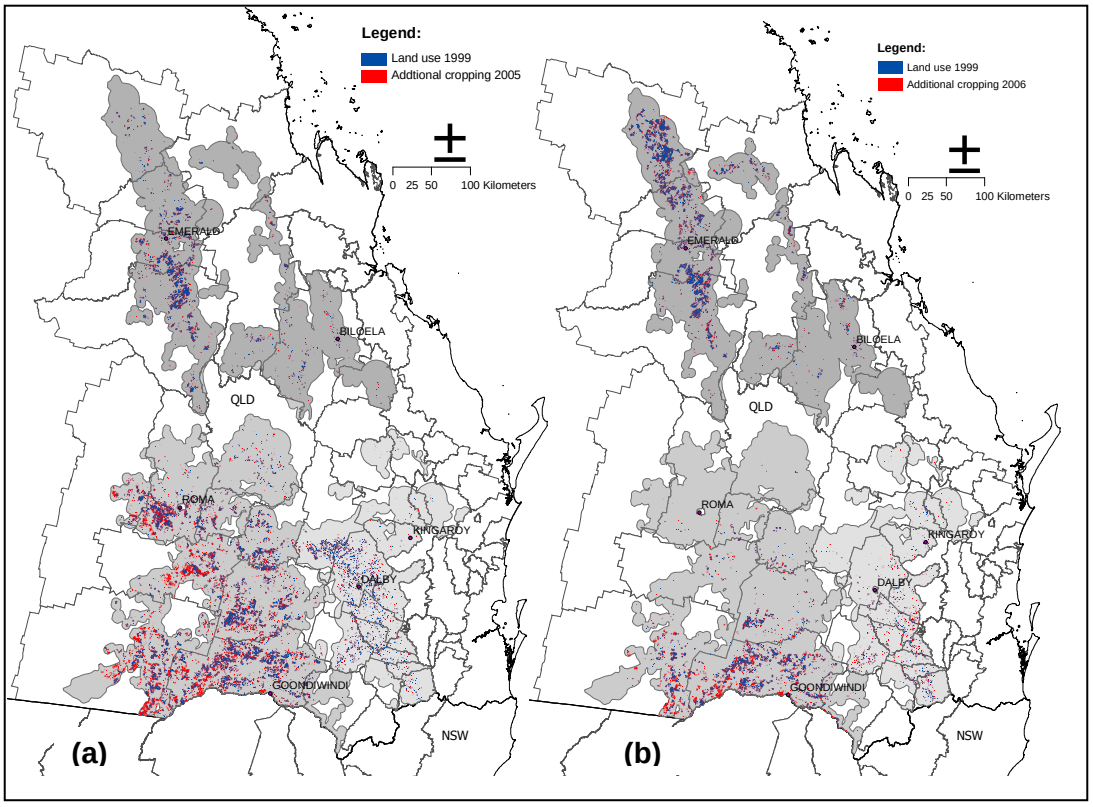

Figure 6.15: The likely difference in land use for winter cropping between 1999 (blue) and either 2005 (a) or 2006 (b). Red areas show the areas likely to be currently cropped and not cropped in 1999.

Closer investigation of the red areas showed temporal EVI trajectories similar to that of winter cropping for both seasons (data not shown). This illustrates the importance of using accurate up-to-date land use maps when determining early-season winter crop area estimates, whereas by the end-of-season, classification of non-cropping areas had high accuracy at pixel scale (Table 6.2). The end-of-season HANTS approach showed high accuracy in correctly classifying non-crops (i.e. Other in Table 6.1) generated from a very large number of sampling points across QLD during both seasons. This suggests that the multi-temporal HANTS approach could be used in detecting changes in land use patterns related to cropping. This concurs with earlier research elucidating the success in the use of time series analysis (e.g. HANTS) in determining broad land use patterns (Hall-Beyer 2007; Menenti et al. 1993; Verhoef et al. 1996; Wannebo et al. 2000).

Table 6.6: End-of-season area estimates (Ha) for each sub-region and at state level for 2005 based on whole of Queensland (a and b) regional training of pixels (c and d). The area estimates were derived either without (a and c) or with (b and d) the 1999 land use overlay.

(a) Method	Region	Total	Wheat	Barley	Chickpea
	CQ	204579	181539	17178	5863
QLD	SWQ	1109216	787018	234712	87486
no land use	SEQ	122827	95371	17056	10400
	QLD	1436622	1063928	268946	103748

(b) Method	Region	Total	Wheat	Barley	Chickpea
	CQ	160961	142827	12627	5507
QLD	SWQ	543692	364722	128769	50201
land use	SEQ	96899	76264	13164	7472
	QLD	801552	583812	154560	63180

(c) Method	Region	Total	Wheat	Barley	Chickpea
	CQ	173736	171633	0	2103
Sub-region	SWQ	778037	655830	84368	37840
no land use	SEQ	105382	51368	54014	0
	QLD	1057155	878830	138382	39943

(d) Method	Region	Total	Wheat	Barley	Chickpea
	CQ	141641	139645	0	1996
Sub-region	SWQ	422262	351292	46621	24349
land use	SEQ	81819	47222	33789	808
	QLD	645722	538159	80410	27154

6.3.4.2.3 Specific Crop Area Estimates

Specific crop area estimates, using the HANTS sub-regional approach and with no land use mask, showed high accuracy for wheat, barley and chickpea for 2005 and for wheat in 2006, but poor accuracy for barley and chickpea in 2006, when compared to the surveyed ABARE data. The deviations in area estimates for wheat, barley and chickpea were 9.9%, -5.2% and 10.9% and -2.8%, -78% and 64% for 2005 and 2006, respectively (Figure 6.16).

The large error in area estimates for barley and chickpea in 2006 can mostly be attributed to the imperfect ABARE estimates, which showed large relative survey errors as discussed earlier. This was further confirmed through anecdotal statistics from experts in the field. An extension officer in CQ (Lynch 2007) and the development officer of pulses Australia's northern region (Cumming 2007), estimated the chickpea area planted during 2006 in CQ to be close to 50,000 ha, which makes the HANTS estimate of 67,000 ha a much more realistic estimate of what could have

occurred during that season across QLD. The ABARE estimate was 41,000 ha for chickpea for the entire QLD cropping region suggesting a large under estimation for chickpea in 2006.

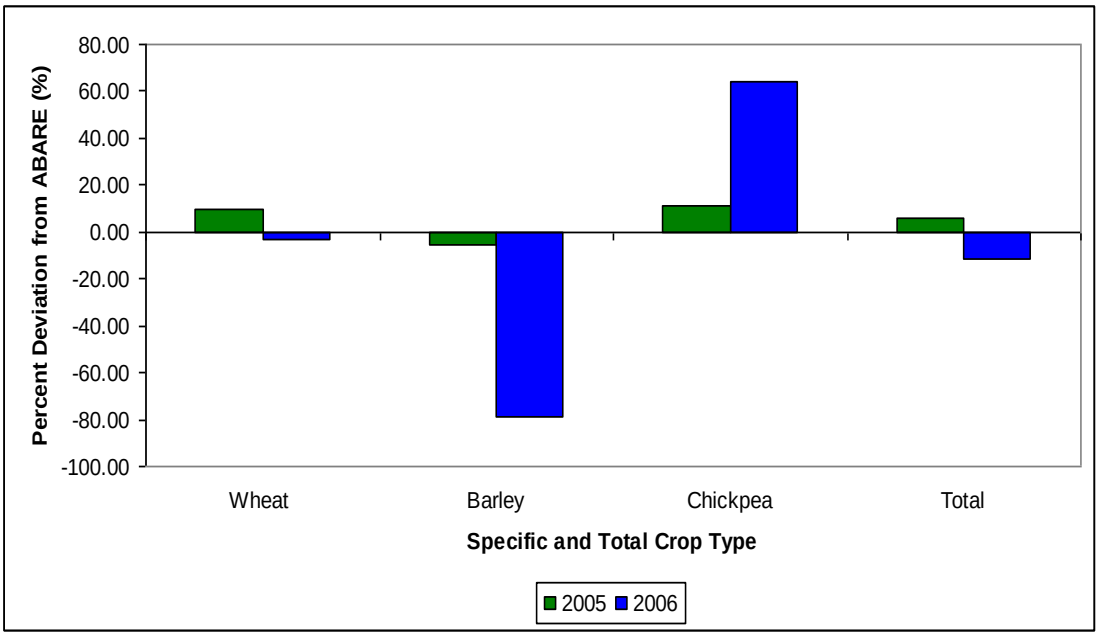

Figure 6.16: Percent deviation (%) of end-of-season area estimates from ABARE estimates fro each crop and total winter crop, using the sub-regional HANTS approach with no land use overlay for both the 2005 and 2006 seasons.

For barley during the 2006 season, the error was likely a result of barley being misclassified as wheat (therefore the over estimation of wheat area). However, some barley crops traditionally get fed-off or could have failed, specifically during the 2006 season when very little rain was recorded in most of the southern Queensland cropping region. Furthermore, no barley paddocks were included in the training samples for CQ and SEQ, which also resulted in no area been classified to barley for the 2006 season for those regions, thus an underestimation of the area planted to barley.

Table 6.7: End-of-season area estimates (Ha) for each sub-region and at state level for 2006 based on whole of Queensland (a and b) regional training of pixels (c and d). The area estimates were derived without (a and c) or with (b and d) the 1999 land use overlay.

(a) Method	Region	Total	Wheat	Barley	Chickpea
	CQ	390517	320998	23470	46049
QLD	SWQ	423223	313151	16038	94034
no land use	SEQ	88820	86438	924	1458
	QLD	902559	720587	40432	141540

(b) Method	Region	Total	Wheat	Barley	Chickpea
	CQ	296713	235551	17656	43506
QLD	SWQ	234444	169334	9729	55381
land use	SEQ	54387	52699	485	1203
	QLD	585545	457584	27871	100090

(c) Method	Region	Total	Wheat	Barley	Chickpea
	CQ	288929	248841	0	40089
Sub-region	SWQ	282122	235774	19100	27248
no land use	SEQ	49923	49820	0	104
	QLD	620975	534434	19100	67440

(d) Method	Region	Total	Wheat	Barley	Chickpea
	CQ	246183	208111	0	38072
Sub-region	SWQ	162513	134173	11532	16809
land use	SEQ	29967	29572	301	95
	QLD	438664	371856	11832	54975

6.3.5 Shire-scale Accuracy for the 2005 Season

High accuracy was evident when contrasting predicted shire-scale crop area estimates against actual shire scale area estimates for total and specific crops in 2005. The predicted area estimate was highly correlated with the actual total winter crop area estimates and not significantly different from the 1:1 relationship (Figure 6.17a and b) for the 2005 season across Queensland. The accuracy of early-season $\sum \Delta EVI_{T500}$ combined and end-of-season (HANTS no land use) time-series approaches to determine area estimates across all main winter crop producing shires for QLD was assessed by contrasting actual area figures (ABS 2008) against predicted area estimates for wheat, barley and chickpea at both periods for the 2005 season. The percentages of variance in observed area explained by end-of-season area estimates using HANTS (with no land use overlay) were 89% (R^2 = 0.89), 82% (R^2 = 0.82) and 52% (R^2 = 0.52) for wheat, barley and chickpea, respectively for that season. This indicated high accuracy for final predictions for wheat and barley across

shires for 2005. The accuracy for determining the final chickpea area was not as good. This suggested a much weaker ability of this approach to discriminate chickpea from the other two crops for 2005 season, which was likely caused by the small training sample size (43 samples in total (SWQ), Table 6.1) collated and subsequently used to classify the image. The low training sample number could mainly be attributed to the small area planted to chickpea for the 2005 season compared to the 2006 season (Lawrance 2007), thus making it even more difficult to capture enough ground truth observations across the region for that season. The early-season approach (combined T500) explained 87% (Figure 6.11a) and the end-of-season explained 92% (Figure 6.17b) of the total variation of the actual observed ABS winter crop area estimate across all shires for 2005. Both the early-season and end-of season approaches had relatively small but similar standard errors (se) of 16,380 ha and 12,850 ha, respectively.

The discrepancies between actual and predicted for the early-season estimate are likely a result of very early or very late planted crops, as well as canopy vigour measured from other crops, such as fodder and/or lucerne, which are traditional winter crops for cattle. The likely error in the land use map of 1999 used as a mask-out, as discussed earlier, is also contributing to the variability in the predictions, especially in shires having planted areas of greater than 50,000 ha (Figure 6.17a). Using the early-season approach to predict total winter crop area showed a useful ability to predict actual crop area across all shires for 2005. The fitted regression was very close (slope (b) = 1.02) to the 1:1 relationship.

Predicted end-of-season crop area estimate was highly correlated with actual area and significantly different from a 1:1 relationship (Figure 6.11b). Differences in the final estimate for total winter crop area and the actual data across all Queensland shires are likely a result of the error associated with the reduction in the temporal information (i.e. from 23 to 7-images) using the HANTS approach. Another likely source of error could be the insufficient collating of crop canopy spectral profiles sampled through the ground truthing process.

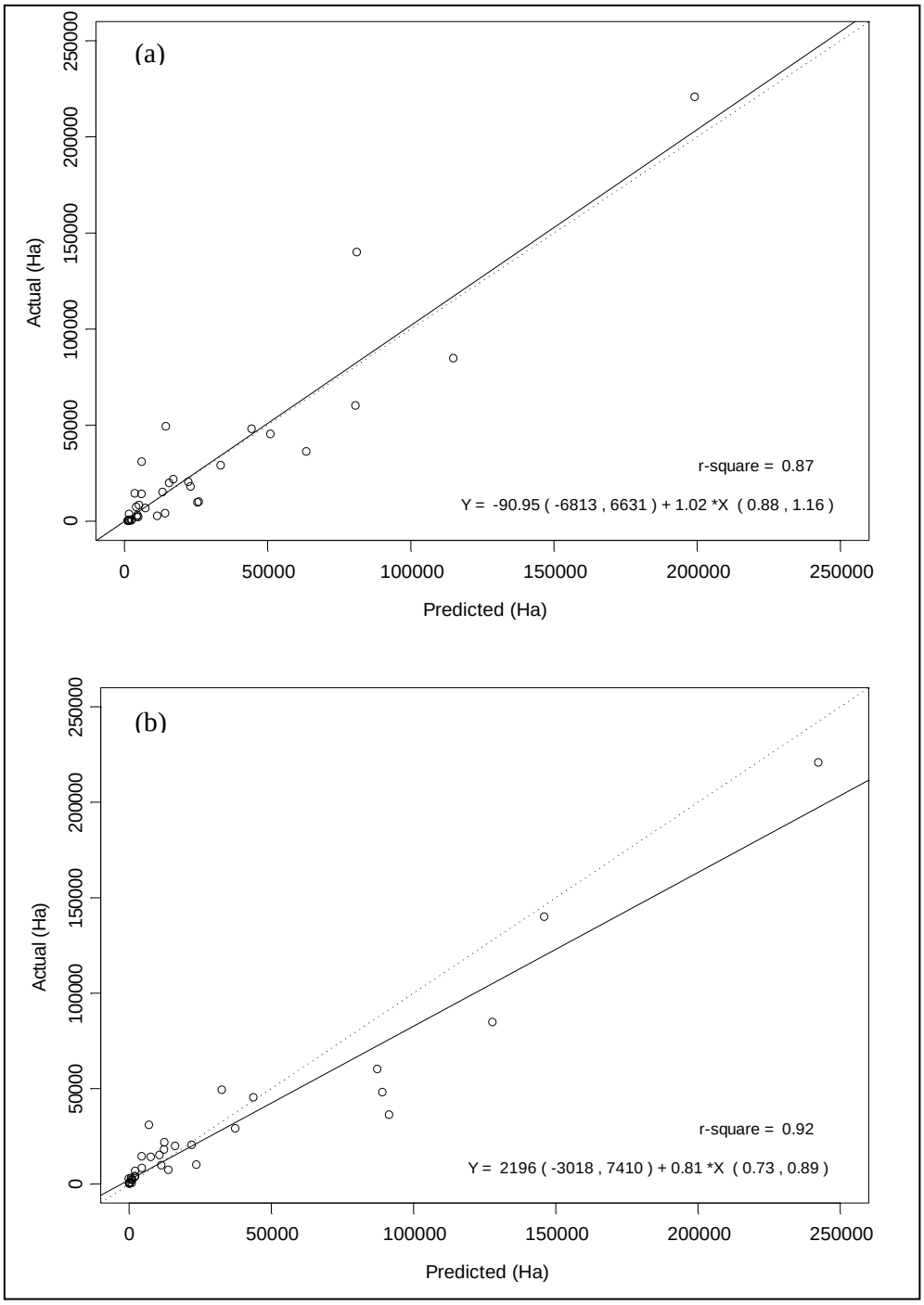

Figure 6.17: Scatter plot of the (a) predicted early-season total winter crop area estimate for each shire (Combined $\sum \Delta EVI_{T500}$ approach) and the (b) end-of-season total winter crop area estimate for each shire (HANTS). The portion of variance explained is given as the r-square on each graph. Lower (ll) and upper (ul) 95% confidence intervals (CI) are included in brackets for each coefficient in the equation: Y = a (llCI, ulCI) + b*X (llCI, ulCI). The 1:1 line is shown as a stippled line, while the solid black line is the fitted regression line. Where a is the intercept and b is the slope.

Conversely, the predicted area estimates could also be closer to the *true* estimate of total cropping area than the census data, since the actual observed ABS census shire data had relative accuracies of between 10% to 25% for wheat and barley and up to 50% for chickpea depending on the sampling numbers within each shire (ABS 2008). Hence, the predictions are within the bounds of the ABS estimates.

Overall, the early-season approach showed significant correlation and comparable accuracy to predict actual total winter crop area across QLD during the 2005 season. This was comparable to that achieved by using the end-of-season approach, which suggests appreciable value in application for industry.

6.3.6 Value to Industry

The combined $\sum \Delta EVI_{T500}$ approach for early-season estimates of total winter crop area as well as the end-of-season HANTS approach to discriminate between wheat, barley and chickpea showed appreciable accuracy. The land use map of 1999 seems to be outdated and the time series analysis approach (e.g. HANTS) could be used to accurately discriminate between cropping and non-cropping areas as illustrated here. This study successfully applied the multi-temporal approaches, derived in Chapters 4 and 5, across different regions and seasons.

This study found that the multi-temporal $\sum \Delta EVI_{T500}$ and the HANTS approach can be used to determine the *missing link* in crop forecasting, i.e. planted area. Further, this could be achieved before flowering as well as after maturity. Such estimates can now be readily integrated with the commodity forecasting system of QDPI&F to create production estimates for winter crops at shire scale across large regions.

It as expected that this technology will be transferable, though with sufficient resource allocation, to different cropping seasons (i.e. summer crops) and other regions across Australia. The utility of this technology will mainly depend on the trade-offs between risk (depending on accuracy) and value (determined by the timeliness of the information) of such information to the grains industry decision-making processes. It is envisaged that the main value of this proposed predictive area

estimate methodology will come from the ability of the system to predict firstly, total winter crop area estimates before harvest, secondly, the ability to transform the area and yield estimates into a production estimate, and finally, the ability to accurately discriminate between specific crops within a growing season.

6.4 Conclusion

Multi-temporal approaches that used MODIS imagery during the season and at end-of-season showed appreciable prediction accuracy for total (1 to 2 months before flowering) as well as specific winter crop area estimates (after harvest) across different seasons and regions. Accurate area estimates were mainly evident using no land use overlay when determining end-of-season area estimates as new areas had likely come into cropping. Early-season crop area estimates showed high accuracy and had a lead time of up to four months before harvest. Higher accuracy in area estimates was achieved when pixel training for crop classification was done at sub-regional level.

It is anticipated that this forecast, which will be integrated with the shire yield prediction of QDPI&F, will be of significant value to agri-business in their decision-making processes, such as bulk handling of grain and hedging of financial risk by forward buying or selling of crops within a current season. Successful implementation will require a systemised approach to ground truthing for pixel classification for each season and sub-region. Further research is necessary to update the land use change patterns, from the 1999 land use overlay. This research contributes to the body of production knowledge within the agricultural industry and is innovative, original and transparent, in determining early-season total winter crop area estimates and crop specific end-of-season area estimates.

Chapter 7

Summary, Concluding Remarks and Recommendations

"To know that you know, and to know that you don't know - that is real wisdom."

Confucious (551-479 BC)

7.1 Summary

Since early settlement, the existence of most rural communities in Australia has depended on agriculture. Dryland cropping has been one of the main activities contributing towards the long-term viability and sustainability of these communities. This is still true today. However, the operating environment of producers has become more challenging. Food producers are increasingly exposed to variability and change in world markets, commodity prices and climate, thus increasing their vulnerability and threatening their livelihoods. Advance knowledge of the associated risk in crop production, however, can mitigate some of the impact of such factors. Hence, easily accessible, near real-time, objective and accurate crop production information is becoming increasingly valuable in decision-making for agricultural industry and government agencies. To date, industry and crop forecasters have had a good idea of the potential crop yield for a specific season, but accurate, timely and objective information on crop area for a shire or region has been mostly unavailable. The main aim of this thesis was to develop approaches to estimate crop area, i.e. the *missing link*, across different regions and seasons using remotely sensed information available in near real-time.

This issue was addressed by developing and applying mutli-temporal remote sensing techniques to determine winter crop area estimates at regional scale. Particularly, this study set out to:

- Assess the ability of a range of approaches to using multi-temporal MODIS imagery to estimate total end-of-season winter crop area;
- Determine the discriminative ability of such remote sensing approaches in estimating area totals for wheat, barley and chickpea within a specific cropping season;

- Develop and evaluate the methodology for determining the predictability of crop area estimates well before harvest for wheat, barley and chickpea; and
- Validate the ability of multi-temporal MODIS approaches, as derived in the study region, to determine the pre-harvest and end-of-season winter crop area estimates for different seasons and regions.

Chapter 4 illustrated the ability of multi-temporal EVI MODIS trajectories to determine total as well as specific winter crop area estimates after harvest (i.e. the first two objectives) for the Jondaryan and Pittsworth shires for 2003 and 2004 winter crop seasons. The multi-temporal HANTS, MEVI, Curve fitting functions (i.e. CF1, CF2) and PCA methods showed high accuracy in discriminating between crops and non-crops as well as non-crops from specific crops like wheat, barley and chickpea at pixel and shire scales. The use of multi-temporal approaches performed significantly better than the traditional single-date approach at maximum canopy growth (around flowering), which is likely to produce spurious crop area estimates at shire scale. This is mainly due to the fact that the timing or acquisition date of the image is usually out of sync with maximum canopy growth, which coincides with flowering, as a result of variable planting dates within a shire. The increased capability, as demonstrated here, of the derived multi-temporal approaches to discriminate total and specific shire scale winter crops is mainly attributed to the use of all available canopy vigour information measured through the crop growth EVI profile of the entire cropping season. This allowed the capturing of all phenological stages and subsequent interactions between soils, climate, crop management practices and pest and diseases at a pixel scale.

The research question of "*how early and with what accuracy?*" area estimates can be determined using multi-temporal MODIS EVI imagery was investigated in Chapter 5. This was done for two study shires (i.e. Jondaryan and Pittsworth) for the 2003 and 2004 seasons. Since discrimination between specific crops was most accurate after harvest (Chapter 4), the focus in this chapter was on deriving total winter crop area estimates (including wheat, barley, chickpea and other minor crops like forage). A simple metric, which measures the green-up rate of the crop canopy, was derived. This was done by calculating the accumulated difference of three

consecutive images for three consecutive 16-day EVI threshold cut-offs ($\sum \Delta EVI_i$, where i = 250, 500 and 750) at monthly intervals from April to October. July showed the highest pixel accuracy with percent correctly classified for all thresholds of 93.7% and 97.9% for 2003 and 2004, respectively. The differences in accuracy between the three cut-offs were minimal and the T500 threshold was selected as the preferred cut-off to avoid measuring too small or too large fluctuations in the differential EVI values.

When compared to the ABS survey data on crop area across shires and seasons, average percent differences for the $\sum \Delta EVI_{T500}$ for July and August ranged from -19% to 9%. To capture most of the variability in green-up within a region, the average $\sum \Delta EVI_{T500}$ of July and August was used for the early-season prediction of total winter crop area estimates. This resulted in high accuracy (R^2 = 0.96; RMSE = 3,157 ha) for predicting the total winter crop from 2000 to 2004 across both shires. This result indicated that this simple multi-temporal approach could be used with confidence in early-season crop area predictions at least one to two months ahead of anthesis.

The rigorousness of the multi-temporal HANTS and $\sum \Delta EVI_{T500}$ approaches were investigated when applied across different regions and seasons (Chapter 6). Thus, extrapolability of these approaches to predict early-season, and determine end-of-season, winter crop area estimates was validated across the entire Queensland cropping region for 2005 and 2006 seasons. Early-season prediction for total winter crop area estimates was done by applying the $\sum \Delta EVI_{T500}$ for July, August, Average (July and August) as well as the Combined area estimate of July and August. The combined approach showed the highest pixel scale accuracy with *kappa coefficients* of 0.99 and 0.78 for 2005 and 2006, respectively. Total winter crop estimates at shire scale were contrasted against ABARE data. The combined approach of July and August had deviations of 8.6% and 26% below the industry estimate of 1 mHA and 700,000 ha for 2005 and 2006, respectively. These estimates were derived using the land use mask.

For end-of-season crop area estimates, the pixel classification of specific winter crops was done using all ground truth data points across Queensland. In addition, classification was done for each sub-region using only ground truth points within that sub-region. In both cases the multi-temporal HANTS was used. Pixel accuracies in the absence of chance (measured through the *kappa coefficient*) were the highest when the sub-region pixel classification approach was used for both seasons. The HANTS approach was used to classify crops within each sub-region without using the land use mask overlay. When results were aggregated only relatively small deviations from the ABARE data for 2005 and 2006 were found. Total winter crop percentage deviations were 5.7% and -11% for the 2005 and 2006 seasons, respectively, while deviations for specific area estimates for wheat, barley and chickpea were 9.9%, -5.2% and 10.9% for 2005 and -2.8%, -78% and 64% for 2006, respectively. Closer investigation suggested a degree of error in the ABARE estimates specifically for chickpea when compared to industry figures.

Accuracy at shire scale was tested by comparing ABS shire scale survey data with predicted area estimates using these multi-temporal approaches for the 2005 season. End-of-season predictions, using HANTS, explained 92%, 89%, 82% and 52% of the observed variability for total winter crop, wheat, barley and chickpea cross all shires. Early-season estimates, using the $\sum \Delta EVI_{T500}$ combined method, had R^2 of 0.87. Importantly, not only did the HANTS approach show high accuracy in discriminating crops from non-crops, it also highlighted the importance of using a contemporary land use pattern mask.

7.2 Concluding Remarks

This study has shown that multi-temporal approaches (i.e. HANTS, MEVI and PCA) can be applied successfully to estimate total winter crop area at harvest and well before harvest. Further, high discriminative ability was achieved in determining crop area for specific crops. This discriminative ability, although after harvest, is not only well in advance of any census or survey estimates disseminated by ABS, but also adds objectiveness and transparency to crop information produced by agencies like ABARE that provide crop statistics on a quarterly basis. Such statistics are usually generated from previous ABS statistics combined with local industry and

government agency input. The results of this study showed that accurate estimates of crop area can be calculated through the application of multi-temporal approaches like HANTS. Accurate, objective and near real-time crop area estimates for specific crops (i.e. wheat, barley, chickpea) are invaluable to bulk grain handlers and agri-industry to aid in logistics of resources and marketing decisions.

In addition, this showed enhanced efficacy in determining total winter crop area as early as July, which is before flowering and at least four months before harvest. This early-season crop area estimates not only assist in bridging the *information gap*, through integration of crop yield predictions, generating accurate, objective crop production estimates, but also aid government and industry in decision making processes, well before harvest. This will enable decision makers to move from a point of passive acceptance to a point of active response to the forecast, well before harvest. Although the end-of-season HANTS approach using regional training data for pixel classification showed total winter crop area predictions similar to what was observed by industry, the early-season approach showed value since it had a forecast lag of up to four months over the end-of season approach. This earlier forecast, however, comes at a price of lower accuracy.

The advent of MODIS satellite platform has augmented the capability of satellite based applications to capture reflectance over large areas at acceptable pixel scale, cost and accuracy. Integrating such information with shire yield forecast will lead to crop production predictions over large areas as early as July. This information is objective and accurate and will assist business and government bodies in marketing, resource management and policy decisions well before harvest. Further, the application of multi-temporal MODIS approaches, as derived and analysed in this thesis, adds transparent production knowledge to the wheat grain industry. This is particularly true in a time in which the industry is increasingly being exposed, not only to fluctuations in domestic and international commodity markets but also climate variability and change at national and global scales.

This thesis exemplified the *novel* use of a time series of MODIS EVI imagery methods, which can be incorporated into an easy accessible and cost effective remote

sensing framework for Queensland. The ability to determine early-season and end-of-season total and specific winter crop area at pixel, shire and regional scales showed high accuracy and thus suggest uptake of outputs from such a system by industry highly likely. However, utility of such an approach to agri-industry will depend on the risk and accuracy industry operates at within their decision and operating regimes.

7.3 Recommendations

A number of implications arose from this study and some recommendations were raised for further investigation:

- Pixel, as well as shire-scale, accuracies for discriminating between crops depend partially on the number of ground truth points collated during a cropping season. Accuracy can be improved by an increase in sampling intensity within a specific region or sub-region. Thus, in the future, more effort should be spent in collating sufficient sampling points by either more extensive field trips or by extending the network of co-workers collating the ground truth data across each region;
- Extending this multi-temporal remote sensing approach to larger regions outside Queensland (i.e. other states or entire Australian cropping region) is plausible but needs to be tested. This will require resources and commitment from multi-agencies at state level and national level. The collaborative arrangement between QDPI&F and federal agencies like ABARE could be the ideal vehicle for extrapolate and test the derived techniques at a national level;
- Further attention should be given to determine sensible error bounds around the area estimates at shire scale. This will increase the robustness of the approach;
- Given the reality of global climate change and the temporal as well as spatial gaps within the ABS census data, especially over the last decade, it is envisaged that this technology could be adapted and linked to biophysical modelling frameworks to determine pixel and shire-scale yield estimates over large regions. This will result in real-time yield predictions, which are less dependent on the impact of technology trends that are intrinsic in the design of highly calibrated agro-climatic shire scale models;

- The application of this methodology to the prediction of grain quality (rather than quantity) across regional scales could be investigated. Deregulation of the wheat market from a single desk to multiple exporters has enhanced the need for quality data. New research would be needed, however, to seek causal relationships between grain quality, crop phenology and multi-temporal spectral indices at regional scales;
- This technology can play a vital role in adding spatial and temporal resolution to ABS agricultural census data by filling the "gaps" for total winter crop area estimates. This would be of more value in years when survey responses in certain regions are very low; for example 2002 season when some agricultural statistics were published at statistical divisions (i.e. cluster of shires) only;
- Measuring changes in land use pattern through the use of the HANTS multi-temporal approach would be possible by extrapolating back to the 1980s via NDVI AVHRR images. This would result in a detailed up-to-date natural resource inventory and additional information on change in land use patterns for cropping; and
- The total area of the shires investigated in this study was relatively small in comparison with other shires in Queensland or Australia. However, the technology derived is not restricted to the MODIS sensor only, but could also be applied to Landsat TM or any other high-resolution platform. Acquisition cost of satellite data from these higher resolution sensors will however be a huge factor in implementation of such and approach in smaller study areas.
- Finally, the issue of a replacement of the MODIS satellite platform needs to be considered. Currently, MODIS is commissioned until 2010 but will likely go beyond that date. The National Polar-orbiting Operational Environmental Satellite System (NPOESS) is scheduled to replace MODIS (http://www.ipo.noaa.gov/). NPOESS is a satellite system similar to MODIS, which is used to monitor global environmental conditions, and collect and disseminate data related to weather, atmosphere, oceans, land and near-space environment.

None of these issues impedes the potential for operational application of multi-temporal remote sensing approaches to crop area estimation, as derived in this thesis,

within the QDPI&F's regional commodity forecasting systems framework. QDPI&F has a strong commitment towards predictive modelling systems such as their regional commodity forecasting system, and the technology derived in this thesis is being integrated into regional production estimate outlook reports delivered on a monthly basis at state level (Potgieter et al. 2007). Any application beyond this will need additional collaboration, resources and long-term commitment from government agencies (state and national) and industry.

References

Aase, JK & Siddoway, FH 1981, 'Assessing Winter Wheat Dry Matter Production Via Spectral Reflectance Measurements', *Remote Sensing of Environment*, vol. 11, pp. 267-77.

ABARE 2005a, *Australian Bureau of Agricultural Resource and Economics Farm Survey for the 2003 and 2004*, Australian Bureau of Agricultural Resource and Economics, Canberra, Australia.

---- 2005b, *Farm Survey for the 2003 and 2004*, Australian Bureau of Agricultural Resource and Economics, Canberra, Australia.

---- 2007, *Australian Commodities*, Australian Bureau of Agricultural Resource and Economics, Canberra, Australia.

ABS 2004, *Agricultural Commodities - Historical Data of Main Commodities for Australia, 1861 to 2003*, Agricultural Bureau of Statistics, Commonwealth of Australia. (http://www.abs.gov.au). viewed July 2004.

---- 2008, *71250do016_200506 Agricultural Commodities: Small Area Data, Australia, 2005-06.*, Agricultural Bureau of Statistics, Commonwealth of Australia (http://www.abs.gov.au),

, viewed 1 April 2008.

ACRES 2004, *Acquired by Landsat 5 Satellite Sensor on the 14 September 2004* Imagery processed by Geoscience Australia © Commonwealth of Australia, ACRES, 2004.

Allan, RJ 2000, 'El Niño and the Southern Oscillation: Multiscale Variability and Its Impacts on Natural Ecosystems and Society.' in HF Diaz & V Markgraf (eds),

Enso and Climatic Variability in the Last 150 Years. , Cambridge Univ. Press., Cambridge, UK., pp. 3 - 55.

Anthony, G, Chambers, S, East, M, Goodwin, T, Gowen, R, Holdom, D, James, C, Lobegeiger, R, Paff, J, Smith, A, Underhill, B & Williams, l 2007, *Prospects for Queensland's Primary Industries 2007-2008*, Queensland Department of Primary Industries and Fisheries., Brisbane.

Asner, GP 1998, 'Biophysical and Biochemical Sources of Variability in Canopy Reflectance', *Remote Sensing of Environment*, vol. 64, pp. 234 - 53.

Badhwar, GD 1980, 'Crop Emergence Date Determination from Spectral Data', *Photogrametric Engineering & Remote Sensing*, vol. 46, no. 3, pp. 369-77.

---- 1984, 'Use of Landsat-Derived Profile Features for Spring Small-Grains Classification', *International Journal of Remote Sensing*, vol. 5, no. 5, pp. 783-97.

Badhwar, GD & Henderson, KE 1981, 'Estimating Development Stages of Corn from Spectral Data - an Initial Model', *Agronomy Journal*, vol. 73, pp. 748-55.

Badhwar, GD, Carnes, JG & Austin, WW 1982a, 'Use of Landsat-Derived Temporal Profiles for Corn-Soybean Feature Extraction and Classification', *Remote Sensing of Environment*, vol. 12, pp. 57-79.

---- 1982b, 'A Semi-Automatic Technique for Mutlitemporal Classification of a Given Crop within a Landsat Scene', *Pattern Recognition*, vol. 15, no. 3, pp. 217 - 30.

Bauer, ME 1985, 'Spectral Inputs to Crop Identification and Condition Assessment', *Proceedings of the IEEE*, vol. 73, no. 6, pp. 1071 - 84.

Bloomfield, P 2000, *Fourier Analysis of Time Series*, second edition edn, vol. Applied Probability and Statistics Section, Wiley Series in Probability and Statistics, John Wiley & Sons, INC. , New York.

Boken, VK & Shaykewich, CF 2002, 'Improving an Operational Wheat Yield Model Using Phenological Phase-Based Normalized Difference Vegetation Index', *International Journal of Remote Sensing*, vol. 23, no. 20, pp. 4155-68.

Campbell, JB 2002, *Introduction to Remote Sensing*, Third edn, Guilford Press, New York.

Chen, Z, Li, S, Ren, J, Gong, P, Zhang, M, Wang, L, Xiao, S & Jiang, D 2008, 'Monitoring and Management of Agriculture with Remote Sensing', in S Liang (ed.), *Advances in Land Remote Sensing - System, Modelling, Inversion and Adaptation*, Springer, University of Maryland, USA, pp. 397 - 421.

Cohen, J 1960, 'A Coefficient of Agreement for Nominal Scales', *Educational and Psychological measurement*, vol. XX, no. 1, pp. 37 - 46.

Commonwealth of Australia 1914, *Governor's Despathce to and from England Vol I, 1788-1796, in Historical Records of Australia*, Canberra.

Cotter, JJ & Tomczak, CM 1994, 'An Image Analysis System to Develop Area Sampling Frames for Agricultural Surveys', *Photogrammetric Engineering & Remote Sensing*, vol. 60, no. 3, pp. 299-306.

Crist, EP & Malila, A 1980, 'A Temporal Spectral Analysis Technique for Vegetation Applications of Landsat.' paper presented to 14th International Symposium on Remote Sensing of Environment, San Jose, Costa Rica, 23-30 April.

Crutchfield, J 2008, *Personal Communication.*, World crop area estimates. edn, International Production Assessment Division (IPAD) within the USDA Washington D.C.

Cumming, G 2007, *Personal Communication.*, CQ chickpea crop area for 2005, 2006 cropping season. edn.

Dabrowska-Zielinska, K, Kogan, F, Ciolkosz, A, Gruszczynska, M & Kowalik, W 2002, 'Modelling of Crop Growth Conditions and Crop Yield in Poland Using AVHRR-Based Indices.' *International Journal of Remote Sensing*, vol. 23, no. 6, pp. 1109-23.

Dadhwal, VK & Ray, SS 2000, 'Crop Assessment Using Remote Sensing - Part-Ii: Crop Condition and Yield Assessment', *Indian Journal of Agricultural Economics*, vol. 55, no. 2, pp. 55 - 67.

Dadhwal, VK, Ruhal, DS, Medhavy, TT, Jarwal, SD, Khera, AP, Sing, J, Sharma, T & Parihar, JS 1991, 'Wheat Acreage Estimation for Haryana Using Satellite Digital Data', *Journal of the Indian Society of Remote Sensing*, vol. 19, no. 1, pp. 1-15.

Davis, JC 2002, *Statistics and Data Analysis in Geology*, Third edn, John Wiley & Sons Inc., New York.

Defries, RS, Hansen, MC & Townshend, JRG 2000, 'Global Continuous Fields of Vegetation Characteristics: A Linear Mixture Model Applied to Multi-Year 8 Km AVHRR Data', *International Journal of Remote Sensing*, vol. 21, no. 6&7, pp. 1389-414.

Del Frate, F, Ferrazzoli, P & Schiavon, G 2003, ' Retrieving Soil Moisture and Agricultural Variables by Microwave Radiometry Using Neural Networks', *Remote Sensing of Environment*, vol. 84, pp. 174 - 83.

Department of Natural Resources and Water 2006, *Queensland Land Use Mapping Program*, http://www.nrm.qld.gov.au/science/lump., May 2005.

DNR&W 2006, *Queensland Land Use Mapping Program*, Department of Natural Resources and Water http://www.nrm.qld.gov.au/science/lump, May 2005.

Doraiswamy, P & Cook, PW 1995, 'Spring Wheat Yield Assessment Using NOAA Avhhr Data', *Canadian Journal of Remote Sensing*, vol. 21, no. 1, pp. 43-51.

Doraiswamy, PC, Hatfield, JL, Jackson, TJ, Akhmedov, B, Prueger, J & Stern, A 2004, 'Crop Condition and Yield Simulations Using Landsat and MODIS.' *Remote Sensing of Environment*, vol. 92, pp. 548-59.

Dubey, RP, Ajwani, ND & Navalgund, RR 1991, 'Relationship of Wheat Yield with Parameters Derived from a Spectral Growth Profile.' *Journal of Indian Society of Remote Sensing.*, vol. 19, no. 1, pp. 27-44.

Evans, LT & Wardlaw, IF 1976, 'Aspects of the Comparative Physiology of Grain Yield in Cereals', in NC Brady (ed.), *Advances in Agronomy*, Academic Press, New York, USA, pp. 301 - 49.

Fecso, R, Tortora, RD & Vogel, FA 1986, 'Sampling Frames for Agriculture in the United States', *Journal of Official Statistics*, vol. 2, no. 3, pp. 279-92.

Fensholt, R 2004, 'Earth Observation of Vegetation Status in the Sahelian and Sudanian West Africa: Comparison of Terra MODIS and NOAA AVHRR', *International Journal of Remote Sensing*, vol. 25, no. 9, pp. 1641-59.

Fuller, DO 1998, 'Trends in NDVI Time Series and Their Relation to Rangeland and Crop Production in Senegal, 1987 - 1993', *International Journal of Remote Sensing*, vol. 19, no. 10, pp. 2013 - 8.

Gitelson, AA, Kaufman, YJ, Stark, R & Rundquist, D 2002, 'Novel Algorithms for Remote Estimation of Vegetation Fraction.' *Remote Sensing of Environment*, vol. 80, pp. 76 - 87.

Granados-Ramirez, R, Reyna-Trujillo, T & Gomez-Rodriguez, G 2004, 'Analysis of NOAA-AVHRR-NDVI Images for Crop Monitoring', *International Journal of Remote Sensing*, vol. 25, no. 9, pp. 1615-27.

Groten, SME 1993, 'NDVI - Crop Monitoring and Early Yield Assessment of Burkina Faso', *Int. J. Remote Sensing*, vol. 14, no. 8, pp. 1495 - 515.

Gutteridge, M & Henry, B 2002, *Land Use and Productivity in the Queensland Murray Darling Basin: 1990-2000.*, Queensland Department of Natural Resources and Mines, Brisbane.

Hall-Beyer, M 2007, 'IHS Co-Representation of Circular and Noncircular Variables Using Harmonic Analysis Parameters ', *Canadian Journal of Remote Sensing*, vol. 33, no. 5, pp. 416-21.

Hammer, GL 1987, 'Effects of Climatic Variability and Possible Climatic Change on Reliability of Wheat Cropping - a Modelling Approach', *Agricultural and Forest Meteorology*, vol. 41, pp. 123-42.

Hammer, GL, Stephens, D & Butler, D 1996, *Wheat Modelling Sub-Project: Development of Predictive Models of Wheat Production.*, 6a, Land and Water Resources Research and Development Corporation.

Hammer, GL, Hansen, JW, Phillips, JG, Mjelde, JW, Hill, H, Love, A & Potgieter, AB 2001, 'Advances in Application of Climate Prediction in Agriculture', *Agricultural systems*, vol. 70, pp. 515-53.

Holben, BN, Tucker, CJ & Fan, C-J 1980, 'Spectral Assessment of Soybean Leaf Are and Leaf Biomass', *Photogrammetric Engineering & Remote Sensing*, vol. 46, pp. 651 - 6.

Huete, A, Justice, C & Liu, H 1994, 'Development of Vegetation and Soil Indices for MODIS-Eos', *Remote Sensing of Environment*, vol. 49, pp. 224-34.

Huete, A, Didan, K, Miura, T, Rodriguez, EP, Gao, X & Ferreira, LG 2002, 'Overview of the Radiometric and Biophysical Performance of the MODIS Vegetation Indices', *Remote Sensing of Environment*, vol. 83, pp. 195-213.

Huete, AR, Liu, HQ, Batchily, K & van Leeuwen, W 1997, 'A Comparison of Vegetation Indices over a Global Set of Tm Images for Eos-MODIS', *Remote Sensing of Environment*, vol. 59, pp. 440-51.

IPCC 2001, *Climate Change 2001: The Scientific Basis. Contribution of Working Group I to the Third Assessment Report of the Intergovernmental Panel on Climate Change.*, Third Assessment Report – Climate, Cambridge University Press, Cambridge, UK.

---- 2007, *Climate Change 2007: The Physical Science Basis; Summary for Policymakers. Contribution of Working Group I to the Fourth Assessment Report of the Intergovernmental Panel on Climate Change.*, Cambridge University Press, Cambridge, United Kingdom and New York, NY, USA.

ITT 2008, *ENVI 4.5 Software*, ITT Visual Information Solutions, http://www.ittvis.com.

Jackson, RD 1983, 'Discrimination of Growth and Water Stress in Wheat by Various Vegetation Indices through Clear Turbid Atmospheres', *Remote Sensing of Environment*, vol. 13, pp. 187-208.

Jakubauskas, ME, Legates, DR & Kastens, JH 2001, 'Harmonic Analysis of Time Series AVHRR NDVI Data', *Photogrammetric Engineering & Remote Sensing*, vol. 67, no. 4, pp. 461-70.

---- 2002, 'Crop Identification Using Harmonic Analysis of Time -Series AVHRR NDVI Data', *Computers and Electronics in Agriculture*, vol. 37, pp. 127-39.

Jensen, JR 2007, *Remote Sensing of the Environment: An Earth Resource Perspective.*, 2nd edn, Pearson Prentice Hall, Upper Saddle River, NJ 07458.

Johnson, RA & Wichern, DW 1988, *Applied Multivariate Statistical Analysis*, Second edn, Prentice-Hall, Inc., New Jersey.

Justice, CO, Townsend, JRG, Vermote, EF, Masuoka, E, Wolfe, RE, Saleous, N, Roy, DP & Morisette, JT 2002, 'An Overview of MODIS Land Data Processing and Product Status', *Remote Sensing of Environment*, vol. 83, pp. 3-15.

Justice, CO, Vermote, E, Townshend, JRG, Defries, R, Roy, DP, Hall, DK, Salomonson, VV, Privette, JL, Riggs, G, Strahler, A, Lucht, W, Myneni, RB, Knyazikhin, Y, Running, SW, Nemani, RR, Wan, Z, Huete, AR, van Leeuwen, W, Wolfe, RE, Giglio, L, Muller, J, Lewis, P & Barsnley, MJ 1998, 'The Moderate Resolution Imaging Spectroradiometer (MODIS): Land Remote Sensing for Global Change Research.' *IEEE Transactions on Geoscience and Remote Sensing*, vol. 36, no. 4, pp. 1228-49.

Kalubarme, MH, Potdat, MB, Manjunath, KR, Mahey, RK & Siddhu, SS 2003, 'Growth Profile Based Crop Yield Models: A Case Study of Large Area Wheat Yield Modelling and Its Extendibility Using Atmospheric Corrected NOAA AVHRR Data.' *International Journal of Remote Sensing*, vol. 24, no. 10, pp. 2037-54.

Kamthonkiat, D, Honda, I, Turral, H, Tripathi, NK & Wuwongse, V 2005, 'Discrimination of Irrigated and Rainfed Rice in a Tropical Agricultural System Using Spot-Vegetation NDVI and Rainfall Data', *International Journal of Remote Sensing*, vol. 26, no. 12, pp. 2527-47.

Keating, BA, Carberry, PS, Hammer, GL, Probert, ME, Robertson, MJ, Holzworth, D, Huth, NI, Hargreaves, JNG, Meinke, H, Hochman, Z, McLean, G, Verburg, K, Snow, V, Dimes, JP, Silburn, M, Wang, E, Brown, S, Bristow, KL, Asseng, S, Chapman, S, McCown, RL, Freebairn, DM & Smith, CJ 2003, 'An Overview of Apsim, a Model Designed for Farming Systems Simulation.' *European Journal of Agronomy*, vol. 18, pp. 267-88.

Kelleher, F 2003, 'Crop Adaptation', in J Pratley (ed.), *Principles of Field Crop Production*, Fourth edn, Oxford University press, Melbourne, pp. 78-158.

Knopke, P, O'Donnell, V & Shepherd, A 2000, *Productivity Growth in the Australian Grains Industry*, 0 642 76413 1, ABARE, Canberra.

Labus, MP, Nielsen, GA, Lawrence, RL & Engel, R 2002, 'Wheat Yield Estimates Using Multi-Temporal NDVI Satellite Imagery', *International Journal of Remote Sensing*, vol. 23, no. 20, pp. 4169-80.

Langridge, P & Barr, AR 2003, 'Preface', *Australian Journal of Agricultural Research*, vol. 54, pp. i - iv.

Lawrance, L 2007, *Queensland Winter Crops*, Australian Bureau of Agricultural Resource and Economics, Canberra, Australia.

Lester, D 2008, *Personal Communication.*, Australian Bureau of Statistics, Hobart, 22 July 2008.

Lillesand, MT, Kiefer, RW & Chipman, JW 2004, *Remote Sensing and Image Interpretation*, Fifth edn, John Wiley & Sons, Hoboken NJ, United States of America.

Liu, HQ & Huete, AR 1995, 'A Feedback Based Modification of the NDVI to Minimise Canopy Background and Atmospheric Noise', *IEEE Transactions on Geoscience and Remote Sensing*, vol. 33, pp. 457-65.

Lobell, DB & Asner, GP 2004, 'Cropland Distributions from Temporal Unmixing of MODIS Data', *Remote Sensing of Environment*, vol. 93, pp. 412 - 22.

Lobell, DB, Asner, GP, Oritz-Monasterio, JI & Benning, TL 2003, 'Remote Sensing of Regional Crop Production in the Yaqui Valley, Mexico: Estimates and Uncertainties', *Agriculture, Ecosystems and Environment*, vol. 94, pp. 205-20.

Lynch, B 2007, *Personal Communication.*, Central Queensland chickpea crop area for 2005, 2006. edn.

MacDonald, RB & Hall, FG 1980, 'Global Crop Forecasting', *Science*, vol. 208.

Markon, CJ & Peterson, KM 2002, 'The Utility of Estimating Net Primary Productivity over Alaska Using Baseline AVHRR Data.' *International Journal of Remote Sensing*, vol. 23, no. 21, pp. 4571-96.

Mather, PM 1999, *Computer Processing of Remote-Sensed Images*, Second edn, John Wiley & Sons, New York.

Meinke, H 1996, 'Improving Wheat Simulation Capabilities in Australia from Cropping Systems Perspective', Wageningen.

Meinke, H, Howden, M & Nelson, R 2006a, 'Integrated Assessments of Climate Variability and Change for Australian Agriculture - Connecting the Islands of Knowledge.' paper presented to 3rd Biennial meeting of the International Environmental Modelling and Software Society, Burlington, Vermont, USA, 9-12 July 2006.

Meinke, H, Hammer, GL, van Keulen, H & Rabbinge, R 1998, 'Improving Wheat Simulation Capabilities in Australia from a Cropping Systems Perspective. Iii. The Integrated Wheat Model (I_Wheat).' *European Journal of Agronomy*, vol. 8, pp. 101-16.

Meinke, H, Wright, W, Hayman, P & Stephens, D 2003, 'Managing Cropping Systems in Variable Climates', in J Pratley (ed.), *Principles of Field Crop Production*, 4 edn, Oxford University press, Melbourne, pp. 26-77.

Meinke, H, Hammer, GL, van Keulen, H, Rabbinge, R & Keating, BA 1997, 'Improving Wheat Simulation Capabilities in Australia from a Cropping Systems Perspective. Water and Nitrogen Effects on Spring Wheat in a Semi-Arid Environment. ' *European Journal of Agronomy*, vol. 7, pp. 75-88.

Meinke, H, Nelson, R, Kokic, P, Stone, R, Selvaraju, R & Baethgen, W 2006b, 'Actionable Climate Knowledge: From Analysis to Synthesis', *Climate Research*, vol. 33, pp. 101-10.

Menenti, M, Azzali, S, Verhoef, W & van Swol, R 1993, 'Mapping Agro-Ecological Zones and Time Lag in Vegetation Growth by Means of Fourier Analysis of Time Series of NDVI', *Advance Space Research*, vol. 13, no. 5, pp. (5)233-(5)7.

Muchoney, D, Borak, J, Chi, M, Friedl, M, Gopal, S, Hodges, J, Morrow, N & Strahler, A 2000, 'Application of MODIS Global Supervised Classification Model to Vegetation and Land Cover Mapping of Central America.' *International Journal of Remote Sensing*, vol. 21, no. 6, pp. 1115-38.

Mueller, R 2008, *Personal Communication.*, Research and development division. edn, United States Department of Agriculture (USDA). Washington D.C.

NASS 2006, *The Yield Forecasting Program of NASS*, Statistical Methods Branch, Estimates Division, National Agricultural Statistics Service, Washington D.C. 20250.

Navulur, K 2007, *Multispectral Image Analysis Using the Object-Orientated Paradigm*, CRC Press, Boca Raton, FL, USA.

Nelson, RA, Holzworth, DP, Hammer, GL & Hayman, PT 2002, 'Infusing the Use of Seasonal Climate Forecasting into Crop Management Practice in North East Australia Using Discussion Support Software', *Agricultural Systems*, vol. 74, pp. 393-414.

Nix, HA 1975, 'The Australian Climate and Its Effects on Grain Yield and Quality', in A Lazenby & EM Matheson (eds), *Australian Field Crops*, Angus and Robertson, Sydney, Australia, vol. 1, pp. 183-226.

Penm, J 2002, *Australian Commodities - Economic Overview*, Volume 9, Number 4, ABARE Canberra.

---- 2006, *Australian Commodities - Economic Overview*, ABARE, Canberra.

Potgieter, AB 2008, *Seasonal Crop Outlook (Http://Www.Dpi.Qld.Gov.Au/Cps/Rde/Dpi/Hs.Xsl/26_6256_Ena_Html.Htm)*, viewed August 2008.

Potgieter, AB, Hammer, GL & Butler, D 2002, 'Spatial and Temporal Patterns in Australian Wheat Yield and Their Relationship with Enso', *Australian Journal of Agricultural Research*, vol. 53, pp. 77-89.

Potgieter, AB, Everingham, Y & Hammer, GL 2003, 'Measuring Quality of a Commodity Forecasting from a System That Incorporates Seasonal Climate Forecasts', *International Journal of Climatology*, vol. 23, pp. 1195-210.

Potgieter, AB, Hammer, GL & deVoil, P 2005a, 'A Simple Regional-Scale Model for Forecasting Sorghum Yield across North-Eastern Australia', *Agriculture and Forest Meteorology*, vol. 132, pp. 143-53.

Potgieter, AB, Hammer, GL & Doherty, A 2006, *Oz-Wheat: A Regional-Scale Crop Yield Simulation Model for Australian Wheat.*, Information Series No,

QI06033, Queensland Department of Primary Industries & Fisheries. , Brisbane, Australia. (ISSN 0727-6273).

---- 2007, 'Integrating Crop Models, Satellite Data and Seasonal Climate Prediction to Forecast Regional Crop Production in Australia', paper presented to The 6th Asian Crop Science Association Conference and the 2nd International Conference on Rice for the Future, Bangkok, Thailand. (ISBN 978-974-229-500-4),, 5-9 November 2007.

Potgieter, AB, Hammer, GL, Meinke, H, Stone, RC & Goddard, L 2005b, 'Three Putative Types of El Nino Revealed by Spatial Variability in Impact on Australian Wheat Yield.' *Journal of Climate*, vol. 18, no. 10, pp. 1566-74.

Pratley, J 2003, *Principles of Field Crop Production*, Oxford University Press, Melbourne.

Price, JC 2003, 'Comparing MODIS and ETM+ Data for Regional and Global Land Classification.' *Remote Sensing of Environment*, vol. 86, pp. 491-9.

Prince, SD 1991, 'A Model of Regional Primary Production for Use with Coarse Resolution Satellite Data', *International Journal of Remote Sensing*, vol. 12, no. 6, pp. 1313-30.

Prince, SD & Goward, SN 1995, 'Global Primary Production: A Remote Sensing Approach.' *Journal of Biogeography*, vol. 22, pp. 815-35.

Reynolds, CA, Yitayew, M, Slack, DC, Hutchinson, CF, Huete, A & Petersen, MS 2000, 'Estimating Crop Yields and Production by Integrating the Fao Crop Specific Water Balance Model with Real-Time Satellite Data and Ground-Based Ancillary Data', *Int. J. Remote Sensing*, vol. 21, no. 18, pp. 3487-508.

Richards, JA & Jia, X 1999, *An Introduction Remote Sensing Digital Image Analysis*, Third edn, Springer-Verlag, Berlin Heidelberg.

Roerink, GJ, Menenti, M, Soepboer, Z & Su, Z 2003, 'Assessment of Climate Impact on Vegetation Dynamics by Using Remote Sensing', *Physics and Chemistry of the Earth*, vol. 28, pp. 103-9.

Rondeaux, G 1995, 'Vegetation Monitoring by Remote Sensing: A Review of Biophysical Indices', *Photo-Interpretation*, vol. 3, pp. 197-216.

Routley, R 2006, *Personal Communication.*, early planting 2006 CQ edn, DPI&F, Emerald, Central Queensland, Australia.

Sakamoto, T, Yokozawa, M, Torintani, H, Shibayama, M, Ishitsuka, N & Ohno, H 2005, 'A Crop Phenology Detection Method Using Time-Series MODIS Data', *Remote Sensing of Environment*, vol. 96, pp. 366-74.

Sharma, T & Navalgund, RR 1989, 'Estimation of Growth Stages of Wheat from Spectral Data', *Journal of the Indian Society of Remote Sensing*, vol. 17, no. 2, pp. 1-6.

Shaw, A 1993, 'Colonial Settlement 1788-1945', in DB Williams (ed.), *Agriculture in the Australian Economy*, Third edn, Sydney University Press, Melbourne, pp. 1-18.

Sim, J & Wright, CC 2005, 'The Kappa Statistic in Reliability Studies: Use, Interpretation, and Sample Size Requirements.' *Physical Therapy*, vol. 85, no. 3, pp. 257 - 68.

Smith, RCG, Adams, J, Stephens, DJ & Hick, PT 1995, 'Forecasting Wheat Yield in a Mediterranean-Type Environment from the NOAA Satellite', *Australian Journal of Agricultural Research*, vol. 46, pp. 113-25.

Stephens, DJ 1995, 'Crop Yield Forecasting over Large Areas in Australia', Murdoch University.

Stephens, DJ & Lyons, TJ 1998, 'Rainfall-Yield Relationships across the Australian Wheatbelt.' *Australian Journal of Agricultural Research*, vol. 49, pp. 211-23.

Stephens, DJ, Lyons, TJ & Lamond, MH 1989, 'A Simple Model to Forecast Wheat Yield in Western Australia', *Journal of the Royal Society of Western Australia*, vol. 71, no. Parts 2 & 3, pp. 77 - 81.

Stephens, DJ, Butler, D & Hammer, GL 2000, 'Using Seasonal Climate Forecasts in Forecasting the Australian Wheat Crop', in GL Hammer, N Nicholls & C Mitchell (eds), *Applications of Seasonal Climate Forecasting in Agriculture an Natural Ecosystems: The Australian Experience*, Kluwer Academic Publishers, Dordrecht, Netherlands, pp. 351-66.

Stone, RC, Nicholls, N & Hammer, G 1996a, 'Frost in Northeast Australia: Trends and Influences of Phases of the Southern Oscillation', *Journal of Climate*, vol. 9, pp. 1896-905.

Stone, RC, Hammer, GL & Marcussen, T 1996b, 'Prediction of Global Rainfall Probabilities Using Phases of the Southern Oscillation Index.' *Nature*, vol. 384, pp. 252-5.

TBRS 2007, *MODIS*, University of Arizona, USA, http://tbrs.arizona.edu/project/MODIS/compositing.php, December 2006.

Thenkabail, PS, Smith, RB & De Pauw, E 2000, 'Hyperspectral Vegetation Indices and Their Relationship with Agricultural Crop Characteristics', *Remote Sensing of Environment*, vol. 71, pp. 158 - 82.

Thomas & Fukai, S 1995, 'Growth and Yield Response of Barley and Chickpea to Water Stress under Three Environments in Southeast Queensland. I. Light Interception, Crop Growth and Grain Yield', *Australian Journal of Agricultural Research*, vol. 46, pp. 17 - 33.

Toll, DL 1985, 'Effect of Landsat Thematic Mapper Sensor Parameters on Land Cover Classification', *Remote Sensing of Environment*, vol. 17, pp. 129 - 40.

Tou, J & Gonzales, R 1974, *Pattern Recognition Principles*, Addison-Wesley, Reading MA.

Tucker, CJ, Holben, BN, Elgin Jr, JH & McMurtrey III, JE 1980, 'Relationship of Spectral Data to Grain Yield Variation.' *Photogrammetric Engineering & Remote Sensing*, vol. 46, no. 5, pp. 657-66.

---- 1981, 'Remote Sensing of Total Dry-Matter Accumulation in Winter Wheat.' *Remote Sensing of Environment*, vol. 11, pp. 171-89.

USGS 2009, *Usgs Announcement: Opening the Landsat Archive* http://landsat.usgs.gov/mission_headlines2009.php, January 2009.

Van Genderen, JL, Lock, BF & Vass, PA 1978, 'Remote Sensing: Statistical Testing of Thematic Map Accuracy', *Remote Sensing of Environment*, vol. 7, no. 3, pp. 3 - 14.

Van Niel, T & McVicar, TR 2004, 'Determining Temporal Windows for Crop Discrimination with Remote Sensing: A Case Study in South-Eastern Australia', *Computers and Electronics in Agriculture*, vol. 45, pp. 91-108.

Verhoef, W, Menenti, M & Azzali, S 1996, 'A Colour Composite of NOAA-AVHRR-NDVI Based on Time Series Analysis (1981-1992)', *International Journal of Remote Sensing*, vol. 17, no. 2, pp. 231-5.

Vogel, FA & Bange, GA 1999, *Understanding USDA Crop Forecasts*, National Agricultural Statistics Service, and World Agricultural Outlook Board, Office of the Chief Economist., Washington D.C. 20250.

Wannebo, A & Rosenzweig, C 2000, 'Using Remote Sensing to Identify Agricultural Areas in the Us Cornbelt Sensitive to the El Niño Southern Oscillation Phenomenon.' *International Journal of Remote Sensing*.

Weisssteiner, CJ & Kuhbauch, W 2005, 'Regional Yield Forecasts of Malting Barley (Hordeum Vulgare L.) by NOAA-AVHRR Remote Sensing Data and Ancillary Data', *Journal of Agronomy & Crop Science*, vol. 191, pp. 308 - 20.

Wessel, KJ, De Fries, RS, J, D, O, AL, Hansen, AJ, L, PS & Moran, EF 2004, 'Mapping Regional Land Cover with MODIS Data for Biological Conservation: Examples from the Greater Yellowstone Ecosystem, USA and Para State, Brazil.' *Remote Sensing of Environment*, vol. 92, pp. 67 - 83.

Wiegand, CL, Richardson, AJ, Escobar, DE & Gerbermann, AH 1991, 'Vegetation Indices in Crop Assessments', *Remote Sensing of Environment*, vol. 35, pp. 105-19.

Xiao, X, Boles, S, Liu, J, Zhuang, D, Frolking, S, Li, C, Salas, W & Moore III, B 2005, 'Mapping Paddy Rice Agriculture in Southern China Using Multi-Temporal MODIS Images', *Remote Sensing of Environment*, vol. 95, pp. 480-92.

Yunasa, IAM, Siddique, KHM, Belford, RK & Karimi, MM 1993, 'Effect of Canopy Structure on Efficiency of Radiation Interception and Use of Spring Wheat Cultivars During the Pre-Anthesis Period in a Mediterranean-Type Environment.' *Field Crops Research*, vol. 35, pp. 113-22.

Zang, P, Anderson, B, Tan, B, Huang, D & Myneni, R 2005, 'Potential Monitoring of Crop Production Using a Satellite-Based Climate-Variability Impact Index.' *Agricultural and Forest Meteorology*, vol. 132, pp. 344-58.

Zhan, X, Sohlberg, RA, Townsend, JRG, DiMiceli, C, Carroll, ML, Eastman, JC, Hansen, MC & DeFries, RS 2002, 'Detection of Land Cover Changes Using MODIS 250 M Data.' *Remote Sensing of Environment*, vol. 83, pp. 336-50.

Zhang, P, Anderson, BT & Myneni, R 2006, 'Monitoring 2005 Corn Belt Yields from Space', *Eos*, vol. 87, no. 15, pp. 150 - 2.

Zhang, P, Anderson, B, Tan, B, Huang, D & Myneni, R 2005, 'Potential Monitoring of Crop Production Using a Satellite-Based Climate-Variability Impact Index.' *Agricultural and Forest Meteorology*, vol. 132, pp. 344-58.

Zhang, X, Friedl, MA, Schaaf, CB, Strahler, AH, Hodges, JCF, Gao, F, Reed, C & Huete, A 2003, 'Monitoring Vegetation Phenology Using MODIS.' *Remote Sensing of Environment*, vol. 84, pp. 471-5.

Appendices

Appendix A: Mathematical equations and program scripts, for the determining the maximum peak EVI.

A.1 Determining $t_{\max}$

A maximum or minimum occurs where $\frac{d\rho}{dt} = 0$. The maximum or peak occurs at point $(t_{\max}, \rho_{\max})$. Setting $\rho_s(t_0) = A$ and applying the product rule of differentiation (i.e. $\frac{duv}{dt} = u\frac{dv}{dt} + v\frac{du}{dt}, \quad u = A(t/t_0)^{\alpha}, v = \exp[\beta({t_0}^2 + t^2)]$) equation 4.4 becomes:

$$\frac{d\rho}{dt} = A\left[\frac{\alpha t^{\alpha-1}}{t_0^{\alpha}}\exp[\beta({t_0}^2 + t^2)] - 2t\beta\exp[\beta({t_0}^2 + t^2)](\frac{t}{t_0})^{\alpha}\right]$$

Simplifying this equation for $\frac{d\rho}{dt} = 0$ is equivalent to finding what t is at the peak (i.e. $t_{\max}$):

$$t_{\max} = \sqrt{\frac{\alpha}{2\beta}}$$

A.2 R-script for determining the curve fitting parameter outputs for curve fitting procedure (CF1) and curve fitting procedure 2 (CF2) as described in Chapter 4.

```
#filters:
#min.EVI.crop <- 2700 #lowest possible value for max (EVI) in crop
rm(list = ls())
fileName<-"data\\evi2004stackENVI.txt"
nrows <- 865
ncols <- 967
nbands <- 23
tot.pix <- nrows*ncols #numbers of pixels
img <- array(scan(fileName, skip=5), dim=c(nrows,ncols,nbands))

#init some output matrices
t.range <- b1 <- b2 <- peak <- peak.t <- A.e <- alpha <- beta <- g1 <- g2 <- D.pos <-
  D.neg <- matrix(NA, nrows, ncols)
#splined <- s.t.range <- s.b1 <- s.b2 <- s.peak <- s.A.e <- s.alpha <- s.beta <-
  s.multipeak <- s.g1 <- s.g2 <- s.D.pos <- s.D.neg <- matrix(NA, nrows, ncols)
n <- 1

#1:nrows
#1:ncols
for (k in 1:nrows ) {
  for (j in 1:ncols) {
    #j <- 363 #rows in ENVI
    #k <- 412  #cols in ENVI

    #a counter
    if(n %% 1000 == 0) print(n)
    n <- n+1
    EVI <- img[k,j,]
    #EVI.l <- loess.smooth(1:length(EVI),EVI) #loess fit
```

```
  #EVI.p <- lm(EVI ~ poly(1:length(EVI),3))
  #EVI.p <- lm(EVI ~ poly(1:length(EVI),3))
  #lines(ht, predict(EVI.p, c(1:length(EVI)))

  EVI.s <- smooth.spline(EVI)
  EVI.s0 <- predict(EVI.s,deriv = 0)$y #0th derivative
  EVI.s1 <- predict(EVI.s,deriv = 1)$y #1st derivative
  EVI.s2 <- predict(EVI.s,deriv = 2)$y #2st derivative
  EVI.s3 <- predict(EVI.s,deriv = 3)$y #3d derivative
  EVI.max <- max(EVI[10:21])
  EVI.maxt <-  c(10:21)[match(EVI.max,EVI[10:21])] # t at which max EVI occurs
  if (EVI.max <= 2700) next

  #Green up
      #only consider n.b bands before maxt
  n.b <- 10
  t1 <- ifelse(EVI.maxt - n.b <= 6, 7, EVI.maxt-10) #start not before middle March

  #the position of last negative value between 1st and 2nd derivative (see Sakamoto
3.2)
  d.1 <- which(diff(sign(EVI.s1[t1:(EVI.maxt-3)]))==2)
  d.2 <- which(diff(sign(EVI.s2[t1:(EVI.maxt-3)]))==2)

 if (length(d.1) == 0) {
  t.0 <- c(t1:(EVI.maxt-2))[max(d.2)]+1 #green up start time
 } else {
  t.0 <- c(t1:(EVI.maxt-2))[max(d.1)]+1 #green up start time
  }
 if ( (length(d.1) == 0) & (length(d.2) == 0)) {
  t.0 <- t1 + 1
  }
```

```
  #Green down
  #position between 1st second and third derivative
  #exclude n.b bands after maxt
   n.b <- 2
   t2 <- ifelse((EVI.maxt+n.b) > length(EVI),length(EVI),(EVI.maxt+n.b))
   d.1 <- which(diff(sign(EVI.s1[(t2):length(EVI)])) == 2)
   d.2 <- which(diff(sign(EVI.s2[(t2):length(EVI)])) == -2)

  if (length(d.1) == 0){
   t.end <- c(t2:length(EVI))[min(d.2)]
  } else {
   t.end <- c(t2:length(EVI))[min(d.1)]
  }
 if ((length(d.1) == 0) & (length(d.2) == 0)) {
  t.end <- length(EVI)-1
  }
  t.end <- ifelse(t.end > length(EVI),length(EVI)-2,t.end)

  #plot(EVI, ylim=c(-4000,10000))
  #lines(EVI.s1, col=3)#green
  #lines(EVI.s2, col=4)#blue
  #lines(EVI.s3, col=5)# cyan
  #lines(c(0,23), c(0,0))
  #lines(c(t.0,t.0), c(0,10000), col=5)
  #lines(c(t.end,t.end), c(0,10000), col=6)
  #print(t.0)
  #print(t.end)
  #print(EVI.maxt)
  if (any(is.na(c(t.0,t.end)))) next
  if (all(EVI.s1[t.0:t.end] < 250) | all(EVI.s1[t.0:t.end] > 250)) next

#peak
  peak[k,j] <- EVI.max
```

```
  peak.t[k,j] <- EVI.maxt

  #range
  t.range[k,j] <- t.end - t.0
  if (t.range[k,j] <= 4) next

  #----------------------------------
  #In crop EVI cycles

  inCrop <- data.frame(EVI=EVI[t.0:t.end],t=t.0:t.end)
  inCrop.1 <- data.frame(EVI=EVI[t.0:EVI.maxt],t=t.0:EVI.maxt)
  inCrop.2 <- data.frame(EVI=EVI[EVI.maxt:t.end],t=EVI.maxt:t.end)

  #-----------------------------------
  #Skewness & Kurtosis
  N <- length(inCrop$EVI)
  X <- inCrop$EVI

  k3 <- (N*sum(X^3)-3*sum(X)*sum(X^2)+2*sum(X)^3*N^-1)/((N-1)*(N-2))
  g1[k,j] <- round(k3/sd(X)^3,2)

  k4 <- ((N^3+N^2)*sum(X^4)-4*(N^2+N)*sum(X^3)*sum(X)-3*(N^2-
N)*sum(X^2)^2+12*N*sum(X^2)*sum(X)^2-6*sum(X)^4)/
       (N*(N-1)*(N-2)*(N-3))
  g2[k,j] <- round(k4/sd(X)^4,2)

  #-----------------------------------
  #avg rate of change, D.pos and D.neg
  D.pos[k,j] <- (EVI[EVI.maxt]-EVI[t.0])/(EVI.maxt-t.0)
  D.neg[k,j] <- (EVI[t.end]-EVI[EVI.maxt])/(t.end-EVI.maxt)

  #Crist and Malila 1980 equation2
  #----------------------------------------
```

```
  nls.1 <- try(nls(EVI ~ EVI.max*exp(b1*(t - EVI.maxt)^2),data=inCrop.1,
start=list(b1=-0.005),trace=F),silent = TRUE)

  nls.2 <- try(nls(EVI ~ EVI.max*exp(b2*(t - EVI.maxt)^2),data=inCrop.2,
start=list(b2=-0.1),trace=F),silent = TRUE)

  if (class(nls.1) == "nls")
    b1[k,j] <- round(coef(nls.1),4)

  if (class(nls.2) == "nls")
    b2[k,j] <- round(coef(nls.2),4)

  #-------------------------------------------------
  # Badhwar & Henderson  1981 - equation 1 page 749
  #-------------------------------------------------
  #estimate for rhozero: EVI.0
  #estimate for time zero: t.0
  EVI.0 <- inCrop$EVI[1]
  alpha.e <- log(EVI.max/EVI.0)/(log(EVI.maxt/t.0)+(t.0^2-
EVI.maxt^2)/(2*EVI.maxt^2))
  beta.e <- alpha.e/(2*EVI.maxt^2)

  nls.3 <- try(nls(EVI ~ A.e*(t/t.0)^alpha*exp(beta*(t.0^2-
t^2)),start=list(A.e=EVI.0,alpha=alpha.e,beta=beta.e),trace=F,data=inCrop),silent =
TRUE)
  if (class(nls.3) == "nls") {
    c3 <- coef(nls.3)
    A.e[k,j] <- round(c3[1],4)
    alpha[k,j] <- round(c3[2],4)
    beta[k,j] <- round(c3[3],4)
  }
 }
}
```

```
  write.table(t(t.range),"output\\2004\\derivative\\trange.dat",quote = F,na = "-999", dec
  = ".", row.names = F,col.names = F)
  write.table(t(b1),"output\\2004\\derivative\\b1.dat",quote = F,na = "-999", dec = ".",
  row.names = F,col.names = F)
  write.table(t(b2),"output\\2004\\derivative\\b2.dat",quote = F,na = "-999", dec = ".",
  row.names = F,col.names = F)
  write.table(t(peak),"output\\2004\\derivative\\peak.dat",quote = F,na = "-999", dec =
  ".", row.names = F,col.names = F)
  write.table(t(A.e),"output\\2004\\derivative\\Ae.dat",quote = F,na = "-999", dec = ".",
  row.names = F,col.names = F)
  write.table(t(alpha),"output\\2004\\derivative\\alpha.dat",quote = F,na = "-999", dec =
  ".", row.names = F,col.names = F)
write.table(t(beta),"output\\2004\\derivative\\beta.dat",quote = F,na = "-999", dec = ".",
  row.names = F,col.names = F)
write.table(t(g1),"output\\2004\\derivative\\g1.dat",quote = F,na = "-999", dec = ".",
  row.names = F,col.names = F)
write.table(t(g2),"output\\2004\\derivative\\g2.dat",quote = F,na = "-999", dec = ".",
  row.names = F,col.names = F)
write.table(t(D.pos),"output\\2004\\derivative\\Dpos.dat",quote = F,na = "-999", dec =
  ".", row.names = F,col.names = F)
write.table(t(D.neg),"output\\2004\\derivative\\Dneg.dat",quote = F,na = "-9999", dec =
  ".", row.names = F,col.names = F)

#Write combined tables
write.table(rbind(t(b1),t(b2),t(peak),t(t.range)),"output\\2004\\derivative\\b1b2peaktran
  ge.txt",sep=" ",quote = F,na = "-999", dec = ".", row.names = F,col.names = F)
write.table(rbind(t(alpha),t(beta),t(A.e)),"output\\2004\\derivative\\alphabetaAe.txt",sep
  =" ", quote = F,na = "-999", dec = ".", row.names = F,col.names = F)
write.table(rbind(t(g1),t(g2),t(D.pos),
  t(D.neg),t(peak)),"output\\2004\\derivative\\g1g2DposDnegpeak.txt",sep=" ",  quote
  = F,na = "-9999", dec = ".", row.names = F,col.names = F)
```

```
write.table(rbind(t(alpha),t(beta),t(peak), t(t.range),
  t(A.e)),"output\\2004\\derivative\\alphabetapeaktrangeAe.txt",sep=" ", quote = F,na =
  "-999", dec = ".", row.names = F,col.names = F)
```

Appendix B: Extension of Tables

Table B.1: Separability measures (*Jeffries-Matusita* (JM) & *Transformed Divergence* (TD)) calculated on the EVI trajectories of each feature class for May to October for 2003.

Feature Classes	JM	TD
Wheat 214 points		
Stubble & Soil 255 points	2.00	2.00
Barley fed off 12 points	2.00	2.00
Barley 100 points	1.41	1.62
Chickpeas 36 points	1.99	2.00
Wheat late 39 points	1.65	1.97
Barley double cropping 70 points	1.87	2.00
Natural Forest 56 points	2.00	2.00
Grazing 292 points	2.00	2.00
Production forestry 315 points	2.00	2.00
Stubble & Soil 255 points		
Wheat 214 points	2.00	2.00
Barley fed off 12 points	2.00	2.00
Barley 100 points	2.00	2.00
Chickpeas 36 points	2.00	2.00
Wheat late 39 points	2.00	2.00
Barley double cropping 70 points	2.00	2.00
Natural Forest 56 points	2.00	2.00
Grazing 292 points	1.99	2.00
Production forestry 315 points	2.00	2.00
Barley fed off 12 points		
Wheat 214 points	2.00	2.00
Stubble & Soil 255 points	2.00	2.00
Barley 100 points	2.00	2.00
Chickpeas 36 points	2.00	2.00
Wheat late 39 points	2.00	2.00
Barley double cropping 70 points	2.00	2.00
Natural Forest 56 points	2.00	2.00
Grazing 292 points	2.00	2.00
Production forestry 315 points	2.00	2.00
Barley 100 points		
Wheat 214 points	1.41	1.62
Stubble & Soil 255 points	2.00	2.00
Barley fed off 12 points	2.00	2.00
Chickpeas 36 points	2.00	2.00
Wheat late 39 points	1.94	2.00
Barley double cropping 70 points	2.00	2.00
Natural Forest 56 points	2.00	2.00
Grazing 292 points	2.00	2.00
Production forestry 315 points	2.00	2.00
Chickpeas 36 points		
Wheat 214 points	1.99	2.00
Stubble & Soil 255 points	2.00	2.00
Barley fed off 12 points	2.00	2.00
Barley 100 points	2.00	2.00
Wheat late 39 points	1.97	2.00
Barley double cropping 70 points	1.99	2.00
Natural Forest 56 points	2.00	2.00
Grazing 292 points	1.99	2.00
Production forestry 315 points	2.00	2.00

Feature Classes	JM	TD
Wheat late 39 points		
Wheat 214 points	1.65	1.97
Stubble & Soil 255 points	2.00	2.00
Barley fed off 12 points	2.00	2.00
Barley 100 points	1.94	2.00
Chickpeas 36 points	1.97	2.00
Barley double cropping 70 points	1.89	2.00
Natural Forest 56 points	2.00	2.00
Grazing 292 points	2.00	2.00
Production forestry 315 points	2.00	2.00
Barley double cropping 70 points		
Wheat 214 points	1.87	2.00
Stubble & Soil 255 points	2.00	2.00
Barley fed off 12 points	2.00	2.00
Barley 100 points	2.00	2.00
Chickpeas 36 points	1.99	2.00
Wheat late 39 points	1.89	2.00
Natural Forest 56 points	2.00	2.00
Grazing 292 points	2.00	2.00
Production forestry 315 points	2.00	2.00
Natural Forest 56 points		
Wheat 214 points	2.00	2.00
Stubble & Soil 255 points	2.00	2.00
Barley fed off 12 points	2.00	2.00
Barley 100 points	2.00	2.00
Chickpeas 36 points	2.00	2.00
Wheat late 39 points	2.00	2.00
Barley double cropping 70 points	2.00	2.00
Grazing 292 points	1.92	2.00
Production forestry 315 points	1.96	2.00
Grazing 292 points		
Wheat 214 points	2.00	2.00
Stubble & Soil 255 points	1.99	2.00
Barley fed off 12 points	2.00	2.00
Barley 100 points	2.00	2.00
Chickpeas 36 points	1.99	2.00
Wheat late 39 points	2.00	2.00
Barley double cropping 70 points	2.00	2.00
Natural Forest 56 points	1.92	2.00
Production forestry 315 points	1.78	1.94
Production forestry 315 points		
Wheat 214 points	2.00	2.00
Stubble & Soil 255 points	2.00	2.00
Barley fed off 12 points	2.00	2.00
Barley 100 points	2.00	2.00
Chickpeas 36 points	2.00	2.00
Wheat late 39 points	2.00	2.00
Barley double cropping 70 points	2.00	2.00
Natural Forest 56 points	1.96	2.00
Grazing 292 points	1.78	1.94

Table B.2: Separability measures (*Jeffries-Matusita* (JM) & *Transformed Divergence* (TD)) calculated on the EVI trajectories of each feature class for May to October for 2004.

Feature Classes	JM	TD
Natural Forest 56 points		
Grazing 292 points	1.99	2.00
Production forestry 315 points	1.96	2.00
Wheat 245 points	2.00	2.00
Stubble & Soil 405 points	2.00	2.00
Barley 46 points	2.00	2.00
Grazing 292 points		
Natural Forest 56 points	1.99	2.00
Production forestry 315 points	1.83	1.94
Wheat 245 points	2.00	2.00
Stubble & Soil 405 points	1.94	1.99
Barley 46 points	2.00	2.00
Production forestry 315 points		
Natural Forest 56 points	1.96	2.00
Grazing 292 points	1.83	1.94
Wheat 245 points	2.00	2.00
Stubble & Soil 405 points	2.00	2.00
Barley 46 points	2.00	2.00
Wheat 245 points		
Natural Forest56 points	2.00	2.00
Grazing292 points	2.00	2.00
Production forestry 315 points	2.00	2.00
Stubble & Soil 405 points	2.00	2.00
Barley 46 points	1.85	1.96
Stubble & Soil 405 points		
Natural Forest 56 points	2.00	2.00
Grazing 292 points	1.94	1.99
Production forestry 315 points	2.00	2.00
Wheat 245 points	2.00	2.00
Barley 46 points	2.00	2.00
Barley 46 points		
Natural Forest 56 points	2.00	2.00
Grazing 292 points	2.00	2.00
Production forestry 315 points	2.00	2.00
Wheat 245 points	1.85	1.96
Stubble & Soil 405 points	2.00	2.00

Table B.3: Area estimates and ABARE surveyed data (actual) across all features (i.e. wheat, barley, chickpea and other) for each method for the 2003 and 2004 seasons for the Jondaryan shire. The accuracy is depicted in the Dev% column, which is calculated as [Estimate-Actual]/Estimate.

Jondaryan	2003 Season			2004 Season		
Single Date	**Estimate**	**Actual**	**Dev(%)**	**Estimate**	**Actual**	**Dev(%)**
Wheat	28597	27358	5	5922	5443	9
Barley	4566	10796	-58	1853	2714	-32
Chickpea	87110	7760	1023	18033	1650	993
Winter Crop	120272	45914	162	25808	9807	163
Multi-date	**Estimate**	**Actual**	**Dev(%)**	**Estimate**	**Actual**	**Dev(%)**
Wheat	74502	27358	172	12417	5443	128
Barley	2865	10796	-73	7259	2714	167
Chickpea	14327	7760	85	0	1650	-100
Winter Crop	91694	45914	100	19676	9807	101
PCA	**Estimate**	**Actual**	**Dev(%)**	**Estimate**	**Actual**	**Dev(%)**
Wheat	72591	27358	165	8978	5443	65
Barley	2865	10796	-73	5521	2714	103
Chickpea	6877	7760	-11	0	1650	-100
Winter Crop	82334	45914	79	14499	9807	48
HANTS	**Estimate**	**Actual**	**Dev(%)**	**Estimate**	**Actual**	**Dev(%)**
Wheat	37824	27358	38	4909	5443	-10
Barley	2674	10796	-75	1509	2714	-44
Chickpea	13850	7760	78	0	1650	-100
Winter Crop	54348	45914	18	6419	9807	-35
CF1	**Estimate**	**Actual**	**Dev(%)**	**Estimate**	**Actual**	**Dev(%)**
Wheat	48178	27358	76	16429	5443	202
Barley	4566	10796	-58	6686	2714	146
Chickpea	49668	7760	540	96	1650	-94
Winter Crop	102411	45914	123	23210	9807	137
CF2	**Estimate**	**Actual**	**Dev(%)**	**Estimate**	**Actual**	**Dev(%)**
Wheat	35341	27358	29	21395	5443	293
Barley	5272	10796	-51	5922	2714	118
Chickpea	64186	7760	727	1242	1650	-25
Winter Crop	104799	45914	128	28559	9807	191

Table B.4: Table 3: Area estimates and ABARE surveyed data (actual) across all features (i.e. wheat, barley, chickpea and other) for each method for the 2003 and 2004 seasons for the Pittsworth shire. The accuracy is depicted in the Dev% column, which is calculated as [Estimate-Actual]/Estimate.

Pittsworth	2003 Season			2004 Season		
Single Date	**Estimate**	**Actual**	**Dev(%)**	**Estimate**	**Actual**	**Dev(%)**
Wheat	13478	13990	-4	4028	2447	65
Barley	1448	4611	-69	1415	1560	-9
Chickpea	44201	1012	4268	16004	525	2948
Winter Crop	59127	19613	201	21447	4532	373
Multi-date	**Estimate**	**Actual**	**Dev(%)**	**Estimate**	**Actual**	**Dev(%)**
Wheat	38757	13990	177	9145	2447	274
Barley	1034	4611	-78	6423	1560	312
Chickpea	10451	1012	933	0	525	-100
Winter Crop	50243	19613	156	15568	4532	244
PCA	**Estimate**	**Actual**	**Dev(%)**	**Estimate**	**Actual**	**Dev(%)**
Wheat	36907	13990	164	6532	2447	167
Barley	1742	4611	-62	4464	1560	186
Chickpea	4355	1012	330	0	525	-100
Winter Crop	43003	19613	119	10996	4532	143
HANTS	**Estimate**	**Actual**	**Dev(%)**	**Estimate**	**Actual**	**Dev(%)**
Wheat	20576	13990	47	2939	2447	20
Barley	653	4611	-86	1219	1560	-22
Chickpea	7621	1012	653	0	525	-100
Winter Crop	28850	19613	47	4159	4532	-8
CF1	**Estimate**	**Actual**	**Dev(%)**	**Estimate**	**Actual**	**Dev(%)**
Wheat	25040	13990	79	13609	2447	456
Barley	1372	4611	-70	5117	1560	228
Chickpea	34838	1012	3342	120	525	-77
Winter Crop	61250	19613	212	18845	4532	316
CF2	**Estimate**	**Actual**	**Dev(%)**	**Estimate**	**Actual**	**Dev(%)**
Wheat	18508	13990	32	17473	2447	614
Barley	1905	4611	-59	4681	1560	200
Chickpea	39193	1012	3773	893	525	70
Winter Crop	59606	19613	204	23048	4532	409

Table B.5: Early-season and end-of-season area estimates (Ha) for 2005 based on whole of QLD MODIS EVI pixels, applying all of QLD sampling points to create a classified image of entire QLD cropping region. The July, August, Average and combined columns (i.e. early-season estimates approach) estimates were accumulated only within the 1999 land use areas. The end-of-season (i.e. HANTS approach) column is the sum of the Wheat, Barley and Chickpea columns and had no land use mask overlay.

Region	Shire	July	August	Average	Combined	End-of-Season	Wheat	Barley	Chickpea
SWQ	Balonne (S)	94047	54722	74384	81228	191943	142664	33689	15589
CQ	Banana (S)	37416	18018	27717	23196	14883	11640	3035	209
CQ	Bauhinia (S)	93192	35532	64362	80762	98693	85174	9582	3937
CQ	Belyando (S)	8303	2581	5442	6094	10559	9985	0	574
SWQ	Bendemere (S)	29291	8854	19073	26018	34678	27153	4511	3015
SWQ	Booringa (S)	9846	7368	8607	7367	33479	27813	2282	3384
CQ	Broadsound (S)	3029	1635	2332	1696	2378	2083	72	224
SWQ	Bungil (S)	68781	34109	51445	63618	119123	94312	18628	6183
SEQ	Cambooya (S) - Pt A	6260	4877	5568	1893	1487	1368	32	86
SEQ	Chinchilla (S)	43232	29891	36562	22423	25670	19204	4738	1728
SEQ	Clifton (S)	15170	12057	13614	4219	3011	2744	173	93
CQ	Duaringa (S)	16705	6360	11532	13379	13279	11580	1675	24
CQ	Emerald (S)	41869	15600	28735	33689	43650	41101	2226	324
SEQ	Gayndah (S)	1818	462	1140	1470	415	385	30	0
SEQ	Inglewood (S)	14204	6957	10580	11571	10801	6186	3009	1607
SEQ	Jondaryan (S) - Pt B	35725	32107	33916	6028	8904	7731	779	394
SEQ	Kilkivan (S)	2129	714	1422	1574	323	223	100	0
SEQ	Kingaroy (S)	8623	4820	6722	4648	1699	1271	217	211
SEQ	Millmerran (S)	31848	21356	26602	17189	15581	10347	4255	979
CQ	Monto (S)	5392	3477	4434	2670	1028	814	184	30
SEQ	Mundubbera (S)	1563	455	1009	1189	283	171	106	6
SEQ	Murgon (S)	2330	999	1664	1595	226	144	75	6
SWQ	Murilla (S)	72306	44362	58334	51062	65548	47933	8972	8644
CQ	Peak Downs (S)	19986	6579	13282	15705	20107	19163	403	542
SEQ	Pittsworth (S)	20893	18818	19856	3724	5825	5053	503	268
SEQ	Rosalie (S) - Pt B	21940	18039	19989	5134	5763	4839	230	693
SWQ	Tara (S)	129420	58997	94209	114954	184824	128347	44703	11774
SWQ	Taroom (S)	41195	21240	31218	25594	25556	18584	3193	3779
SWQ	Waggamba (S)	227548	123922	175735	199210	337818	201310	104770	31738
SEQ	Wambo (S)	93918	85830	89874	14538	35644	29645	2145	3854
SWQ	Warroo (S)	47737	17490	32613	44508	116245	98902	13964	3379
SEQ	Warwick (S) - East	18426	6630	12528	14294	3486	2892	242	352
SEQ	Warwick (S) - North	10205	6060	8133	4899	1658	1519	70	69
SEQ	Warwick (S) - West	3315	1212	2264	2450	585	499	75	12
SEQ	Wondai (S)	6682	2982	4832	4374	1466	1147	277	41
	Total	1284345	715113	999729	913962	1436622	1063928	268946	103748

Table B.6: Early-season and end-of-season area estimates (Ha) for 2005 based on whole of QLD MODIS EVI pixels, applying all of QLD sampling points to create a classified image for entire QLD cropping region. All column estimates were accumulated within the 1999 land use area overlay.

Region	Shire	July	August	Average	Combined	End-of-Season	Wheat	Barley	Chickpea
SWQ	Balonne (S)	94047	54722	74384	81228	77314	53041	15395	8878
CQ	Banana (S)	37416	18018	27717	23196	11445	8854	2447	145
CQ	Bauhinia (S)	93192	35532	64362	80762	77324	66984	6534	3806
CQ	Belyando (S)	8303	2581	5442	6094	9973	9404	0	569
SWQ	Bendemere (S)	29291	8854	19073	26018	20736	16069	2923	1744
SWQ	Booringa (S)	9846	7368	8607	7367	9833	7171	1288	1374
CQ	Broadsound (S)	3029	1635	2332	1696	1729	1450	61	219
SWQ	Bungil (S)	68781	34109	51445	63618	57173	42460	12008	2705
SEQ	Cambooya (S) - Pt A	6260	4877	5568	1893	1306	1216	28	62
SEQ	Chinchilla (S)	43232	29891	36562	22423	20599	15365	3971	1263
SEQ	Clifton (S)	15170	12057	13614	4219	2661	2439	152	70
CQ	Duaringa (S)	16705	6360	11532	13379	10248	8880	1345	24
CQ	Emerald (S)	41869	15600	28735	33689	32636	30653	1726	257
SEQ	Gayndah (S)	1818	462	1140	1470	364	339	26	0
SEQ	Inglewood (S)	14204	6957	10580	11571	6169	3199	1987	982
SEQ	Jondaryan (S) - Pt B	35725	32107	33916	6028	7611	6585	724	302
SEQ	Kilkivan (S)	2129	714	1422	1574	209	126	83	0
SEQ	Kingaroy (S)	8623	4820	6722	4648	1199	904	138	156
SEQ	Millmerran (S)	31848	21356	26602	17189	11905	8124	2980	801
CQ	Monto (S)	5392	3477	4434	2670	796	608	171	17
SEQ	Mundubbera (S)	1563	455	1009	1189	120	61	53	6
SEQ	Murgon (S)	2330	999	1664	1595	173	103	65	5
SWQ	Murilla (S)	72306	44362	58334	51062	49292	35335	6719	7238
CQ	Peak Downs (S)	19986	6579	13282	15705	16810	15995	344	471
SEQ	Pittsworth (S)	20893	18818	19856	3724	4933	4306	446	181
SEQ	Rosalie (S) - Pt B	21940	18039	19989	5134	3950	3357	126	468
SWQ	Tara (S)	129420	58997	94209	114954	96823	63491	26641	6690
SWQ	Taroom (S)	41195	21240	31218	25594	16335	12166	1750	2418
SWQ	Waggamba (S)	227548	123922	175735	199210	175167	100604	56689	17873
SEQ	Wambo (S)	93918	85830	89874	14538	30114	25383	1926	2805
SWQ	Warroo (S)	47737	17490	32613	44508	41019	34384	5356	1279
SEQ	Warwick (S) - East	18426	6630	12528	14294	2741	2293	160	289
SEQ	Warwick (S) - North	10205	6060	8133	4899	1482	1359	68	54
SEQ	Warwick (S) - West	3315	1212	2264	2450	398	354	38	5
SEQ	Wondai (S)	6682	2982	4832	4374	966	752	192	22
	Total	1284345	715113	999729	913962	801552	583812	154560	63180

Table B.7: Early-season and end-of-season area estimates (Ha) for 2005 based on regional training of MODIS EVI pixels, applying sub-regional sampling points to create endogenous classified sub-regional imagery. The July, August, Average and combined columns (i.e. early-season estimates approach) estimates were accumulated only within the 1999 land use areas. The end-of-season (i.e. HANTS approach) column is the sum of the Wheat, Barley and Chickpea columns and had no land use mask overlay.

Region	Shire	July	August	Average	Combined	End-of-Season	Wheat	Barley	Chickpea
SWQ	Balonne (S)	94047	54722	74384	81228	146032	117294	21800	6939
CQ	Banana (S)	37416	18018	27717	23196	12371	12359	0	12
CQ	Bauhinia (S)	93192	35532	64362	80762	87361	85533	0	1827
CQ	Belyando (S)	8303	2581	5442	6094	7073	7073	0	
SWQ	Bendemere (S)	29291	8854	19073	26018	23724	22114	496	1113
SWQ	Booringa (S)	9846	7368	8607	7367	2217	0	2000	217
CQ	Broadsound (S)	3029	1635	2332	1696	2049	2030	0	18
SWQ	Bungil (S)	68781	34109	51445	63618	91476	86212	4714	550
SEQ	Cambooya (S) - Pt A	6260	4877	5568	1893	1022	622	400	0
SEQ	Chinchilla (S)	43232	29891	36562	22423	22117	9888	12229	0
SEQ	Clifton (S)	15170	12057	13614	4219	13888	1659	12229	0
CQ	Duaringa (S)	16705	6360	11532	13379	10813	10813	0	0
CQ	Emerald (S)	41869	15600	28735	33689	37434	37314	0	120
SEQ	Gayndah (S)	1818	462	1140	1470	142	24	118	0
SEQ	Inglewood (S)	14204	6957	10580	11571	0	0	0	0
SEQ	Jondaryan (S) - Pt B	35725	32107	33916	6028	7723	5031	2692	0
SEQ	Kilkivan (S)	2129	714	1422	1574	218	0	218	0
SEQ	Kingaroy (S)	8623	4820	6722	4648	834	178	656	0
SEQ	Millmerran (S)	31848	21356	26602	17189	12511	3742	8769	0
CQ	Monto (S)	5392	3477	4434	2670	362	362	0	0
SEQ	Mundubbera (S)	1563	455	1009	1189	254	18	236	0
SEQ	Murgon (S)	2330	999	1664	1595	132	0	132	0
SWQ	Murilla (S)	72306	44362	58334	51062	43771	34963	4133	4675
CQ	Peak Downs (S)	19986	6579	13282	15705	16274	16148	0	126
SEQ	Pittsworth (S)	20893	18818	19856	3724	4538	2749	1789	0
SEQ	Rosalie (S) - Pt B	21940	18039	19989	5134	4579	3241	1339	0
SWQ	Tara (S)	129420	58997	94209	114954	127840	111557	11386	4898
SWQ	Taroom (S)	41195	21240	31218	25594	11449	9194	825	1431
SWQ	Waggamba (S)	227548	123922	175735	199210	242382	191047	34435	16901
SEQ	Wambo (S)	93918	85830	89874	14538	32710	22296	10414	0
SWQ	Warroo (S)	47737	17490	32613	44508	89146	83451	4580	1115
SEQ	Warwick (S) - East	18426	6630	12528	14294	2199	739	1460	0
SEQ	Warwick (S) - North	10205	6060	8133	4899	1294	972	323	0
SEQ	Warwick (S) - West	3315	1212	2264	2450	313	69	244	0
SEQ	Wondai (S)	6682	2982	4832	4374	908	141	767	0
	Total	1284345	715113	999729	913962	1057155	878830	138382	39943

Table B.8: Early-season and end-of-season area estimates (Ha) for 2005 based on regional training of MODIS EVI pixels, applying sub-regional sampling points to create endogenous classified sub-regional imagery. All column estimates were accumulated within the 1999 land use area overlay.

Region	Shire	July	August	Average	Combined	End-of-Season	Wheat	Barley	Chickpea
SWQ	Balonne (S)	94047	54722	74384	81228	61859	48735	9473	3651
CQ	Banana (S)	37416	18018	27717	23196	9746	9743	0	3
CQ	Bauhinia (S)	93192	35532	64362	80762	71033	69318	0	1714
CQ	Belyando (S)	8303	2581	5442	6094	6690	6690	0	0
SWQ	Bendemere (S)	29291	8854	19073	26018	15681	14544	365	773
SWQ	Booringa (S)	9846	7368	8607	7367	8225	6541	1527	158
CQ	Broadsound (S)	3029	1635	2332	1696	1513	1495	0	18
SWQ	Bungil (S)	68781	34109	51445	63618	48994	45408	3182	405
SEQ	Cambooya (S) - Pt A	6260	4877	5568	1893	928	562	366	0
SEQ	Chinchilla (S)	43232	29891	36562	22423	18643	8766	9877	0
SEQ	Clifton (S)	15170	12057	13614	4219	2292	1590	702	0
CQ	Duaringa (S)	16705	6360	11532	13379	8600	8571	0	28
CQ	Emerald (S)	41869	15600	28735	33689	30075	29965	0	110
SEQ	Gayndah (S)	1818	462	1140	1470	126	24	102	0
SEQ	Inglewood (S)	14204	6957	10580	11571	2833	2025	0	808
SEQ	Jondaryan (S) - Pt B	35725	32107	33916	6028	6761	4333	2428	0
SEQ	Kilkivan (S)	2129	714	1422	1574	161	0	161	0
SEQ	Kingaroy (S)	8623	4820	6722	4648	596	144	452	0
SEQ	Millmerran (S)	31848	21356	26602	17189	9748	3457	6291	0
CQ	Monto (S)	5392	3477	4434	2670	289	289	0	0
SEQ	Mundubbera (S)	1563	455	1009	1189	97	0	97	0
SEQ	Murgon (S)	2330	999	1664	1595	110	13	96	0
SWQ	Murilla (S)	72306	44362	58334	51062	35048	27520	3506	4022
CQ	Peak Downs (S)	19986	6579	13282	15705	13694	13572	0	122
SEQ	Pittsworth (S)	20893	18818	19856	3724	3971	2427	1545	0
SEQ	Rosalie (S) - Pt B	21940	18039	19989	5134	3345	2560	785	0
SWQ	Tara (S)	129420	58997	94209	114954	76736	65923	7525	3288
SWQ	Taroom (S)	41195	21240	31218	25594	7428	5948	480	1001
SWQ	Waggamba (S)	227548	123922	175735	199210	134946	105284	19033	10630
SEQ	Wambo (S)	93918	85830	89874	14538	28513	19706	8807	0
SWQ	Warroo (S)	47737	17490	32613	44508	33344	31390	1532	422
SEQ	Warwick (S) - East	18426	6630	12528	14294	1783	596	1187	0
SEQ	Warwick (S) - North	10205	6060	8133	4899	1168	872	295	0
SEQ	Warwick (S) - West	3315	1212	2264	2450	185	68	116	0
SEQ	Wondai (S)	6682	2982	4832	4374	561	79	481	0
	Total	1284345	715113	999729	913962	645722	538159	80410	27154

Table B.9: : Early-season and end-of-season area estimates (Ha) for 2006 based on whole of QLD MODIS EVI pixels, applying all of QLD sampling points to create a classified image of entire QLD cropping region. The July, August, Average and combined columns (i.e. early-season estimates approach) estimates were accumulated only within the 1999 land use areas. The end-of-season (i.e. HANTS approach) column is the sum of the Wheat, Barley and Chickpea columns and had no land use mask overlay.

Region	Shire	July	August	Average	Combined	End-of-Season	Wheat	Barley	Chickpea
SWQ	Balonne (S)	11608	32320	21964	38866	114476	82738	1441	30297
CQ	Banana (S)	21315	17618	19466	32957	45236	39679	5379	179
CQ	Bauhinia (S)	49677	13190	31434	54440	79507	61315	7933	10260
CQ	Belyando (S)	85735	26804	56270	93031	106734	84589	1762	20383
SWQ	Bendemere (S)	2957	978	1968	3408	5128	3876	726	527
SWQ	Booringa (S)	166	80	123	207	872	854	0	18
CQ	Broadsound (S)	17967	3009	10488	19425	25932	23685	1608	640
SWQ	Bungil (S)	1334	190	762	1487	7525	7202	146	177
SEQ	Cambooya (S) - Pt A	166	1128	647	1278	5535	5512	0	23
SEQ	Chinchilla (S)	285	454	369	630	1251	1245	0	6
SEQ	Clifton (S)	566	2079	1323	2518	3390	3378	12	0
CQ	Duaringa (S)	17732	9594	13663	24609	36803	30974	5505	324
CQ	Emerald (S)	19126	9204	14165	24289	36413	33008	865	2540
SEQ	Gayndah (S)	61	133	97	175	253	253	0	0
SEQ	Inglewood (S)	1799	7160	4480	7681	12043	10602	669	772
SEQ	Jondaryan (S) - Pt B	1528	4919	3224	5884	10812	10621	110	81
SEQ	Kilkivan (S)	460	618	539	1011	651	651	0	0
SEQ	Kingaroy (S)	178	593	385	719	2390	2390	0	0
SEQ	Millmerran (S)	116	3819	1968	3916	13655	13273	46	336
CQ	Monto (S)	3932	2450	3191	5167	2465	2435	30	0
SEQ	Mundubbera (S)	349	468	408	771	685	685	0	0
SEQ	Murgon (S)	429	705	567	1022	1225	1225	0	0
SWQ	Murilla (S)	5299	4358	4829	8161	16160	13334	467	2359
CQ	Peak Downs (S)	39913	20575	30244	50336	57426	45313	389	11724
SEQ	Pittsworth (S)	253	1470	862	1630	4114	4085	12	17
SEQ	Rosalie (S) - Pt B	464	1487	976	1804	8733	8651	29	54
SWQ	Tara (S)	4428	7987	6208	10681	34598	25432	435	8732
SWQ	Taroom (S)	447	478	463	834	5153	5135	18	0
SWQ	Waggamba (S)	21786	91140	56463	96905	217887	159834	12303	45750
SEQ	Wambo (S)	552	2619	1585	3015	8246	8106	18	122
SWQ	Warroo (S)	6862	1620	4241	7759	21423	14747	502	6175
SEQ	Warwick (S) - East	917	5231	3074	5943	6363	6334	6	23
SEQ	Warwick (S) - North	281	1794	1038	2025	3167	3138	23	6
SEQ	Warwick (S) - West	195	1630	912	1763	2029	2017	0	12
SEQ	Wondai (S)	349	871	610	1136	4279	4273	0	6
	Total	319234	278773	299003	515483	902559	720587	40432	141540

Table B.10: Early-season and end-of-season area estimates (Ha) for 2006 based on whole of QLD MODIS EVI pixels, applying all of QLD sampling points to create a classified image for entire QLD cropping region. All column estimates were accumulated within the 1999 land use area overlay.

Region	Shire	July	August	Average	Combined	End-of-Season	Wheat	Barley	Chickpea
SWQ	Balonne (S)	11608	32320	21964	38866	54659	38909	1116	14633
CQ	Banana (S)	21315	17618	19466	32957	23507	19217	4128	162
CQ	Bauhinia (S)	49677	13190	31434	54440	65640	49976	5716	9948
CQ	Belyando (S)	85735	26804	56270	93031	92411	71417	1646	19348
SWQ	Bendemere (S)	2957	978	1968	3408	3222	2645	244	333
SWQ	Booringa (S)	166	80	123	207	300	286	0	14
CQ	Broadsound (S)	17967	3009	10488	19425	16063	14577	1010	477
SWQ	Bungil (S)	1334	190	762	1487	1576	1368	57	151
SEQ	Cambooya (S) - Pt A	166	1128	647	1278	3342	3336	0	6
SEQ	Chinchilla (S)	285	454	369	630	849	849	0	0
SEQ	Clifton (S)	566	2079	1323	2518	2822	2811	12	0
CQ	Duaringa (S)	17732	9594	13663	24609	21075	16627	4191	258
CQ	Emerald (S)	19126	9204	14165	24289	30935	27797	716	2422
SEQ	Gayndah (S)	61	133	97	175	115	115	0	0
SEQ	Inglewood (S)	1799	7160	4480	7681	5976	5003	277	696
SEQ	Jondaryan (S) - Pt B	1528	4919	3224	5884	7478	7322	90	66
SEQ	Kilkivan (S)	460	618	539	1011	230	230	0	0
SEQ	Kingaroy (S)	178	593	385	719	1467	1467	0	0
SEQ	Millmerran (S)	116	3819	1968	3916	8557	8263	40	254
CQ	Monto (S)	3932	2450	3191	5167	1349	1336	13	0
SEQ	Mundubbera (S)	349	468	408	771	104	104	0	0
SEQ	Murgon (S)	429	705	567	1022	314	314	0	0
SWQ	Murilla (S)	5299	4358	4829	8161	13411	10920	299	2192
CQ	Peak Downs (S)	39913	20575	30244	50336	45732	34604	236	10892
SEQ	Pittsworth (S)	253	1470	862	1630	3111	3082	12	17
SEQ	Rosalie (S) - Pt B	464	1487	976	1804	3983	3937	25	20
SWQ	Tara (S)	4428	7987	6208	10681	25252	17341	348	7563
SWQ	Taroom (S)	447	478	463	834	841	829	12	0
SWQ	Waggamba (S)	21786	91140	56463	96905	123941	89351	7280	27310
SEQ	Wambo (S)	552	2619	1585	3015	5861	5738	18	104
SWQ	Warroo (S)	6862	1620	4241	7759	11244	7685	373	3186
SEQ	Warwick (S) - East	917	5231	3074	5943	4770	4742	5	23
SEQ	Warwick (S) - North	281	1794	1038	2025	2225	2213	6	6
SEQ	Warwick (S) - West	195	1630	912	1763	1290	1282	0	8
SEQ	Wondai (S)	349	871	610	1136	1894	1891	0	3
	Total	319234	278773	299003	515483	585545	457584	27871	100090

Table B.11: Early-season and end-of-season area estimates (Ha) for 2006 based on regional training of MODIS EVI pixels, applying sub-regional sampling points to create endogenous classified sub-regional imagery. The July, August, Average and combined columns (i.e. early-season estimates approach) estimates were accumulated only within the 1999 land use areas. The end-of-season (i.e. HANTS approach) column is the sum of the Wheat, Barley and Chickpea columns and had no land use mask overlay.

Region	Shire	July	August	Average	Combined	End-of-Season	Wheat	Barley	Chickpea
SWQ	Balonne (S)	11608	32320	21964	38866	65136	55954	2414	6768
CQ	Banana (S)	21315	17618	19466	32957	11320	11249	0	71
CQ	Bauhinia (S)	49677	13190	31434	54440	67460	60846	0	6614
CQ	Belyando (S)	85735	26804	56270	93031	100009	76624	0	23385
SWQ	Bendemere (S)	2957	978	1968	3408	2777	1261	1293	222
SWQ	Booringa (S)	166	80	123	207	141	141	0	0
CQ	Broadsound (S)	17967	3009	10488	19425	16987	16812	0	175
SWQ	Bungil (S)	1334	190	762	1487	718	473	211	35
SEQ	Cambooya (S) - Pt A	166	1128	647	1278	2615	2615	0	0
SEQ	Chinchilla (S)	285	454	369	630	824	824	0	0
SEQ	Clifton (S)	566	2079	1323	2518	1961	1961	0	0
CQ	Duaringa (S)	17732	9594	13663	24609	15877	15877	0	0
CQ	Emerald (S)	19126	9204	14165	24289	27108	25015	0	2093
SEQ	Gayndah (S)	61	133	97	175	151	151	0	0
SEQ	Inglewood (S)	1799	7160	4480	7681	5083	4979	0	104
SEQ	Jondaryan (S) - Pt B	1528	4919	3224	5884	6851	6851	0	0
SEQ	Kilkivan (S)	460	618	539	1011	558	558	0	0
SEQ	Kingaroy (S)	178	593	385	719	1192	1192	0	0
SEQ	Millmerran (S)	116	3819	1968	3916	8119	8119	0	0
CQ	Monto (S)	3932	2450	3191	5167	77	77	0	0
SEQ	Mundubbera (S)	349	468	408	771	407	407	0	0
SEQ	Murgon (S)	429	705	567	1022	425	425	0	0
SWQ	Murilla (S)	5299	4358	4829	8161	6301	4813	1256	233
CQ	Peak Downs (S)	39913	20575	30244	50336	50091	42341	0	7750
SEQ	Pittsworth (S)	253	1470	862	1630	2237	2237	0	0
SEQ	Rosalie (S) - Pt B	464	1487	976	1804	4782	4782	0	0
SWQ	Tara (S)	4428	7987	6208	10681	26385	22896	1094	2395
SWQ	Taroom (S)	447	478	463	834	401	330	71	0
SWQ	Waggamba (S)	21786	91140	56463	96905	174755	146481	11159	17116
SEQ	Wambo (S)	552	2619	1585	3015	4662	4662	0	0
SWQ	Warroo (S)	6862	1620	4241	7759	5508	3426	1604	478
SEQ	Warwick (S) - East	917	5231	3074	5943	4823	4823	0	0
SEQ	Warwick (S) - North	281	1794	1038	2025	1923	1923	0	0
SEQ	Warwick (S) - West	195	1630	912	1763	1461	1461	0	0
SEQ	Wondai (S)	349	871	610	1136	1850	1850	0	0
	Total	319234	278773	299003	515483	620975	534434	19100	67440

Table B.12: Early-season and end-of-season area estimates (Ha) for 2006 based on regional training of MODIS EVI pixels, applying sub-regional sampling points to create endogenous classified sub-regional imagery. All column estimates were accumulated within the 1999 land use area overlay.

Region	Shire	July	August	Average	Combined	End-of-Season	Wheat	Barley	Chickpea
SWQ	Balonne (S)	11608	32320	21964	38866	31082	27018	1488	2575
CQ	Banana (S)	21315	17618	19466	32957	9193	9122	0	71
CQ	Bauhinia (S)	49677	13190	31434	54440	58459	52011	0	6448
CQ	Belyando (S)	85735	26804	56270	93031	87338	65223	0	22115
SWQ	Bendemere (S)	2957	978	1968	3408	1364	784	479	101
SWQ	Booringa (S)	166	80	123	207	75	75	0	0
CQ	Broadsound (S)	17967	3009	10488	19425	11976	11874	0	102
SWQ	Bungil (S)	1334	190	762	1487	436	336	100	0
SEQ	Cambooya (S) - Pt A	166	1128	647	1278	1871	1871	0	0
SEQ	Chinchilla (S)	285	454	369	630	587	587	0	0
SEQ	Clifton (S)	566	2079	1323	2518	1674	1674	0	0
CQ	Duaringa (S)	17732	9594	13663	24609	15181	13144	0	2036
CQ	Emerald (S)	19126	9204	14165	24289	23089	23089	0	0
SEQ	Gayndah (S)	61	133	97	175	55	55	0	0
SEQ	Inglewood (S)	1799	7160	4480	7681	3622	3227	301	95
SEQ	Jondaryan (S) - Pt B	1528	4919	3224	5884	5077	5077	0	0
SEQ	Kilkivan (S)	460	618	539	1011	228	228	0	0
SEQ	Kingaroy (S)	178	593	385	719	750	750	0	0
SEQ	Millmerran (S)	116	3819	1968	3916	5256	5256	0	0
CQ	Monto (S)	3932	2450	3191	5167	70	70	0	0
SEQ	Mundubbera (S)	349	468	408	771	72	72	0	0
SEQ	Murgon (S)	429	705	567	1022	103	103	0	0
SWQ	Murilla (S)	5299	4358	4829	8161	4975	3774	999	203
CQ	Peak Downs (S)	39913	20575	30244	50336	40880	33579	0	7300
SEQ	Pittsworth (S)	253	1470	862	1630	1839	1839	0	0
SEQ	Rosalie (S) - Pt B	464	1487	976	1804	2350	2350	0	0
SWQ	Tara (S)	4428	7987	6208	10681	19524	16481	914	2129
SWQ	Taroom (S)	447	478	463	834	226	165	61	0
SWQ	Waggamba (S)	21786	91140	56463	96905	100144	81881	6660	11603
SEQ	Wambo (S)	552	2619	1585	3015	3181	3181	0	0
SWQ	Warroo (S)	6862	1620	4241	7759	4687	3659	829	198
SEQ	Warwick (S) - East	917	5231	3074	5943	1296	1296	0	0
SEQ	Warwick (S) - North	281	1794	1038	2025	996	996	0	0
SEQ	Warwick (S) - West	195	1630	912	1763	1009	1009	0	0
SEQ	Wondai (S)	349	871	610	1136	0	0	0	0
	Total	319234	278773	299003	515483	438664	371856	11832	54975

Appendix C: Extension of Figures

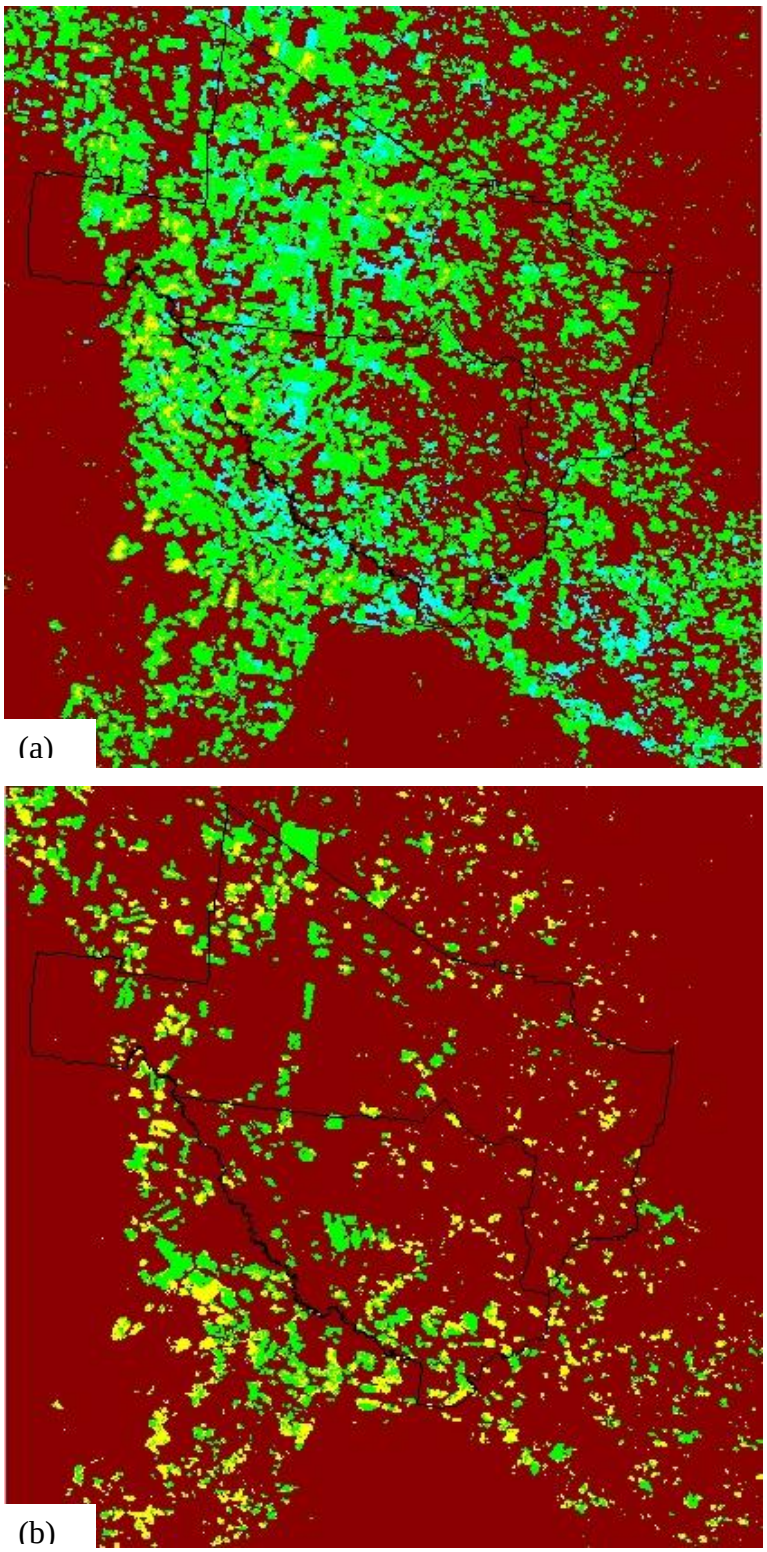

Figure C.1: Multi date EVI classification for the (a) 2003 and (b) 2004 seasons for the study area. The black line delineates the Jondaryan and Pittsworth shire boundaries. Only 3 classes were used during the 2004 season due to insufficient ground truth samples for chickpea for that season.

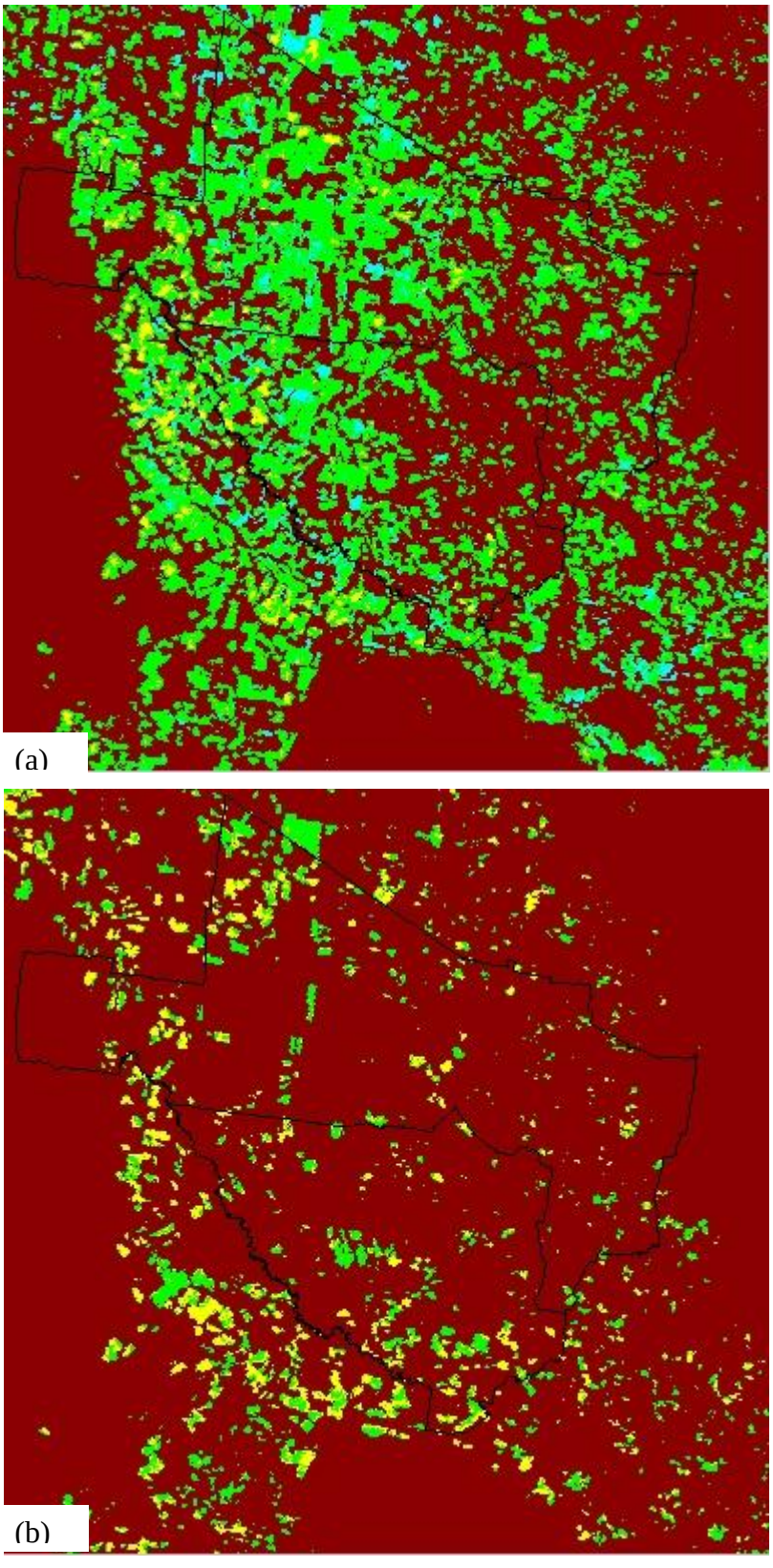

Figure C.2: PCA EVI classification for the (a) 2003 and (b) 2004 seasons for the study area. The black line delineates the Jondaryan and Pittsworth shire boundaries. Only 3 classes were used during the 2004 season due to insufficient ground truth samples for chickpea for that season.

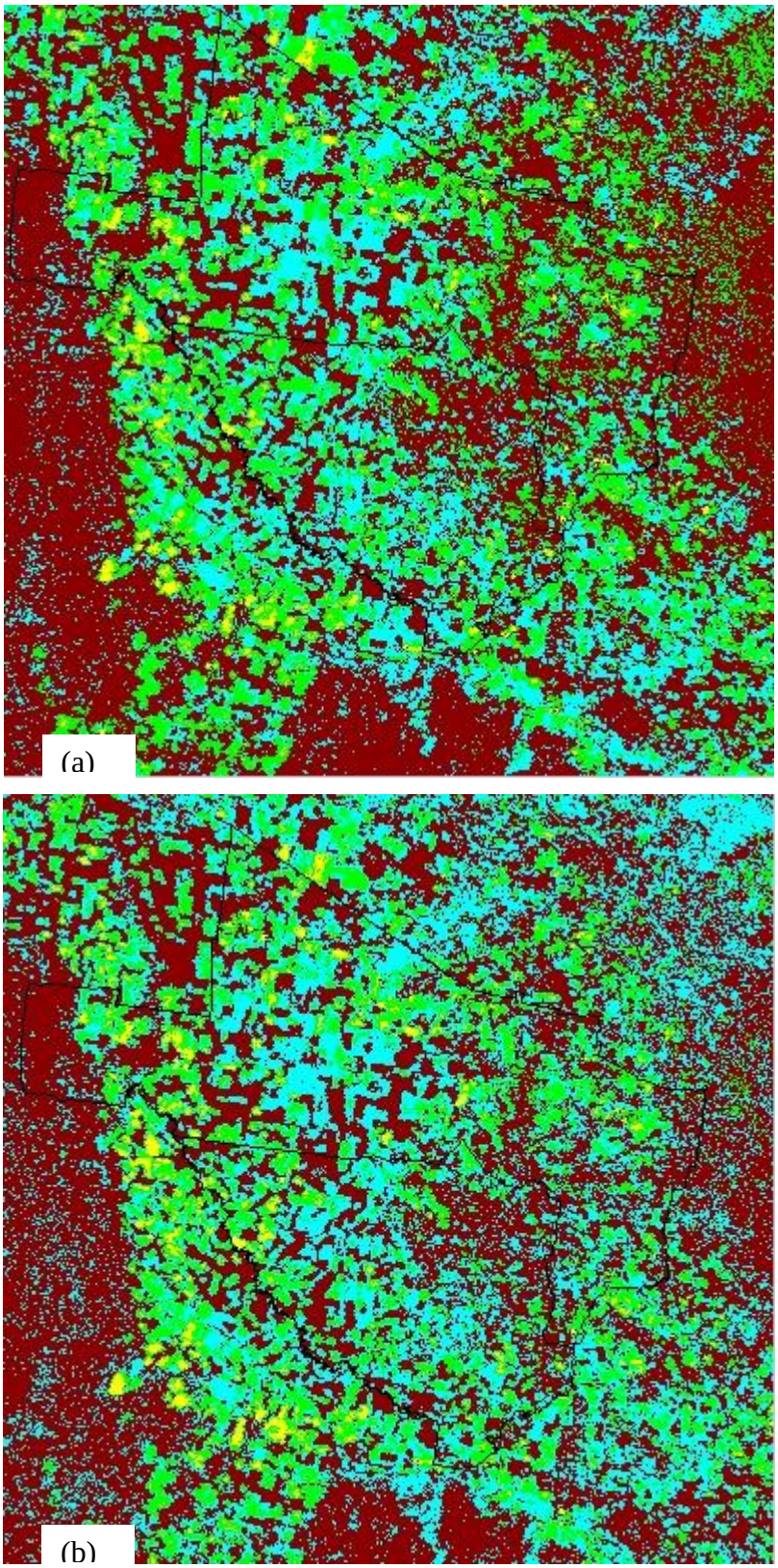

Figure C.3: Curve fitting EVI classifications for the 2003 season for the (a) CF1 and (b) CF2 approaches for the study area. The black line delineates the Jondaryan and Pittsworth shire boundaries.

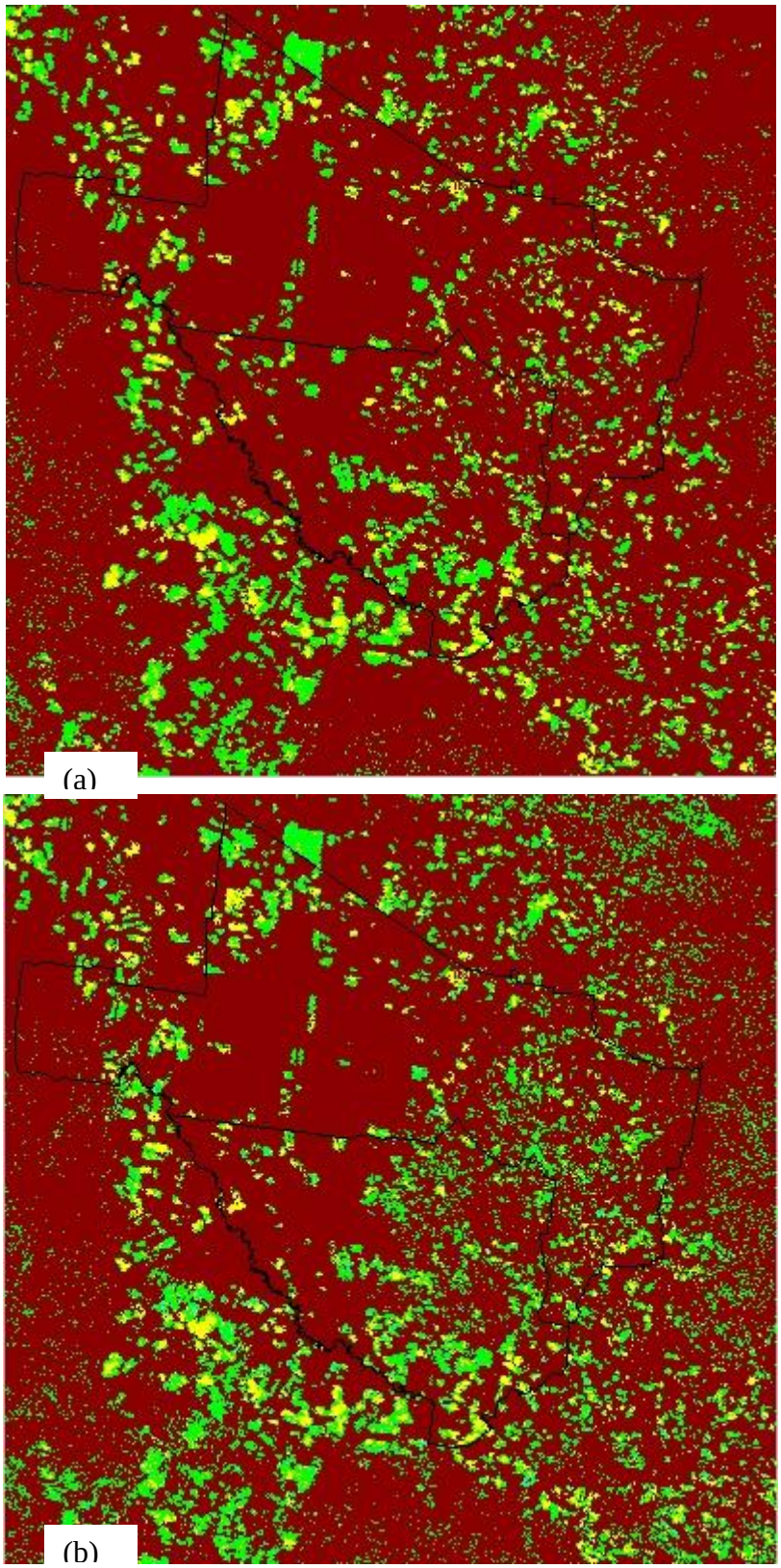

Figure C.4: Curve fitting EVI classifications for the 2004 season for the (a) CF1 and (b) CF2 approaches for the study area. The black line delineates the Jondaryan and Pittsworth shire boundaries.